"The pursuit of truth and beauty is a sphere of activity in which we are permitted to remain children all our lives."

Albert Einstein

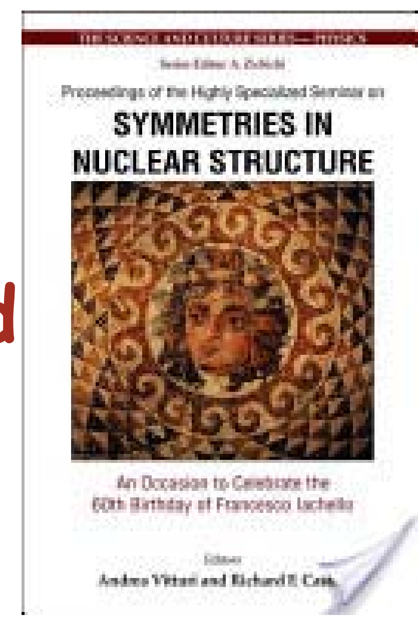

auty in Physics Theory and Experiment

Hacienda Cocoyoc, Morelos,
May 14-18, 2012

My personal Journey

Beauty in Physics：Theory and Experiment

eauty in Physics Theory and Experiment

Hacienda Cocoyoc, Morelos,
May 14-18, 2012

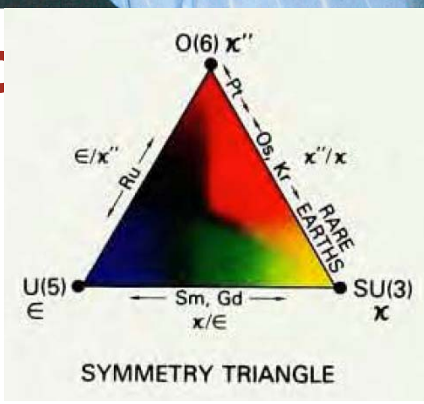

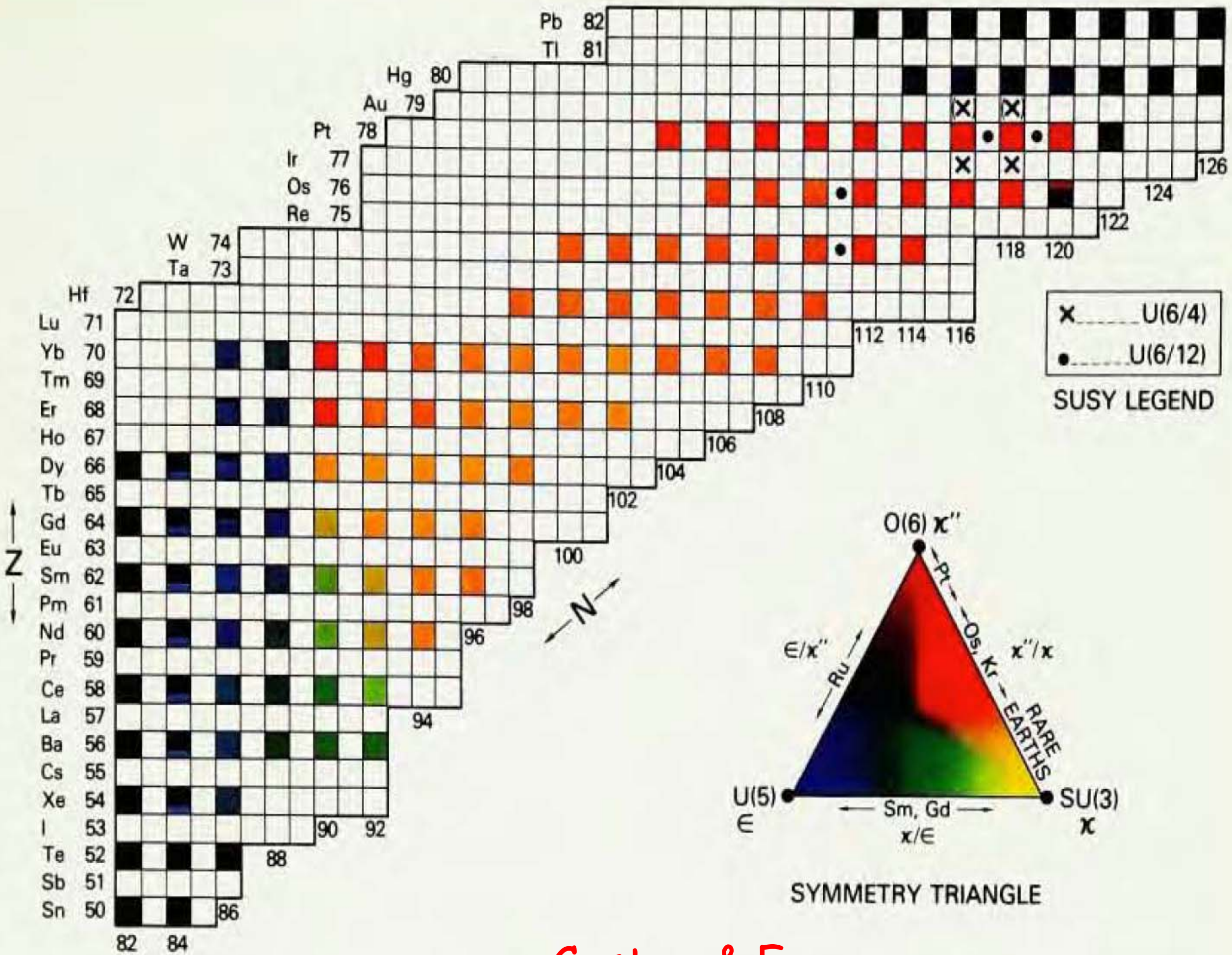

Casten & Feng
Physics Today 37, 26 (1984)

uty in Physics Theory and Experiment

Hacienda Cocoyoc, Morelos,

VOLUME 59, NUMBER 5 PHYSICAL REVIEW LETTERS 3 AUGUST 1987

First Observation of a Near-Harmonic Vibrational Nucleus

A. Aprahamian
Clark University, Worcester, Massachusetts 01610, and
Lawrence Livermore National Laboratory, Livermore, California 94550

D. S. Brenner
Clark University, Worcester, Massachusetts 01610

and

R. F. Casten, R. L. Gill, and A. Piotrowski[(a)]
Brookhaven National Laboratory, Upton, New York 11973

(Received 4 May 1987)

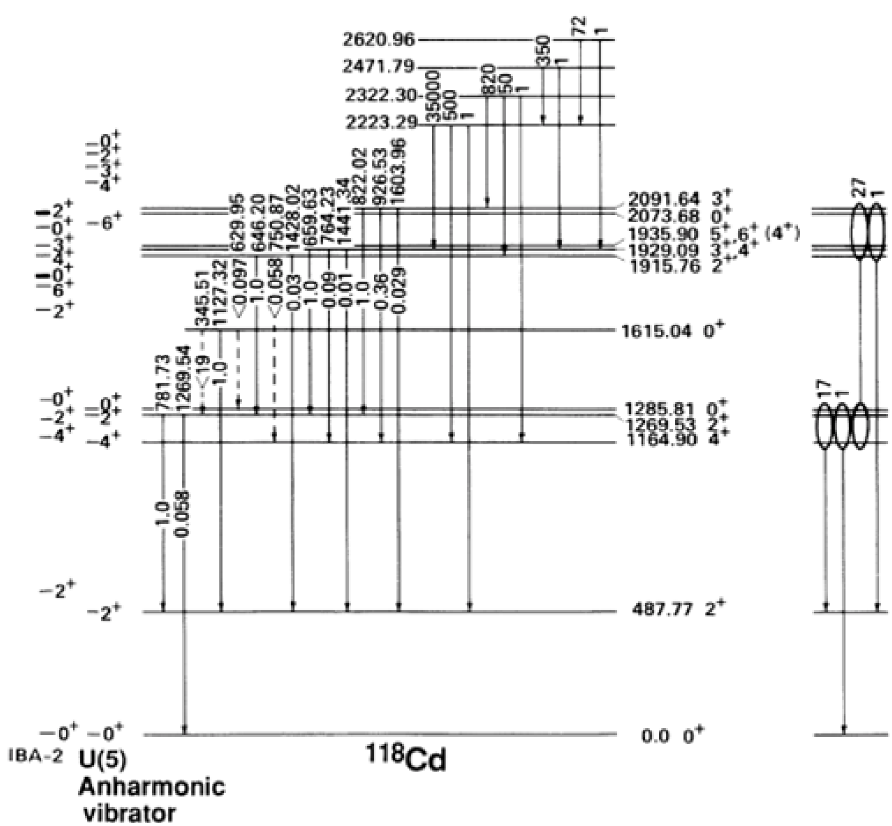

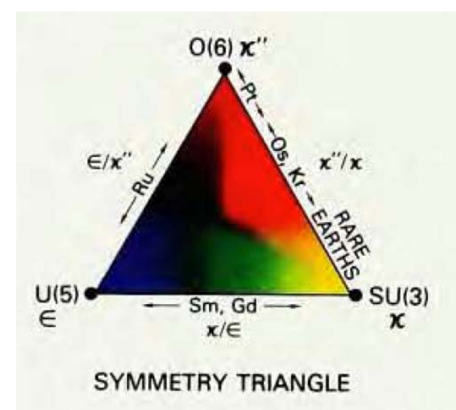

I S N A P

Institute for Structure and Nuclear Astrophysics

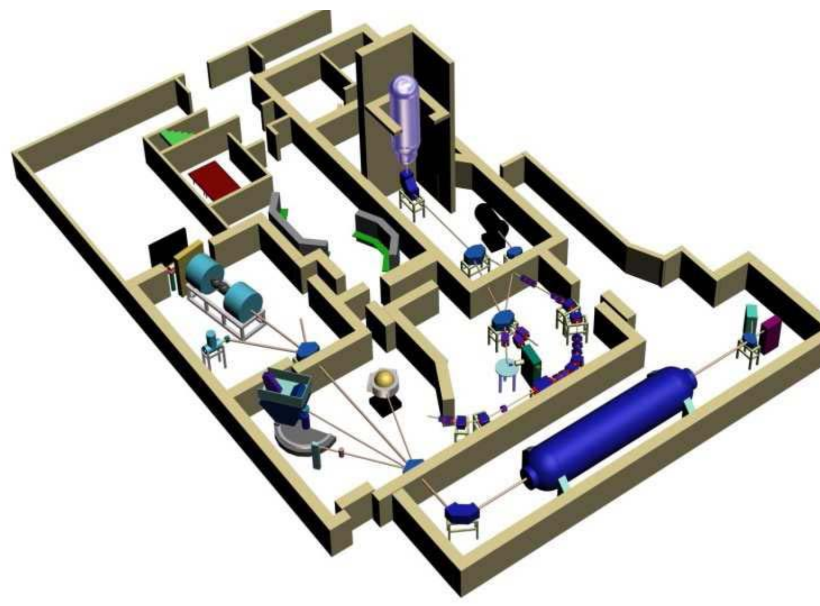

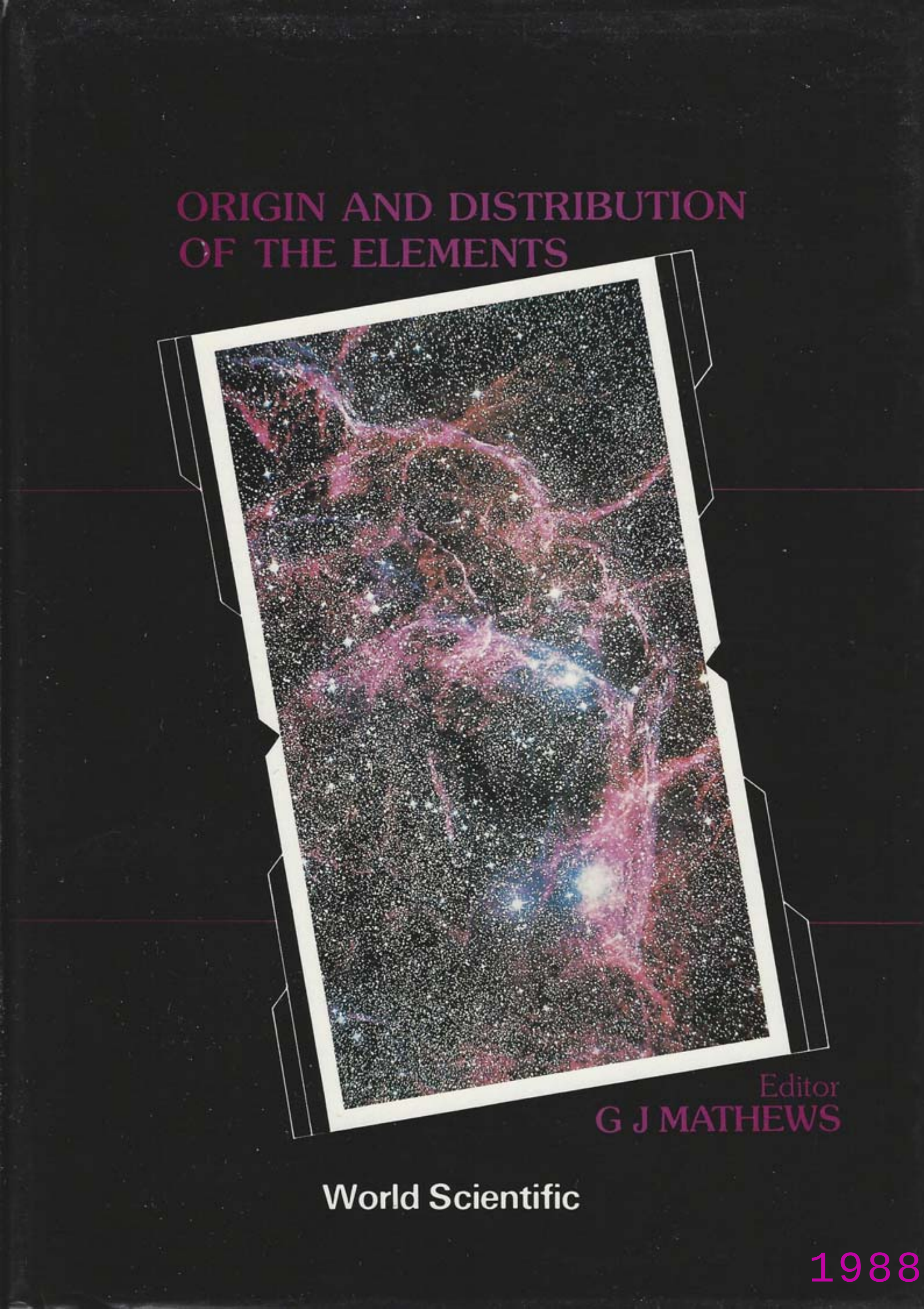

1988

Nuclear Properties Along the r-Process Path

A. APRAHAMIAN
Lawrence Livermore National Laboratory
Livermore, California 94550
USA

Effective Boson Number

ABSTRACT

The uniformity of different nuclear regions as ... e number of valence protons and neutrons (counted ... c closed shell) has been exploited for the parameterization of calculations for nuclei far from stability within the IBA model. Predictions are given for low lying levels, E2 transition rates, and binding energies for nuclei in the process path in the A = 150 and A ~ 190 mass regions

NpNn scheme

nuclei that have been calculated.

F-spin

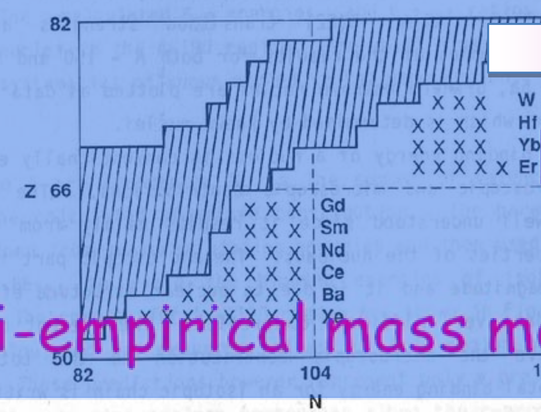

Semi-empirical mass model

Fig. 4 The relevant portion of the N-Z plane. The shaded parts indicate known nuclei. The x's show the calculated nuclei.



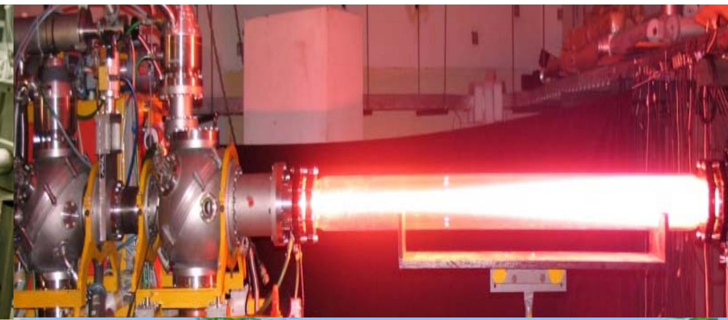
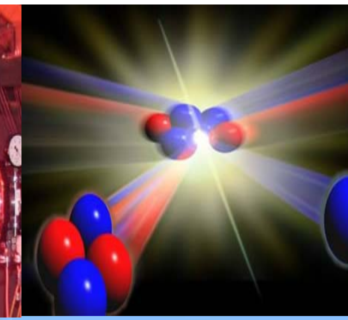
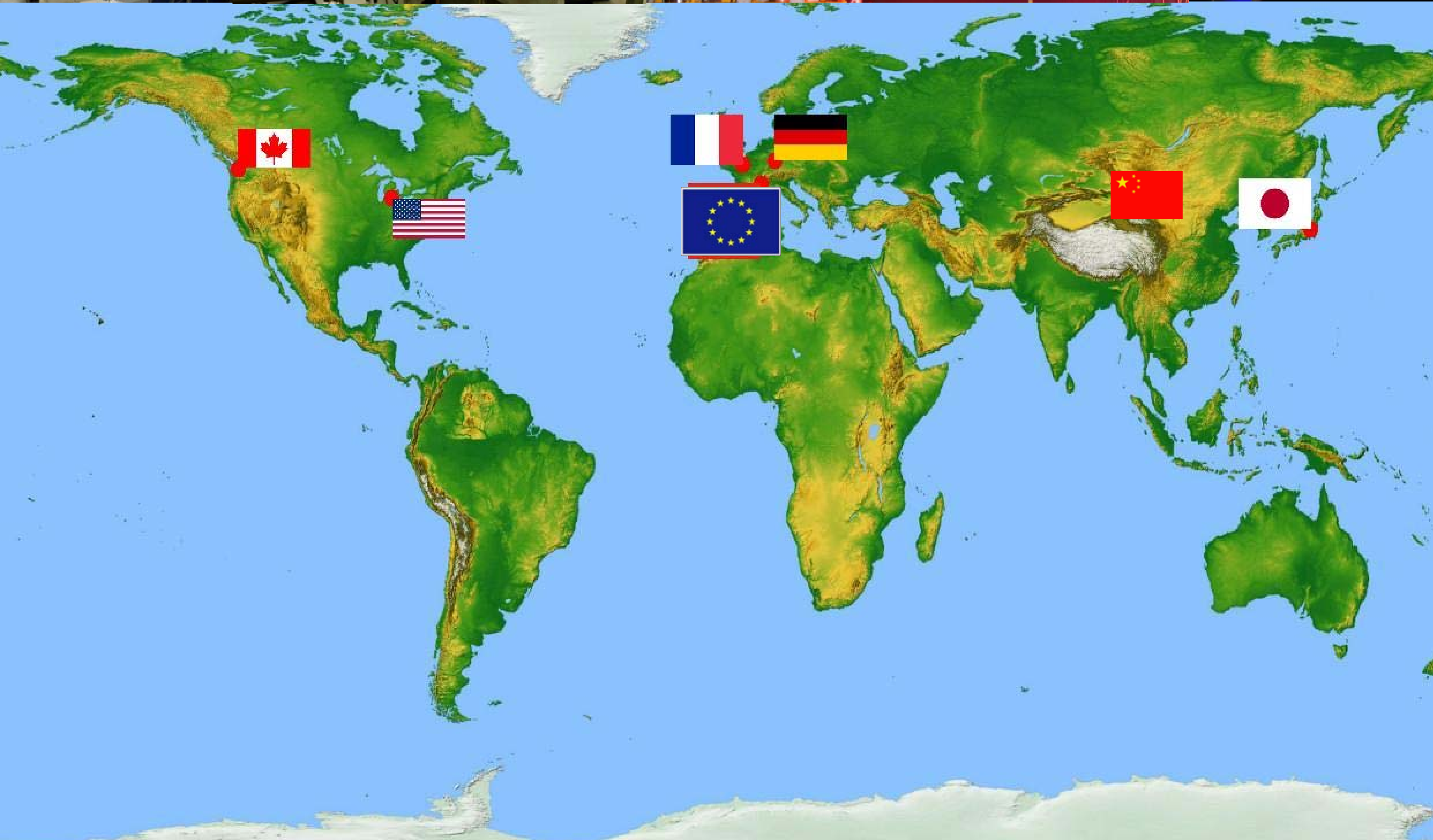

Sensitivities of the r-process to

…masses, β-decay rates, cross-sections

nuclear structure

Institute for Structure & Nuclear Astrophysics

University of Notre Dame, Notre Dame, IN (USA)

The r-process problem

New precision observations of r-process elements

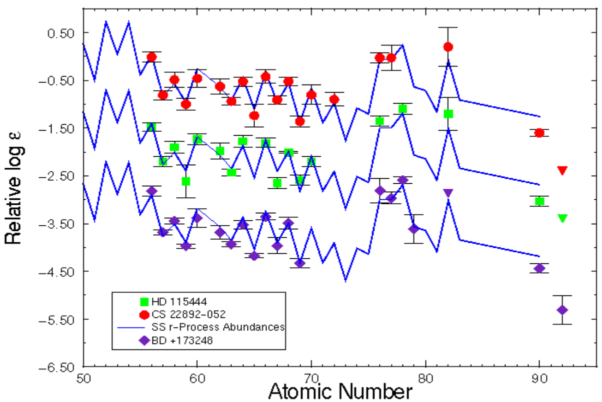

graph by J. Cowan

Nuclear Physics

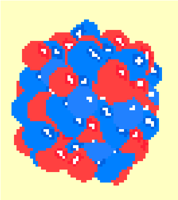

Missing link

r-process models

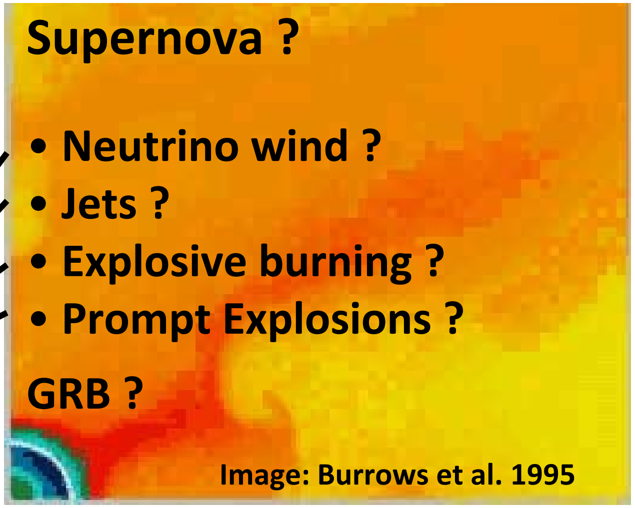

Supernova ?

- **Neutrino wind ?**
- **Jets ?**
- **Explosive burning ?**
- **Prompt Explosions ?**

GRB ?

Image: Burrows et al. 1995

Neutron star mergers ?

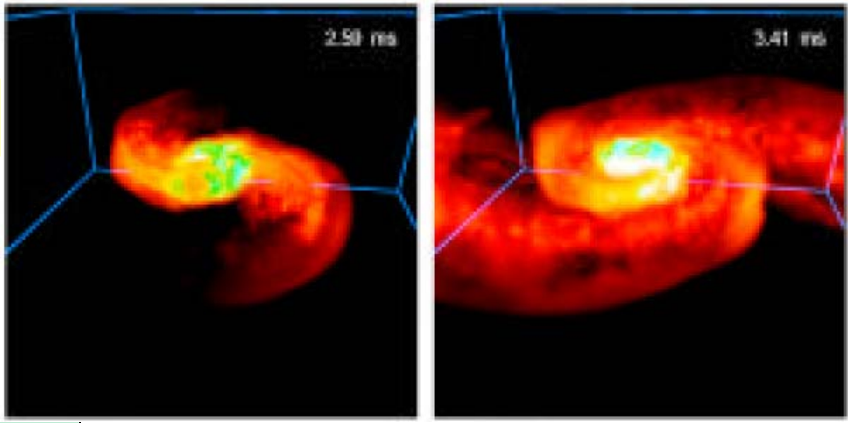

SDSS-2 Nuclear Physics driven observations

Need nuclear physics:

→ With abundance observations the only experimental constraint of r-process environment

→ Disentangle contributions from various s- and r-processes to observed abundances

→ Use r-process as probe for extreme environment

H. Schatz

r-process

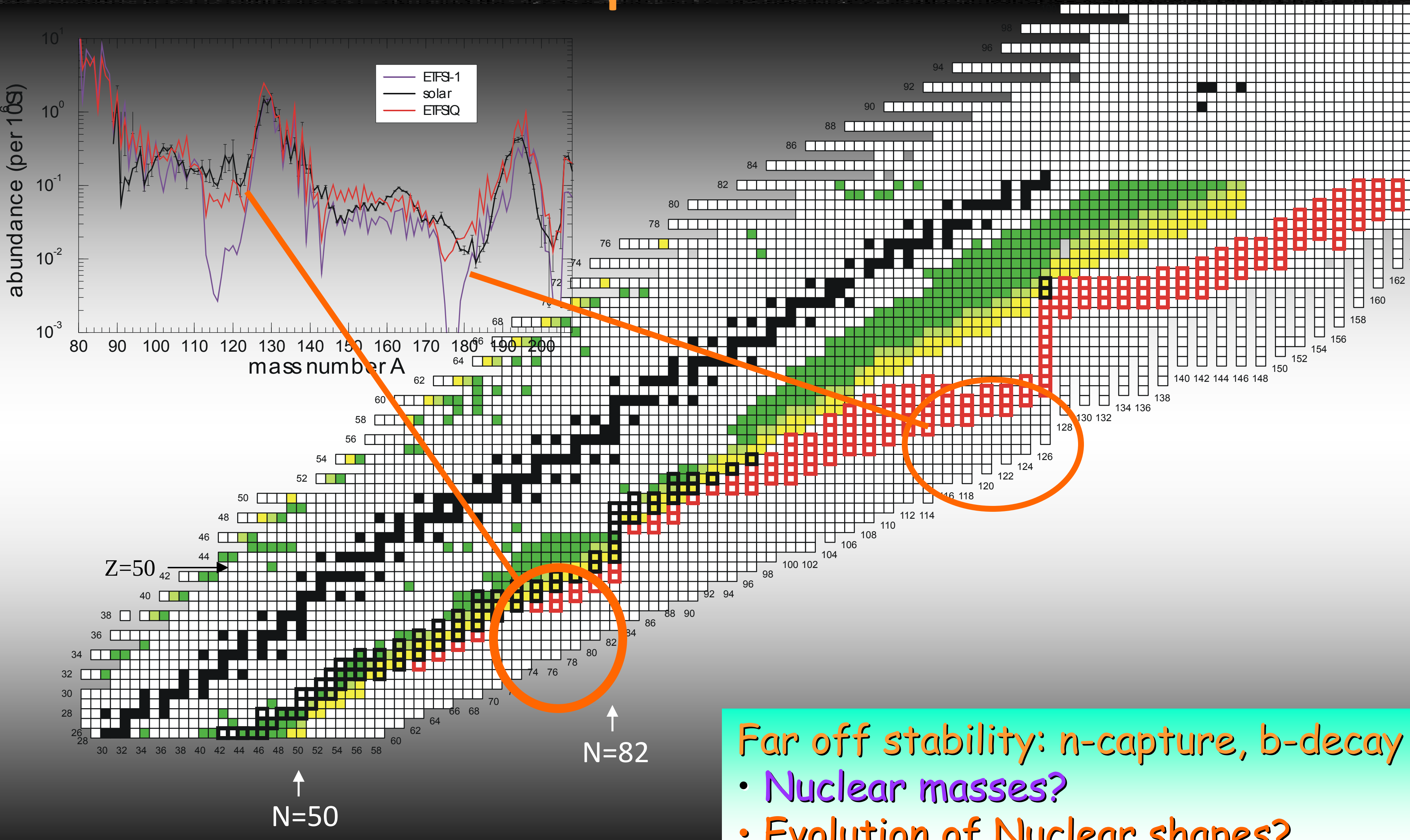

Far off stability: n-capture, b-decay
- Nuclear masses?
- Evolution of Nuclear shapes?

Masses
β-decay rates
n- capture

Major Shells and evolution of shells…

Experimental & Theoretical Challenges

ELSEVIER

Available online at www.sciencedirect.com
SCIENCE DIRECT®

Progress in Particle and Nuclear Physics 54 (2005) 535–613

Progress in Particle and Nuclear Physics

www.elsevier.com/locate/ppnp

Review

Nuclear structure aspects in nuclear astrophysics

A. Aprahamian[a], K. Langanke[b], M. Wiescher[a,*]

[a] Department of Physics and the Joint Institute for Nuclear Astrophysics, University of Notre Dame, Notre Dame, IN 46556, USA

How do you decide which nuclei to measure???

Pt –

Xe –

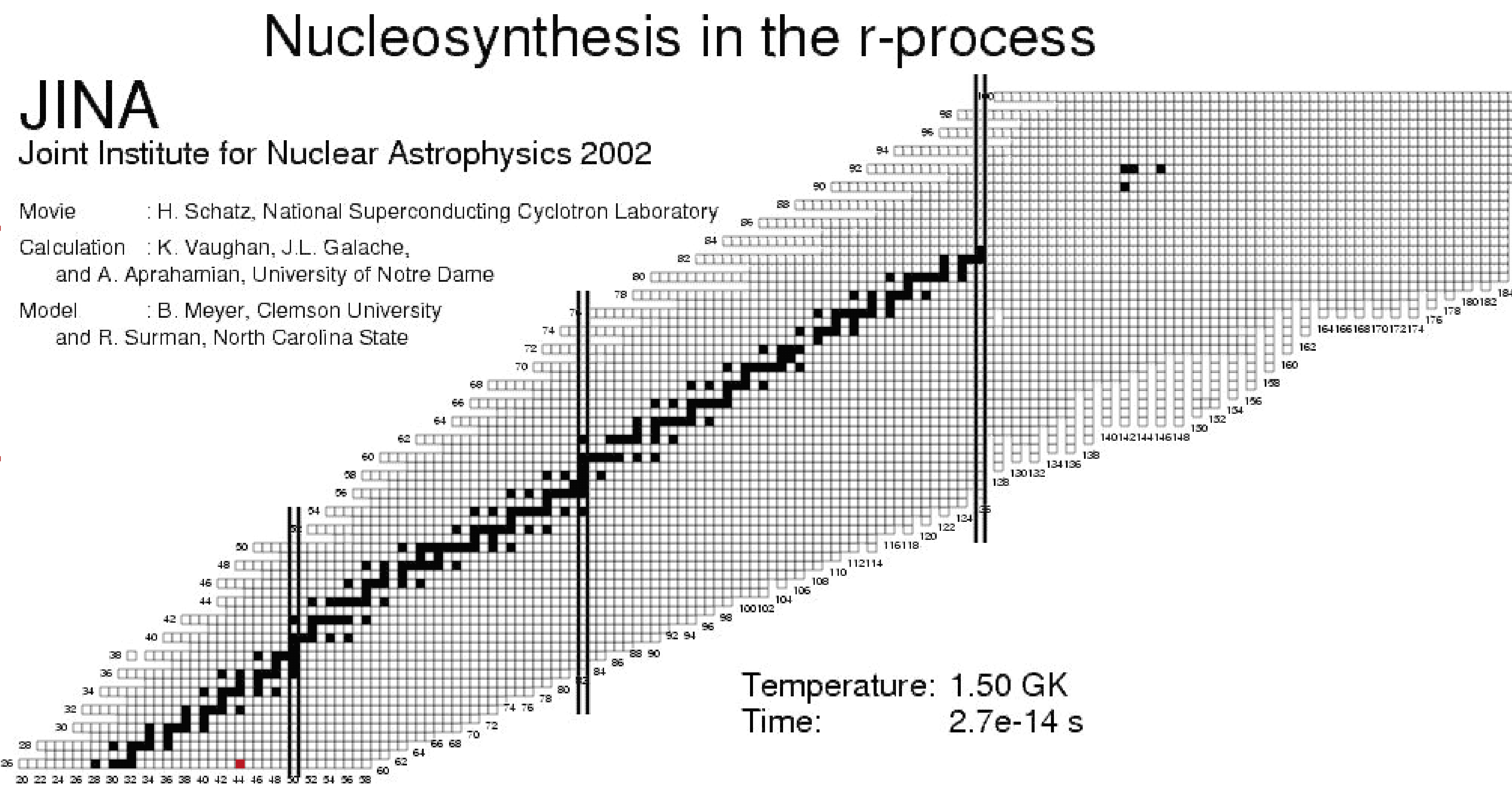

Masses
beta-decay half-lives

First experiment: r-process in the Ni region

Hosmer et al. PRL 94, 112501 (2005)

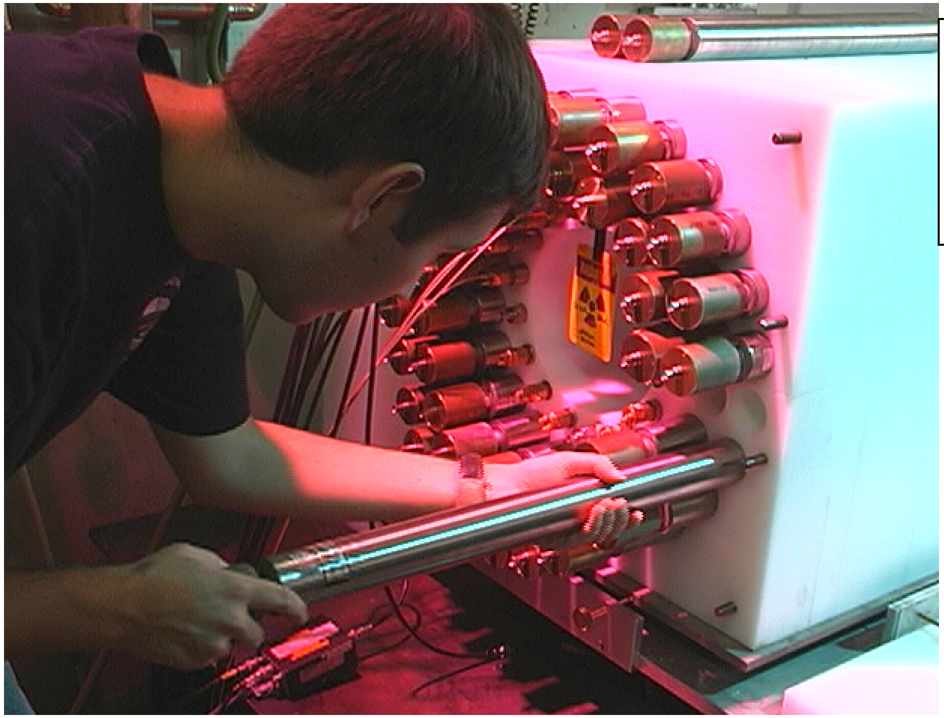

Measure:

- β-decay half-lives
- Branchings for β-delayed n-emission

Neutron detector
NERO

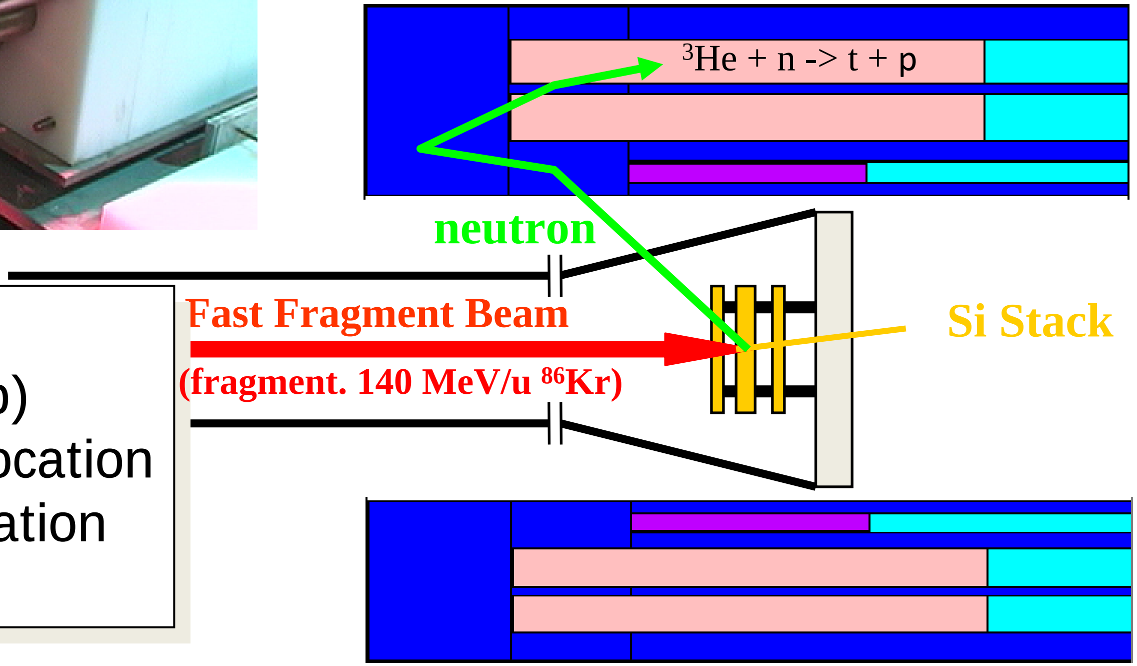

Detect:

- Particle type (TOF, dE, p)
- Implantation time and location
- β-emission time and location
- Neutron-β coincidences

Particle Identification:

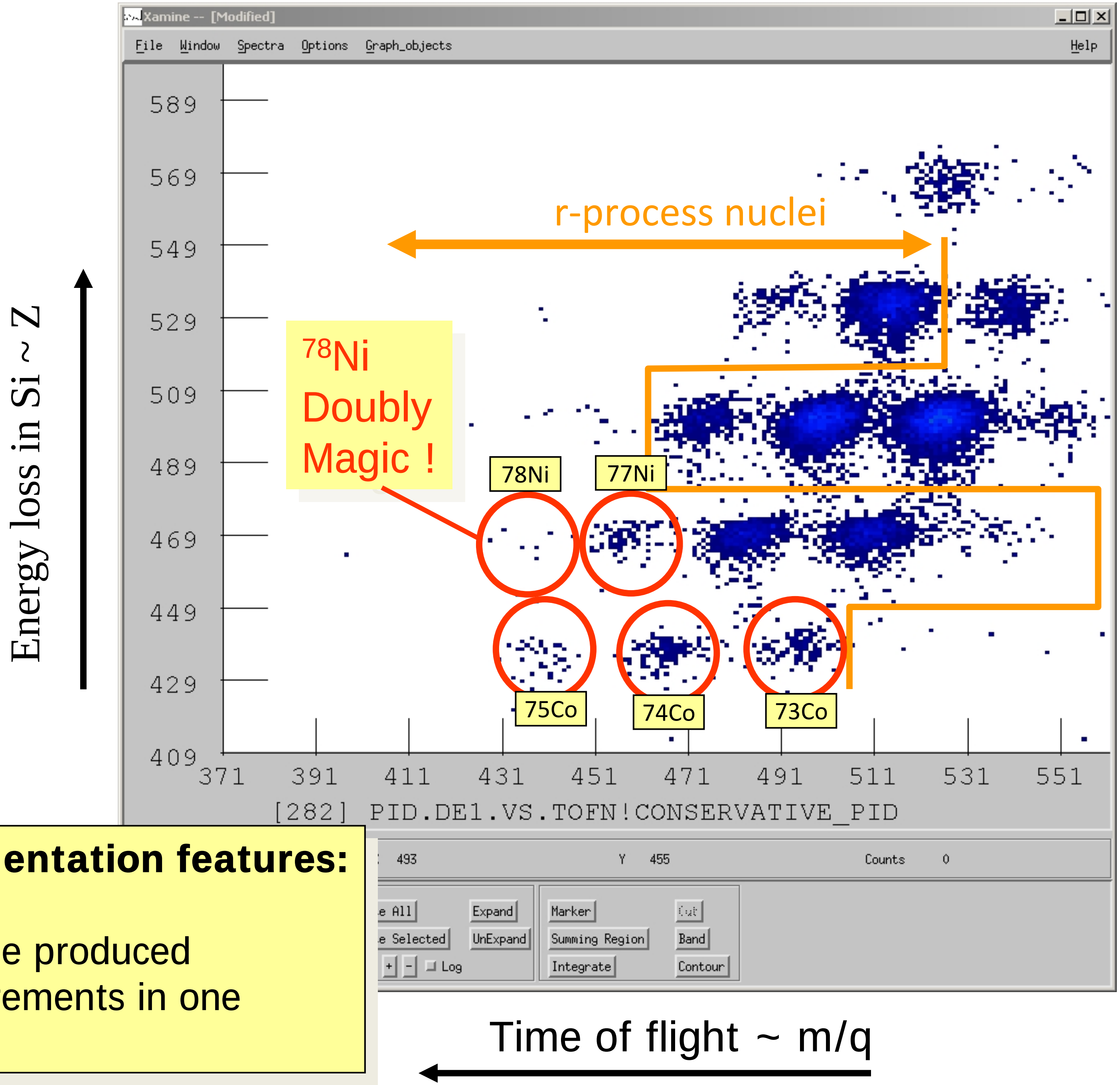

RIB from fragmentation features:

- no decay losses
- any beam can be produced
- multiple measurements in one
- high sensitivity

Impact of ^{78}Ni half-life on r-process models

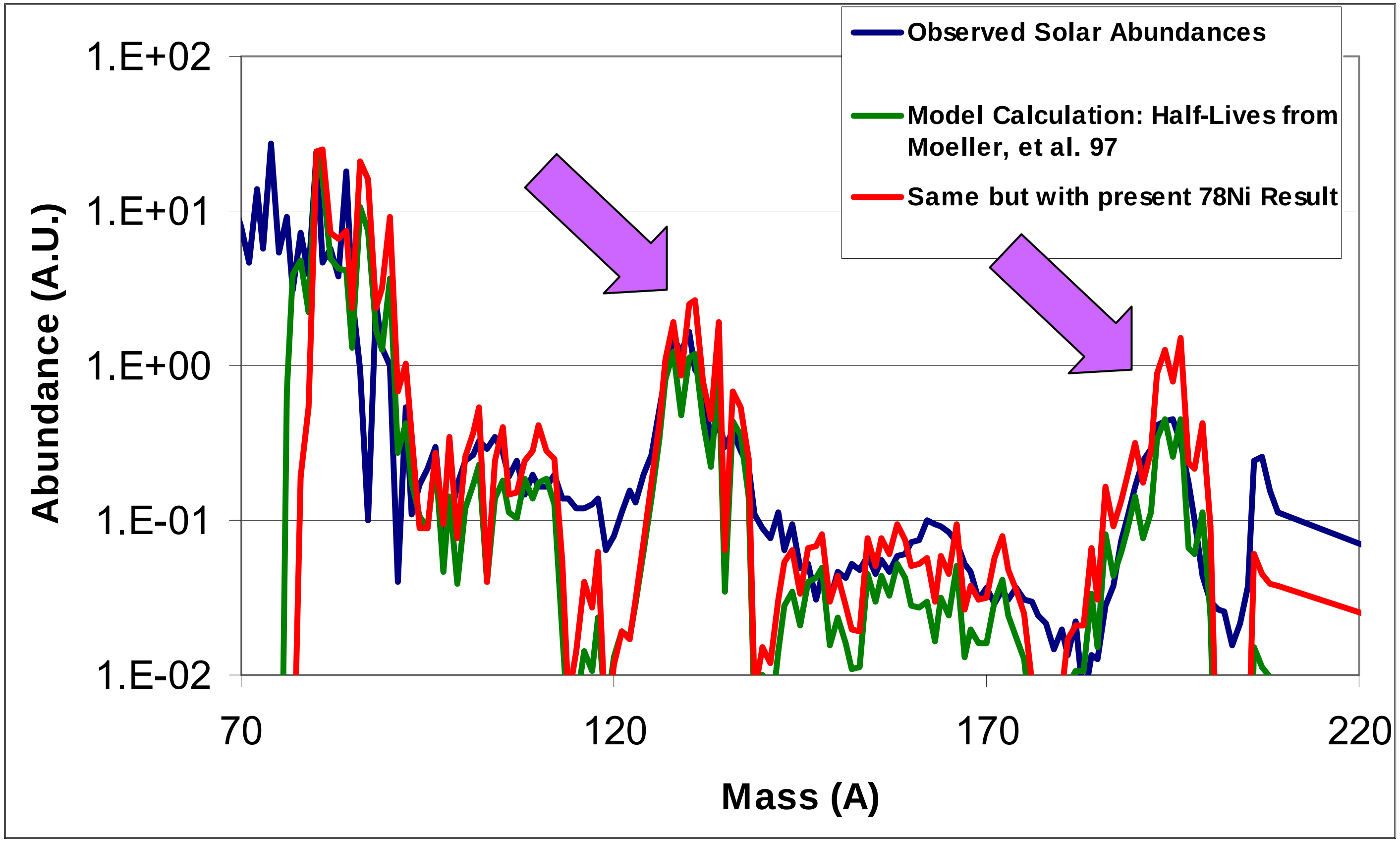

→need to readjust r-process model parameters

→Can obtain Experimental constraints for r-process models from observations and solid nuclear physics

N=56 subshell with Z=34???

Fragmentation of 120 MeV/u ^{136}Xe beam

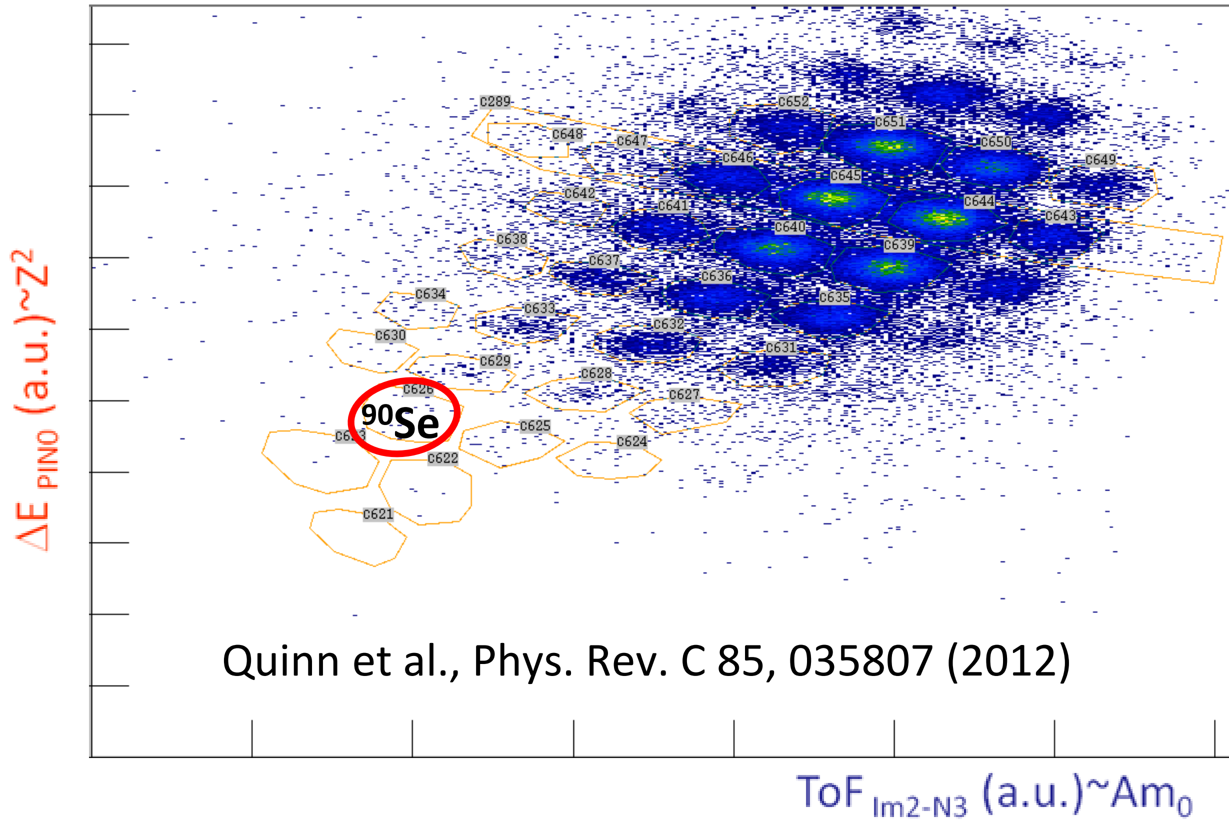

	Implantations		Maximum Likelihood Method (ms)
^{87}As	27	12	$1450(550)^{+3900}_{-1250}$
^{88}As	16	8	$200(10)^{+200}_{-90}$
^{88}Se	144	74	$650(35)^{+175}_{-140}$
^{89}Se	180	90	$345(25)^{+95}_{-80}$
^{90}Se	70	30	$195(10)^{+95}_{-65}$

Impact of ^{90}Se half-life on r-process models

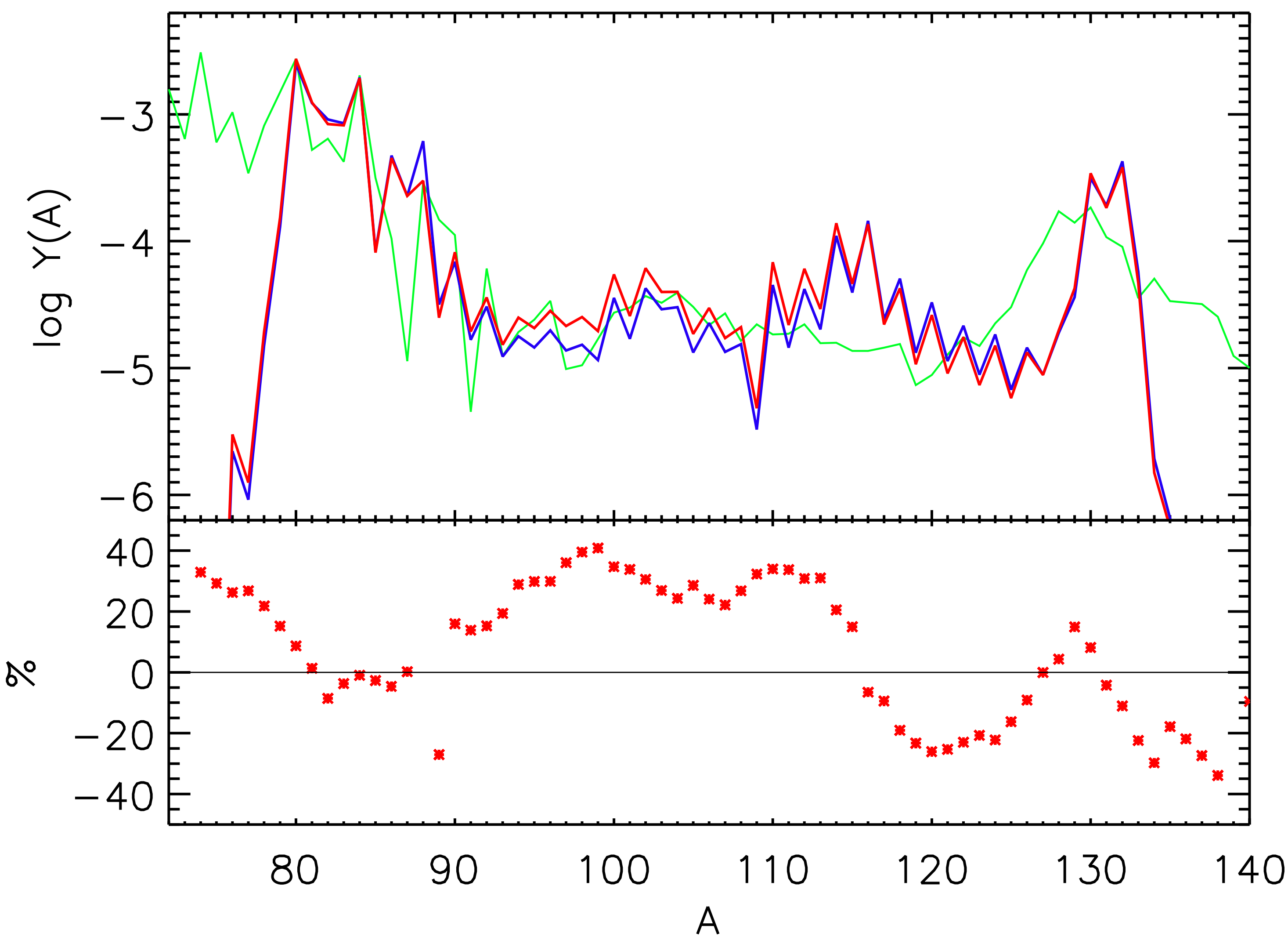

Quinn et al., Phys. Rev. C 85, 035807 (2012)

r-process sensitivities...masses

More quantitative approach to choosing to measure nuclei that would have the greatest impact on

What?

Brad Meyer code modified by R. Surman

various **mass models**-

FRDM, Duflo-Zuker, ETFSIQ, HFB-21, F-spin

Method:

Adjusted the separation energy of each nucleus ± 25%

(**3010 nuclei twice....**)

Calculated the max and fractional change from final abundances

What did we find?

Some consistent set of nuclei that are the most important to measure

So, What did we do?

Simulations….. Varied astrophysical conditions
varied seed nuclei
varied mass models

Input initial astrophysical conditions

Temperature/density
neutron/seed ratios
Freeze-out times

Input nuclear physics

masses
n-capture rates
beta decay half-lives
(fission recycling, alpha recycling, neutrino interactions off)

Why 25%

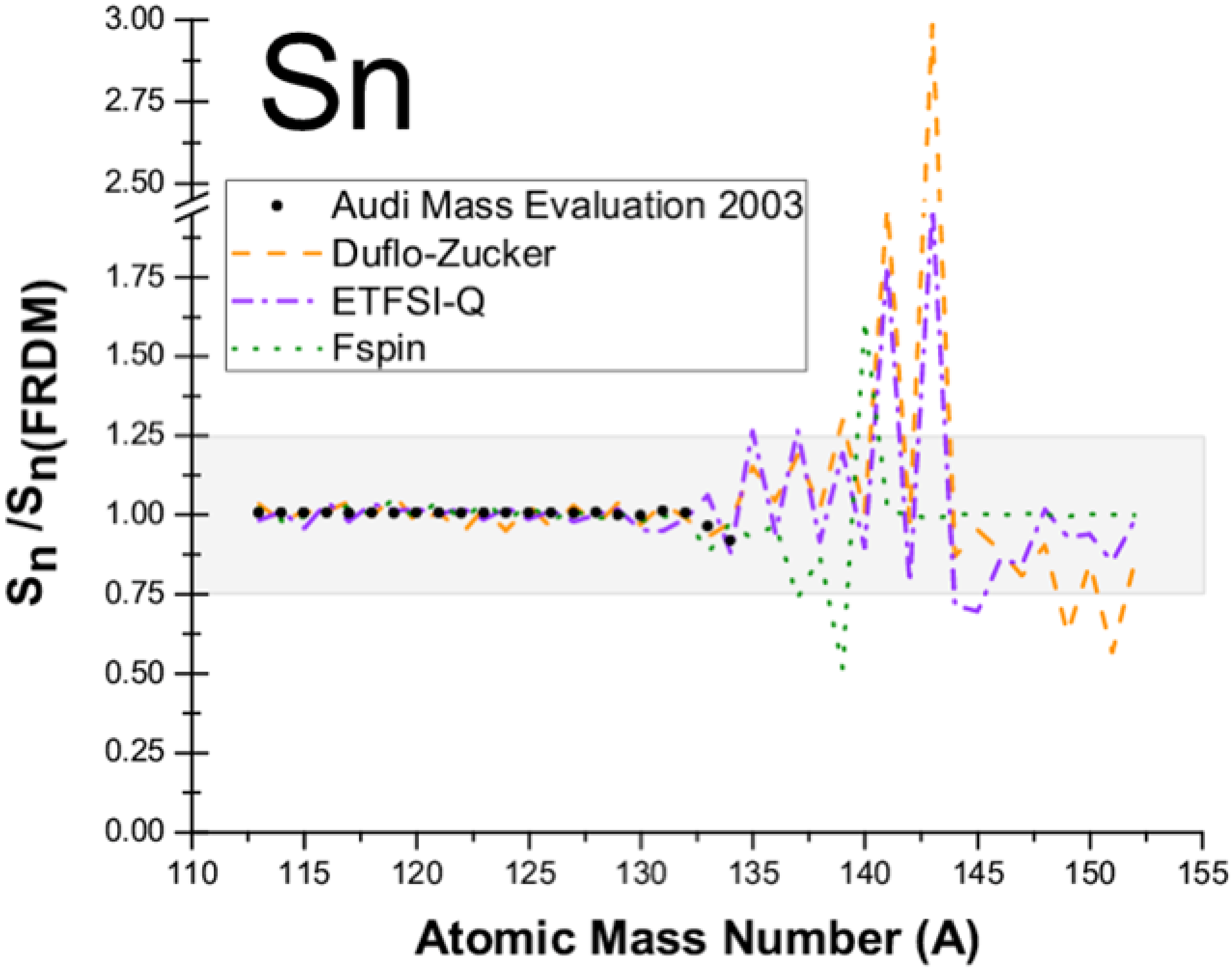
Sn
Audi Mass Evaluation 2003
Duflo-Zucker
ETFSI-Q
Fspin
S_n / S_n(FRDM)
Atomic Mass Number (A)
3.00
2.75
2.50
1.75
1.50
1.25
1.00
0.75
0.50
0.25
0.00
110
115
120
125
130
135
140
145
150
155

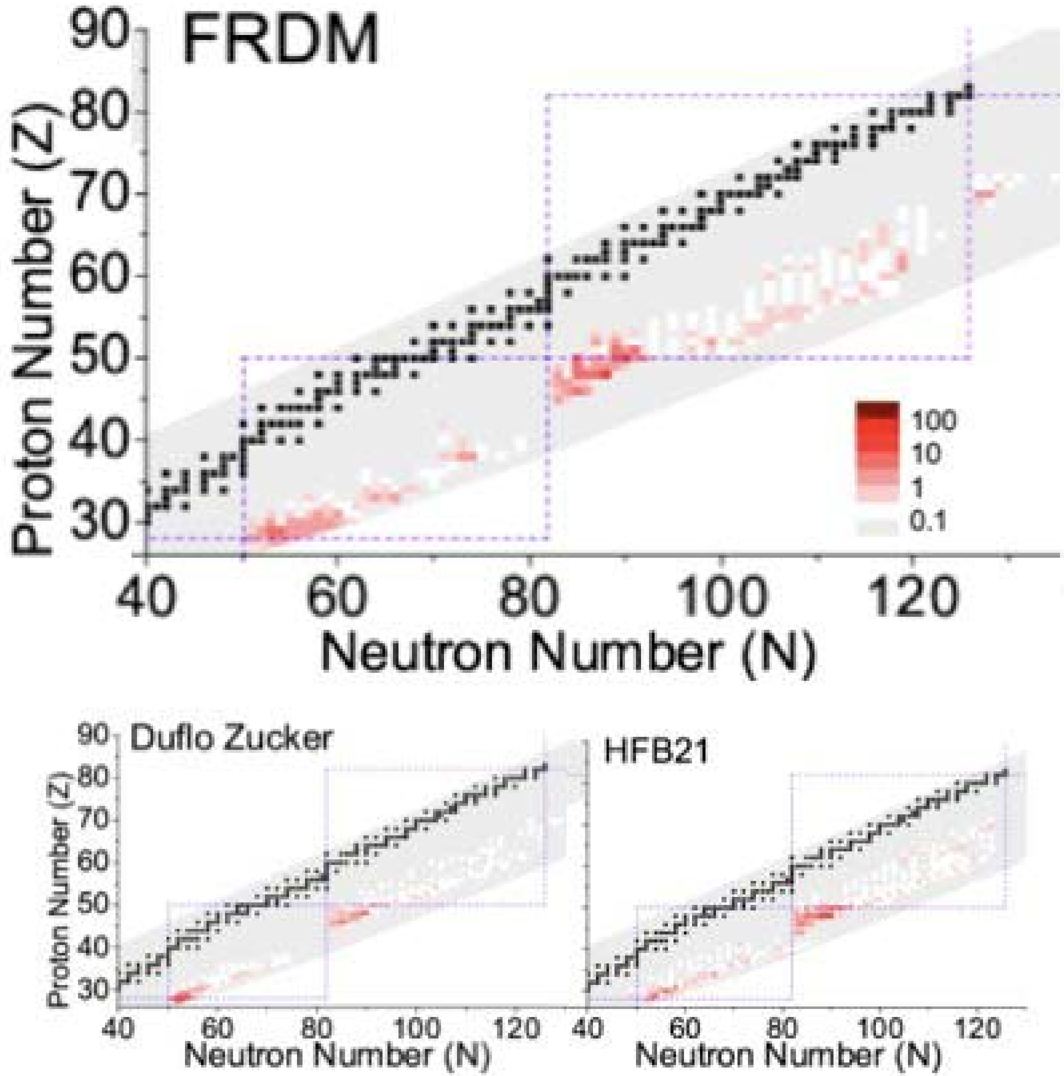

$$\Delta Y_{\pm 25\%}(N, Z) = \sum_{A} \left| Y(A) - Y(A, \pm\Delta S_n(N, Z)) \right|.$$

ΔY for FRDM

Nucleus	
^{136}Cd	20.2
^{140}Sn	12.1
^{135}Cd	8.80
^{83}Cu	8.42
^{139}Sn	8.19
^{142}Sb	5.64
^{135}Sn	5.44
^{133}Cd	5.38
^{140}Sb	5.25
^{134}Cd	5.23
^{82}Cu	4.14
^{134}In	4.14
^{131}Pd	3.29
^{137}Sn	2.94
^{141}Sn	2.91
^{83}Zn	2.89
^{85}Zn	2.71
^{85}Cu	2.66
^{130}Pd	2.39
^{132}Pd	2.39

ΔY for ETFSI-Q

Nucleus	
^{140}Sn	20.1
^{136}Cd	19.0
^{142}Sn	17.3
^{137}Cd	15.3
^{79}Ni	12.5
^{80}Ni	12.0
^{135}Cd	11.5
^{134}Cd	11.5
^{138}Cd	8.57
^{132}Pd	7.66
^{130}Pd	7.34
^{132}In	7.33
^{129}Pd	5.12
^{139}Sn	4.63
^{131}Pd	4.37
^{138}In	3.98
^{139}In	3.95
^{86}Zn	3.21
^{141}Sn	2.92
^{85}Zn	2.86

ΔY for DZ

Nucleus	
^{80}Ni	13.63
^{79}Ni	9.96
^{138}Cd	7.08
^{137}Cd	5.49
^{83}Cu	4.27
^{131}Pd	3.54
^{82}Cu	3.36
^{132}Pd	3.12
^{136}Cd	3.00
^{130}Pd	2.97
^{86}Zn	2.84
^{129}Pd	1.88
^{85}Zn	1.81
^{134}Ag	1.49
^{142}Sn	1.42
^{135}Ag	1.39
^{135}Cd	1.36
^{133}Cd	1.10
^{141}Sn	1.08
^{144}Sn	1.07

- The same isotopes are present in each evaluation:
  - Sn, Sb, and In,
  - Cd,
  - Pd,
  - Cu, Zn, and Ni.

What about β-decay rates?

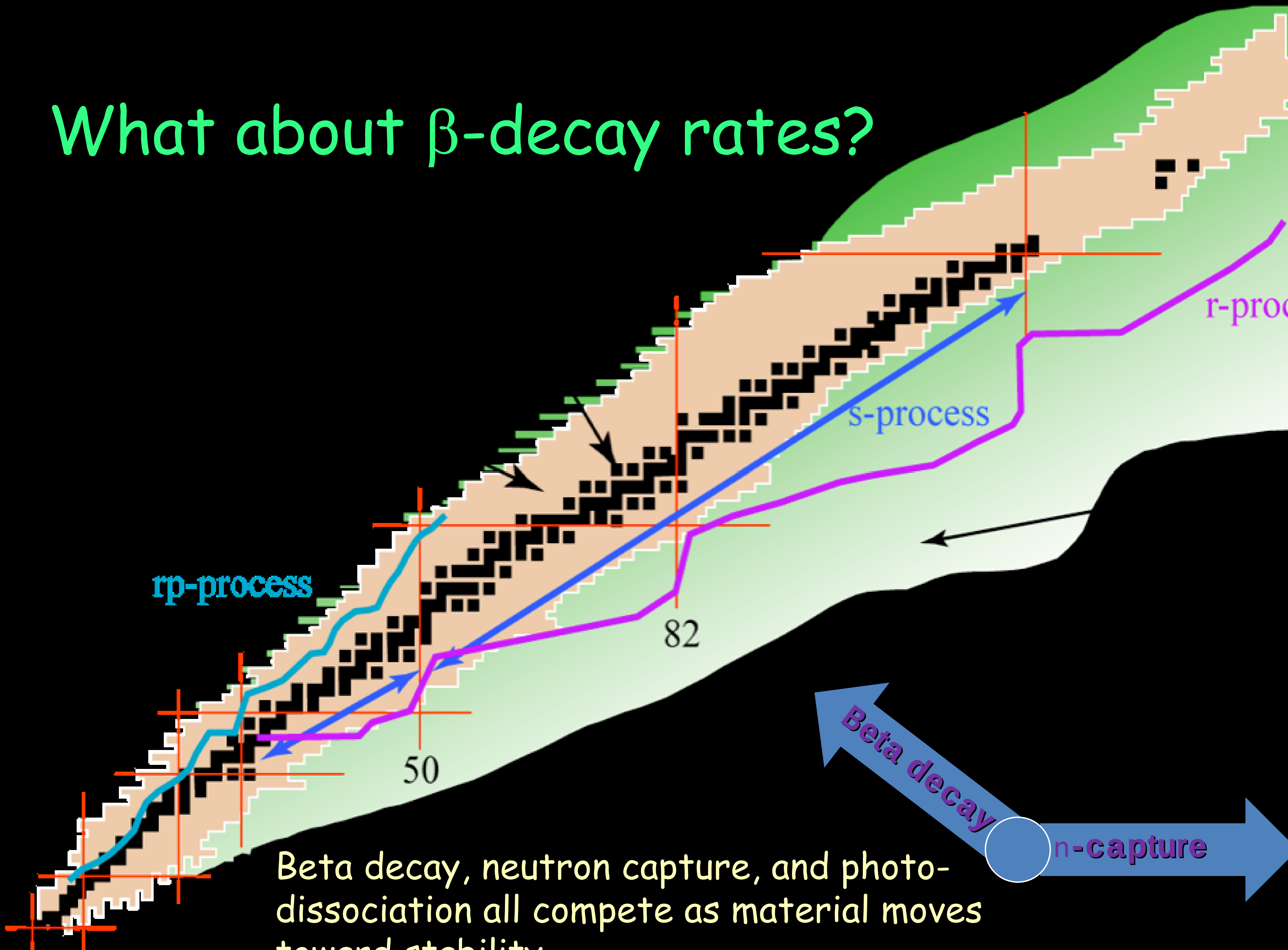

Beta decay, neutron capture, and photo-dissociation all compete as material moves toward stability

So, What are we doing?

Simulations….. Varied astrophysical conditions
varied seed nuclei
varied mass models
varied beta-decay rates

Input initial astrophysical conditions

Temperature/density
neutron/seed ratios
Freeze-out times

Input nuclear physics

masses
n-capture rates
beta decay half-lives
(fission recycling, alpha recycling, neutrino interactions off)

r-process sensitivities…beta-decay rates

J. Cass, G. Passucci, R. Surman, A. Aprahamian

To start…

Vary one beta decay rate by an order of magnitude, rerun the simulation, and compare the final abundance pattern to the baseline

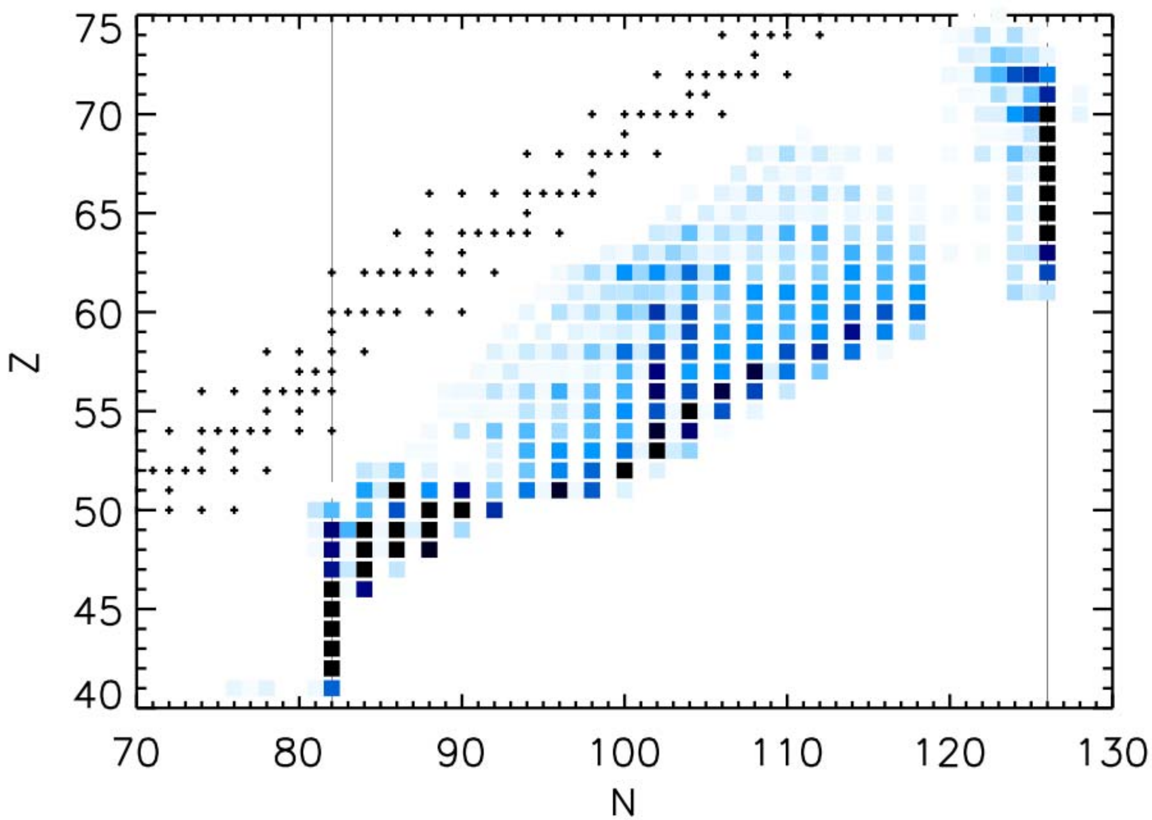

White to black = 0-10% change in the final abundance patterns

Beta decay rate sensitivity study

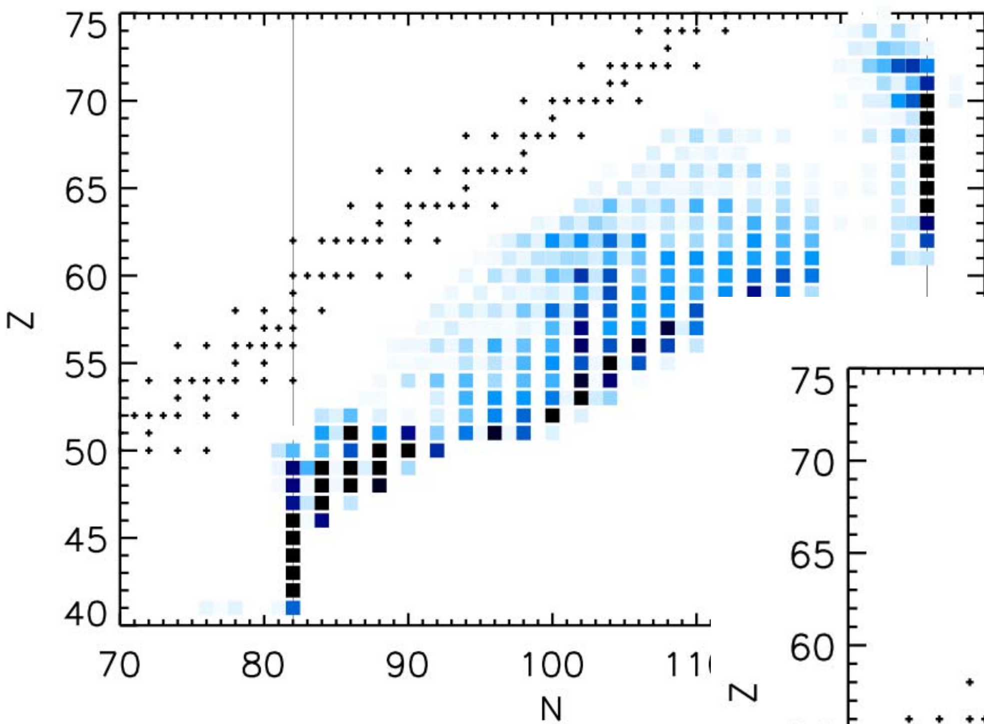

hot r-process

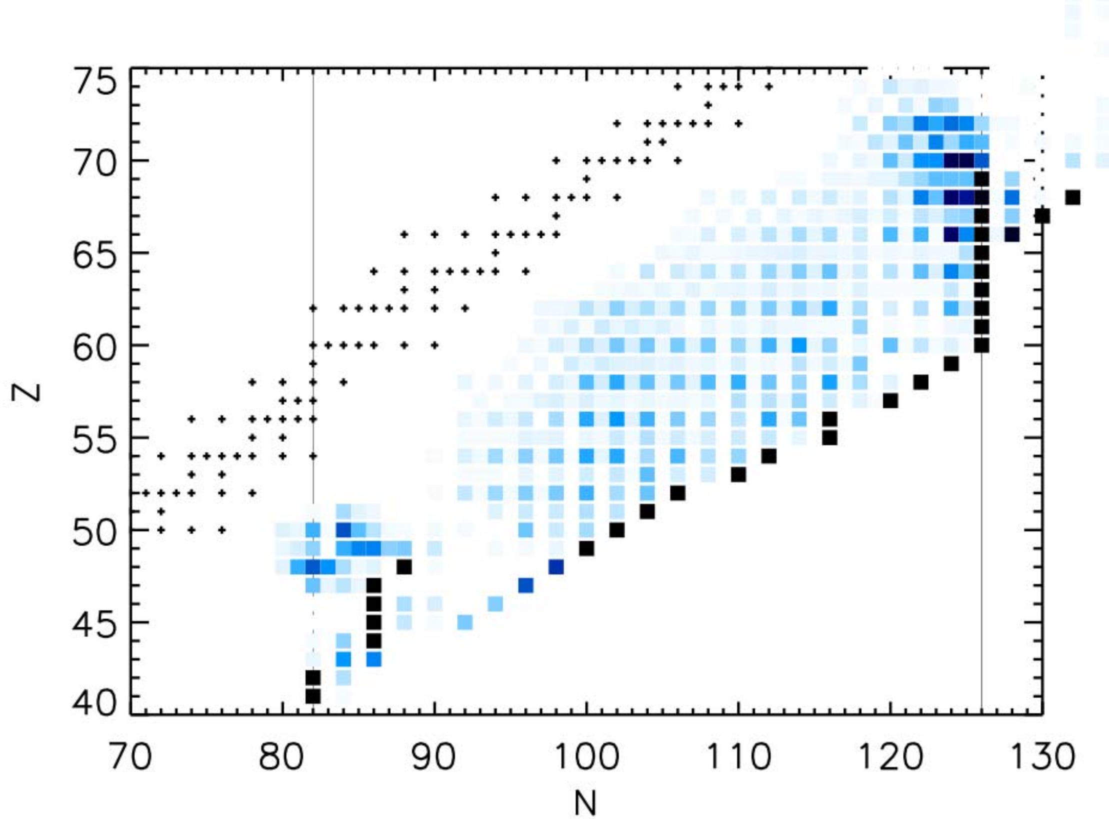

cold r-process

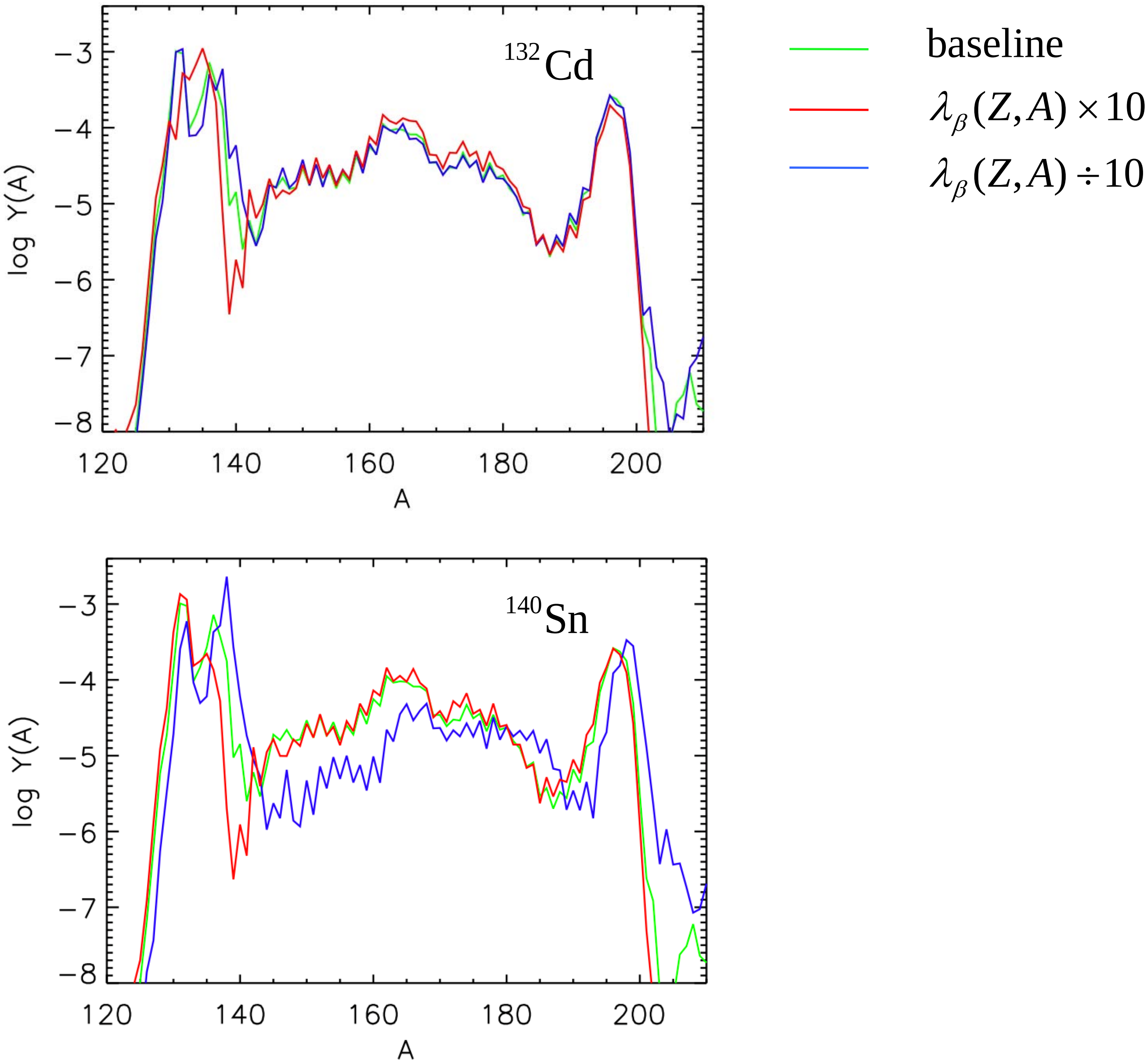

^{132}Cd
^{140}Sn
log Y(A)
A
−3
−4
−5
−6
−7
−8
120
140
160
180
200
baseline
$\lambda_\beta(Z,A)\times 10$
$\lambda_\beta(Z,A)\div 10$

conclusions

We have carried out the first quantitative/comprehensive sensitivity study of an r-process simulation to masses, beta decay rates, neutron capture cross sections.

- we varied mass models
- we varied decay rates
- consistent set of nuclei that we

Sensitivity Study Masses

Samuel Brett

Ian Bentley

Nancy Paul

Rebecca Surman

A^2

Sensitivity Study β-decay rates

Julie Cass

Giuseppe Passucci

Rebecca Surman

A^2

COLLABORATORS (Experiment)

Notre Dame

Mathew Quinn

Andreas Woehr

Sergio Almaraz

Boris Skorodumov

A^2

MSU

Jorge Pereira

Paul Mantica

Hendrik Schatz

Ana Becerril

Thom Elliot

Alfredo Estrade

Daniel Galaviz

Giuseppe Lorusso

Milan Matos

Fernando Montes

Mainz

Stefan Hennrich

Karl-Ludwig Kratz

Bernd Pfeiffer

Ruben Kessler

Florian Schertz

Univ. of Maryland

W. Walters

The role of neutron separation energies in a hot *r*-process

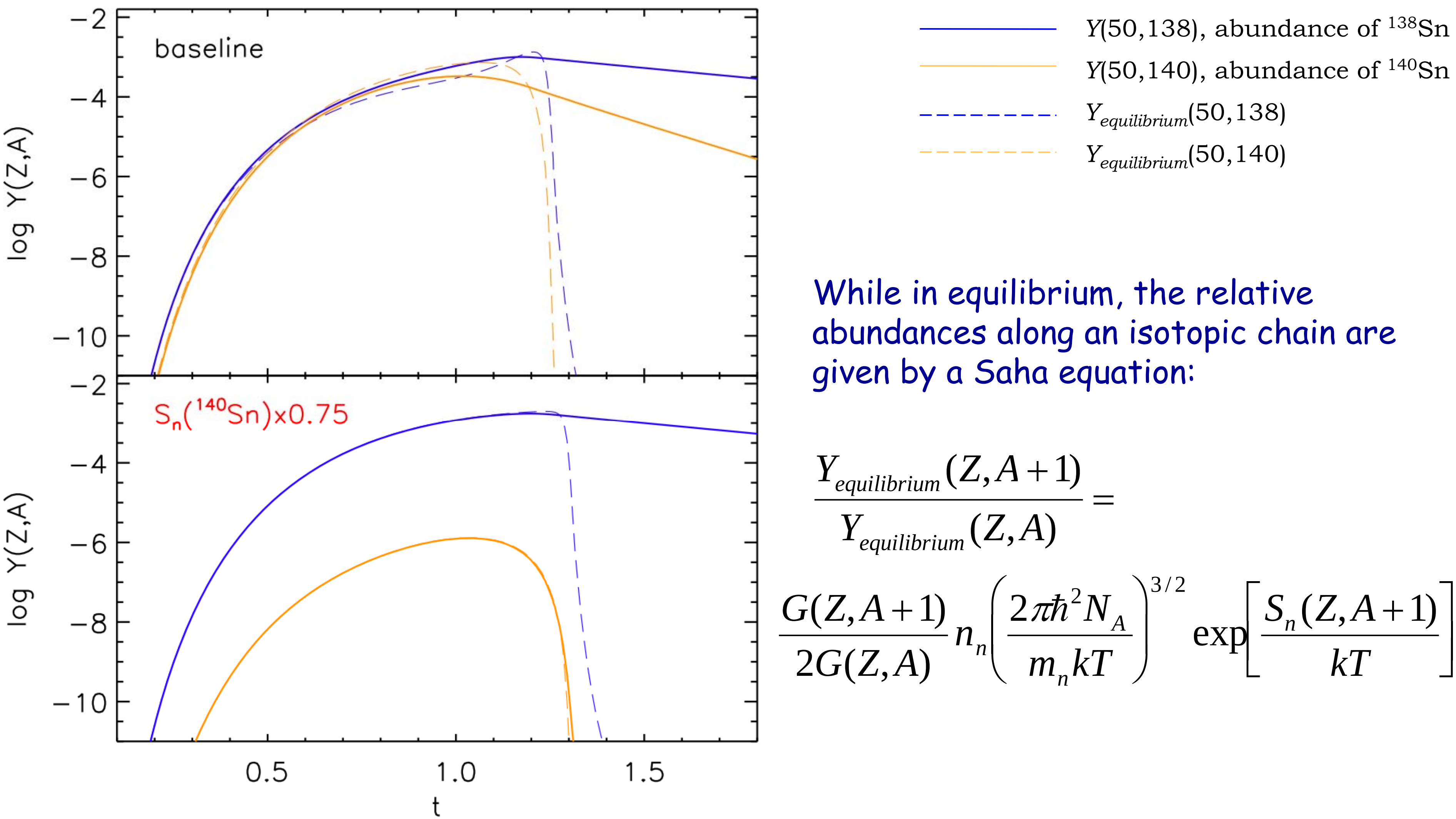

While in equilibrium, the relative abundances along an isotopic chain are given by a Saha equation:

$$\frac{Y_{equilibrium}(Z,A+1)}{Y_{equilibrium}(Z,A)} = \frac{G(Z,A+1)}{2G(Z,A)} n_n \left(\frac{2\pi\hbar^2 N_A}{m_n kT}\right)^{3/2} \exp\left[\frac{S_n(Z,A+1)}{kT}\right]$$

ΔY for FRDM

Nucleus	
^{136}Cd	20.2
^{140}Sn	12.1
^{135}Cd	8.80
^{83}Cu	8.42
^{139}Sn	8.19
^{142}Sb	5.64
^{135}Sn	5.44
^{133}Cd	5.38
^{140}Sb	5.25
^{134}Cd	5.23
^{82}Cu	4.14
^{134}In	4.14
^{131}Pd	3.29
^{137}Sn	2.94
^{141}Sn	2.91
^{83}Zn	2.89
^{85}Zn	2.71
^{85}Cu	2.66
^{130}Pd	2.39
^{132}Pd	2.39

ΔY for ETFSI-Q

Nucleus	
^{140}Sn	20.1
^{136}Cd	19.0
^{142}Sn	17.3
^{137}Cd	15.3
^{79}Ni	12.5
^{80}Ni	12.0
^{135}Cd	11.5
^{134}Cd	11.5
^{138}Cd	8.57
^{132}Pd	7.66
^{130}Pd	7.34
^{132}In	7.33
^{129}Pd	5.12
^{139}Sn	4.63
^{131}Pd	4.37
^{138}In	3.98
^{139}In	3.95
^{86}Zn	3.21
^{141}Sn	2.92
^{85}Zn	2.86

ΔY for DZ

Nucleus	
^{80}Ni	13.63
^{79}Ni	9.96
^{138}Cd	7.08
^{137}Cd	5.49
^{83}Cu	4.27
^{131}Pd	3.54
^{82}Cu	3.36
^{132}Pd	3.12
^{136}Cd	3.00
^{130}Pd	2.97
^{86}Zn	2.84
^{129}Pd	1.88
^{85}Zn	1.81
^{134}Ag	1.49
^{142}Sn	1.42
^{135}Ag	1.39
^{135}Cd	1.36
^{133}Cd	1.10
^{141}Sn	1.08
^{144}Sn	1.07

- The same isotopes are present in each evaluation:
  - Sn, Sb, and In,
  - Cd,
  - Pd,
  - Cu, Zn, and Ni.

CARIBU possibilities

^{130}In	10^4	900
$^{133\text{-}134}$Sn	10^4	10^3
$^{128\text{-}136}$Sb		
$^{113\text{-}119}$Pd		
$^{120\text{-}121}$Ag		

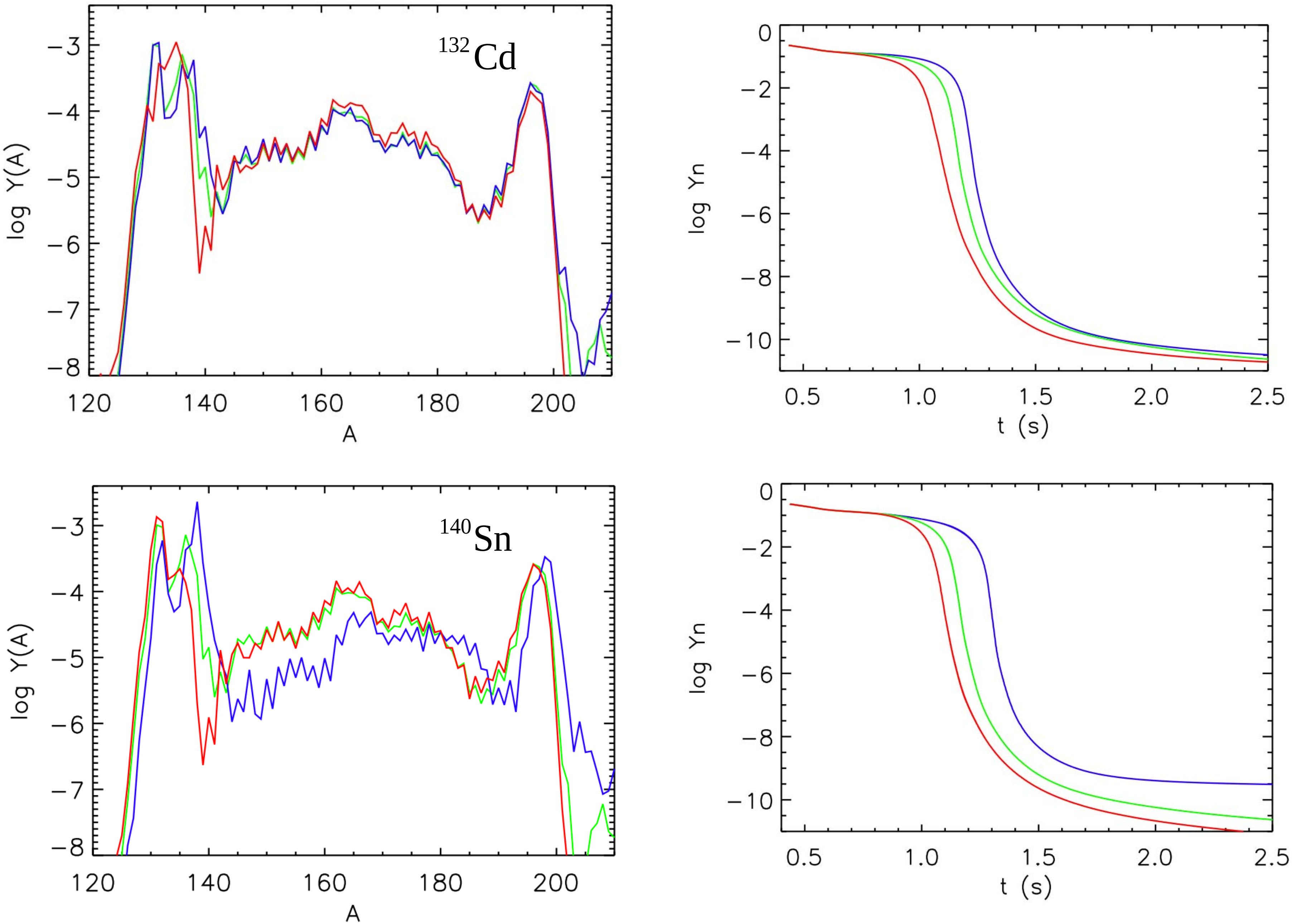

132Cd
log Y(A)
A
log Yn
t (s)
140Sn
log Y(A)
A
log Yn
t (s)

Why 25%

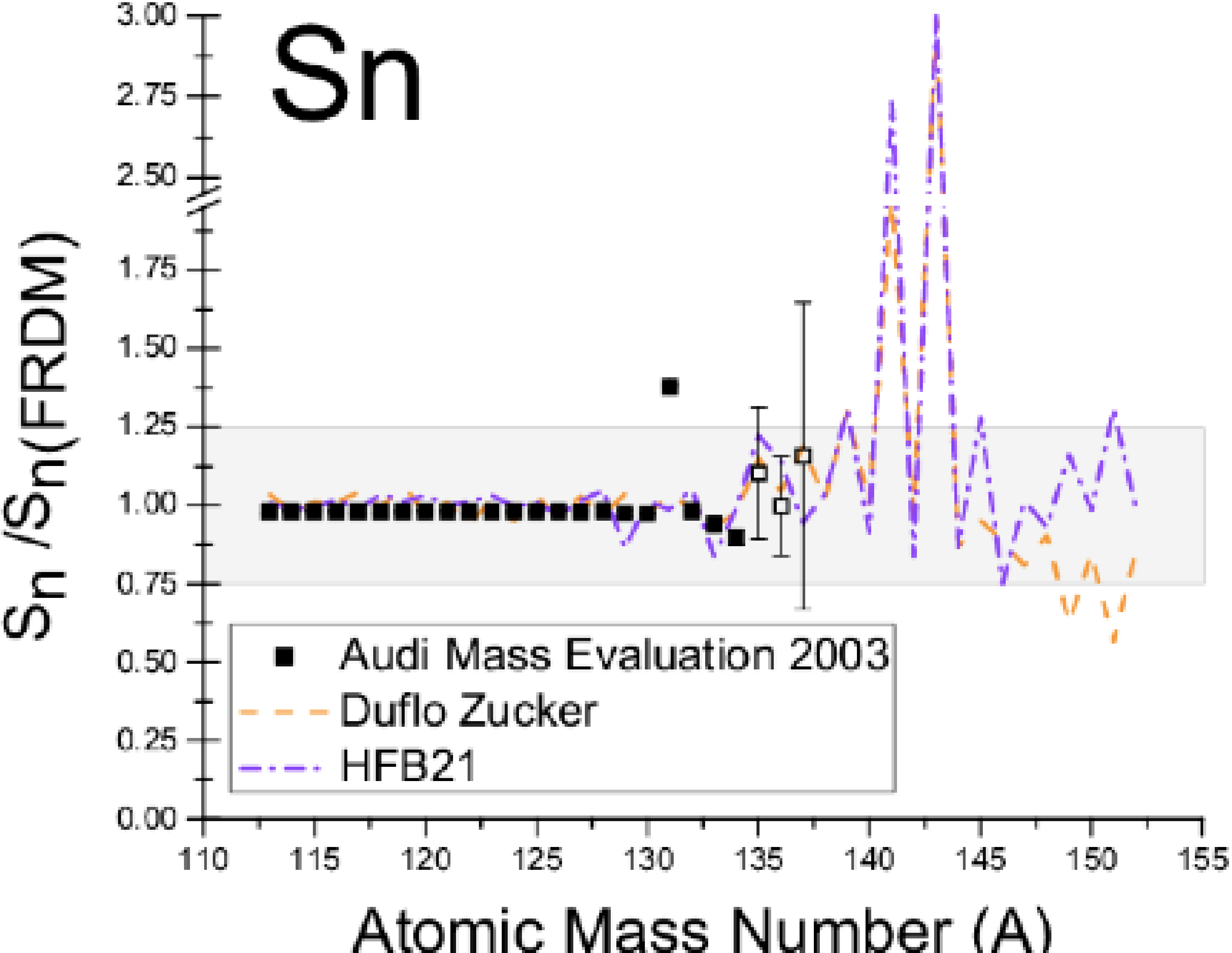
Sn
3.00
2.75
2.50
1.75
1.50
1.25
1.00
0.75
0.50
0.25
0.00
S_n / S_n(FRDM)
Audi Mass Evaluation 2003
Duflo Zucker
HFB21
110
115
120
125
130
135
140
145
150
155
Atomic Mass Number (A)

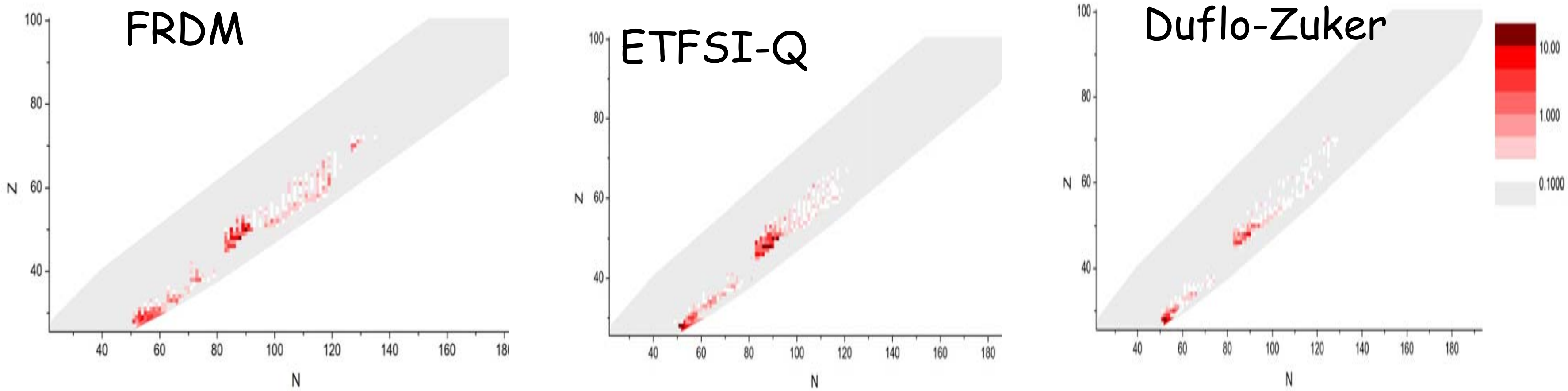

$$\Delta Y_{\pm 25\%}(N,Z) = \sum_{A} |Y(A) - Y(A, \pm\Delta S_n(N,Z))|.$$

Absolute differences

Heavy Ion Accelerator at Notre Dame

Sta. ANA: Stable beam **A**ccelerator for **N**uclear **A**strophysics

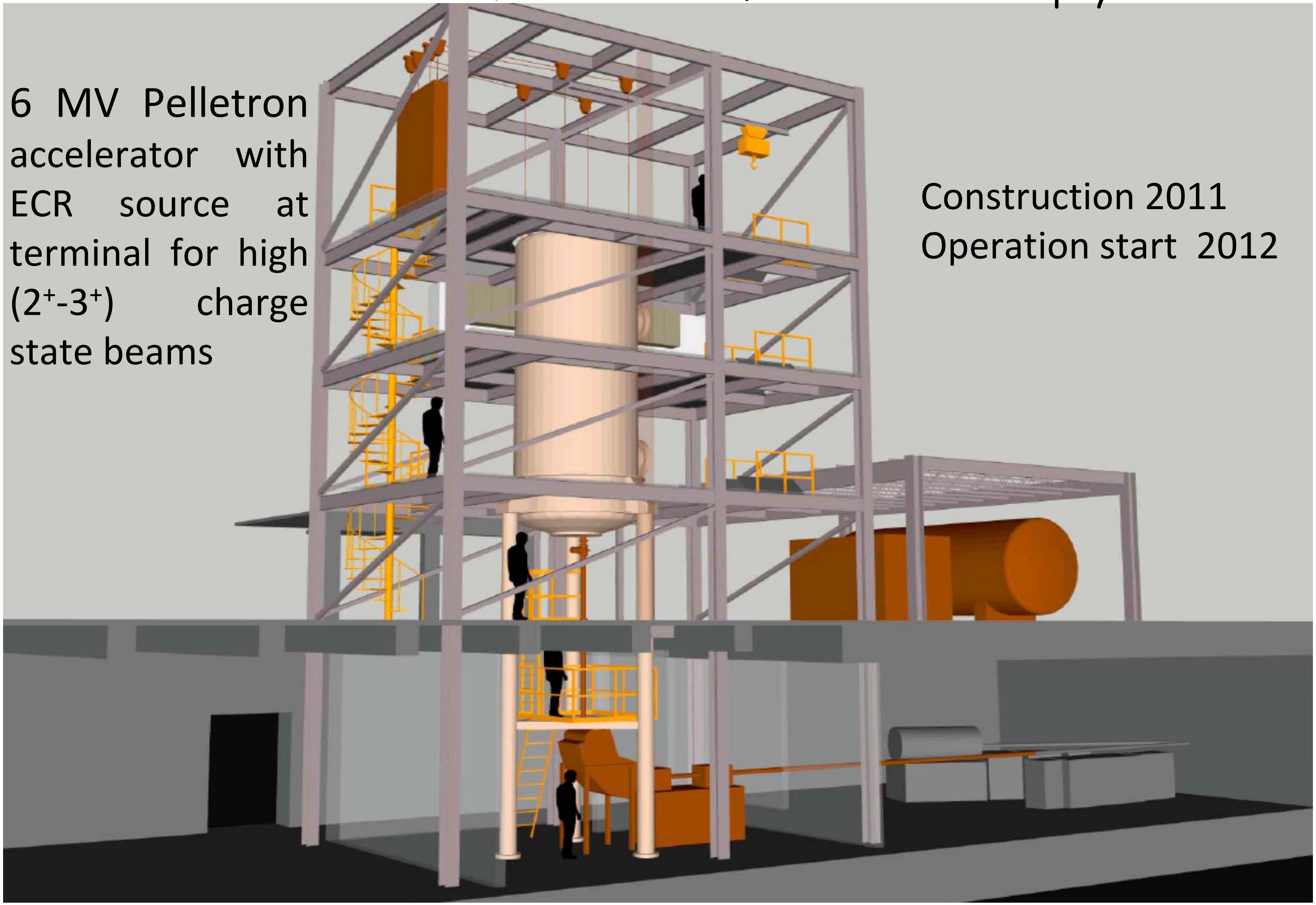

6 MV Pelletron accelerator with ECR source at terminal for high (2^+-3^+) charge state beams

Construction 2011
Operation start 2012

Delivery of Sta. ANA






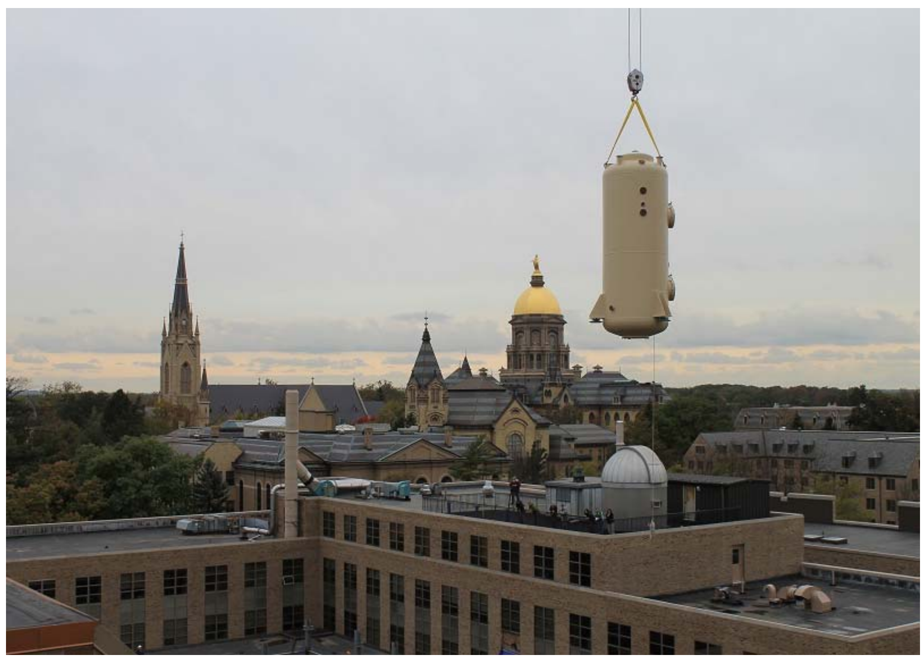


RIKEN, Japan (2008)

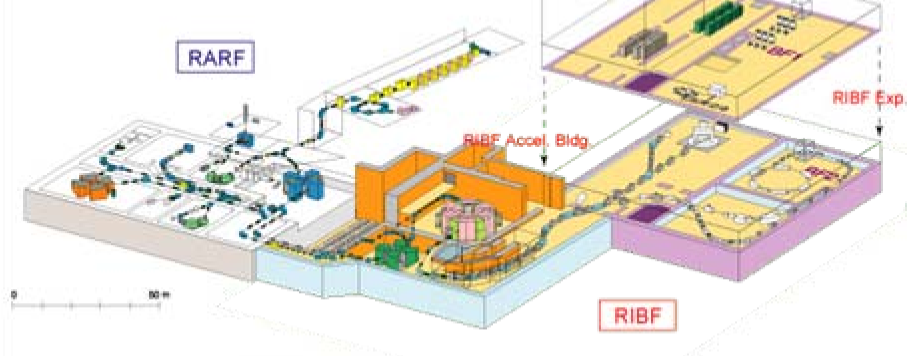

GSI/FAIR Germany (2017)

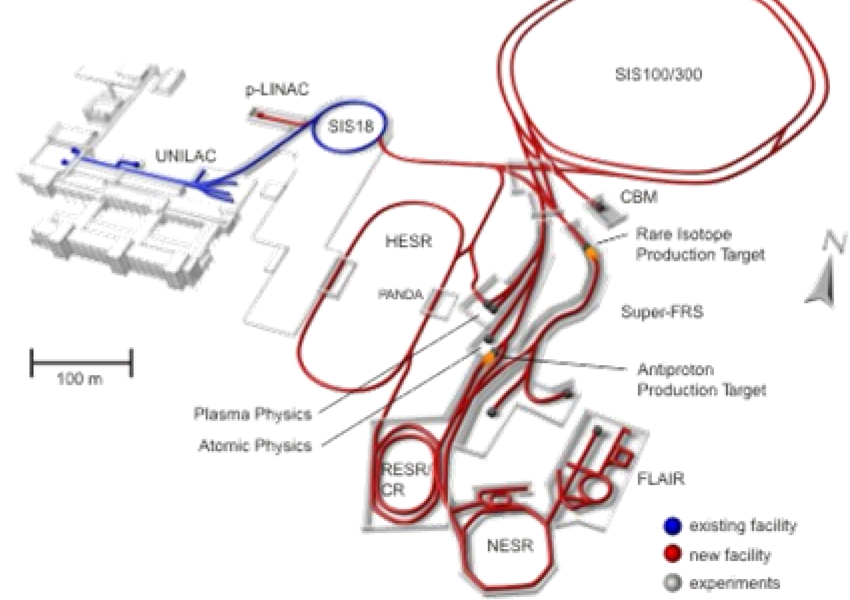

GANIL, France (2013)

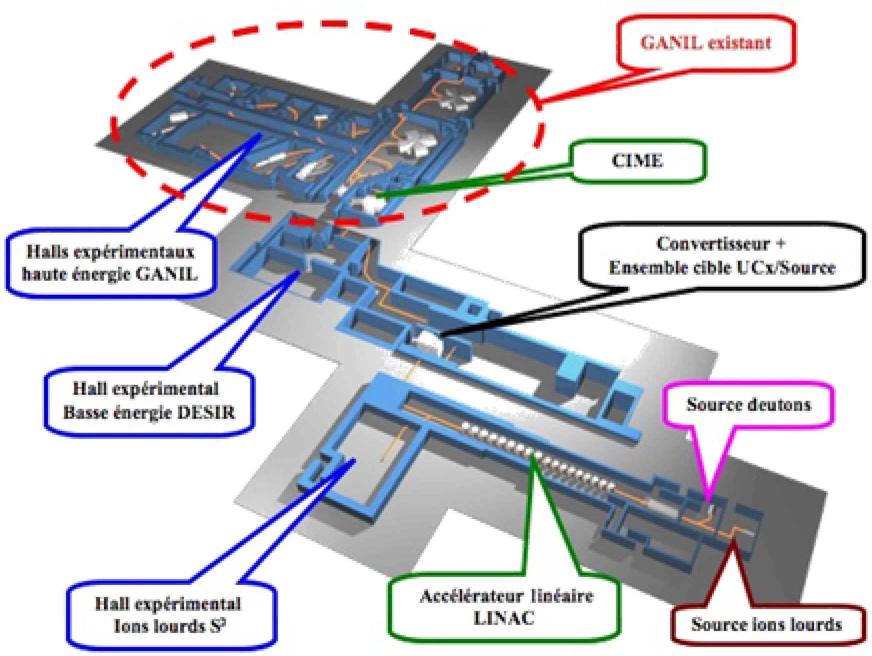

FRIB at NSCL/MSU (2018)

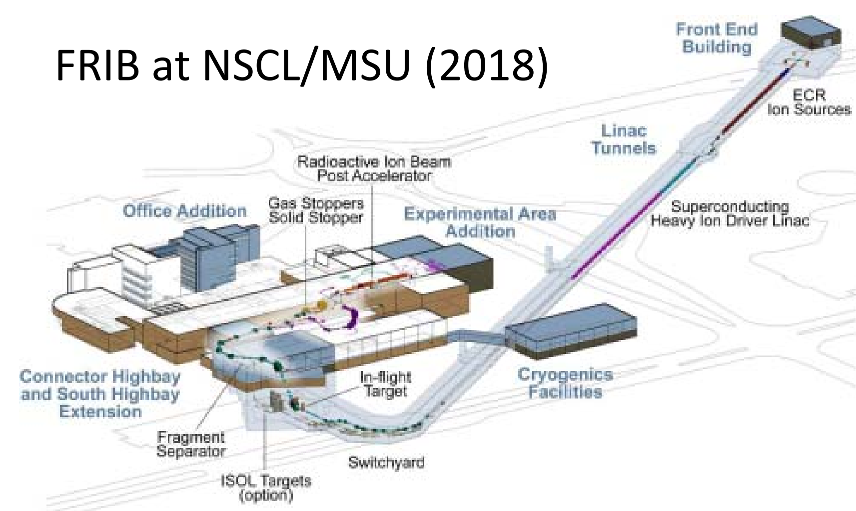

Elemental history of the universe

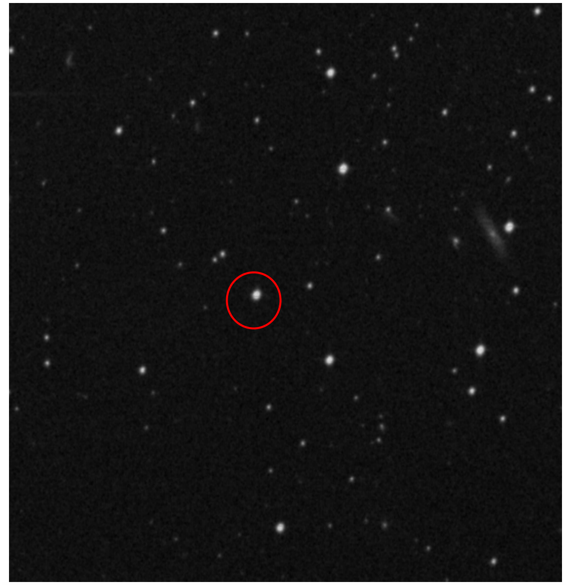

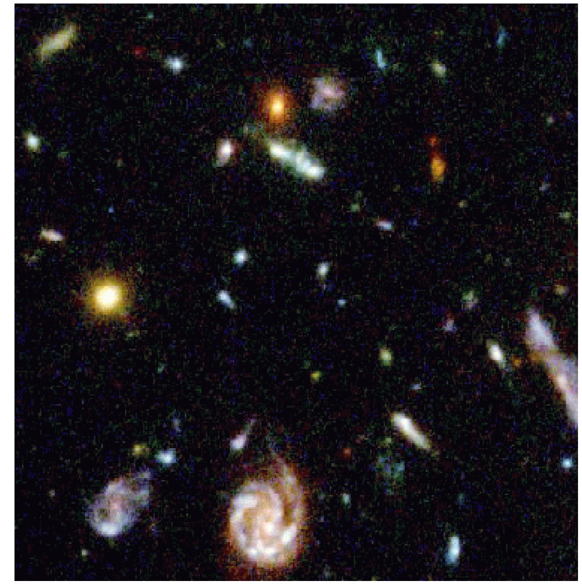

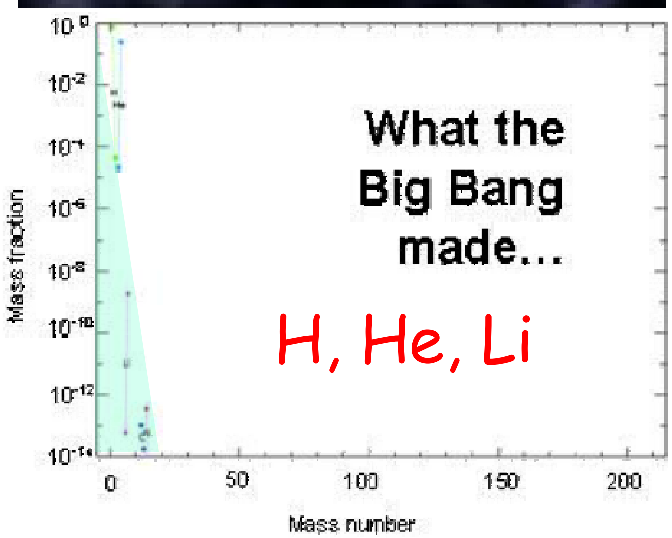

(The primordial abundance pattern)
Brian Fields (2002)

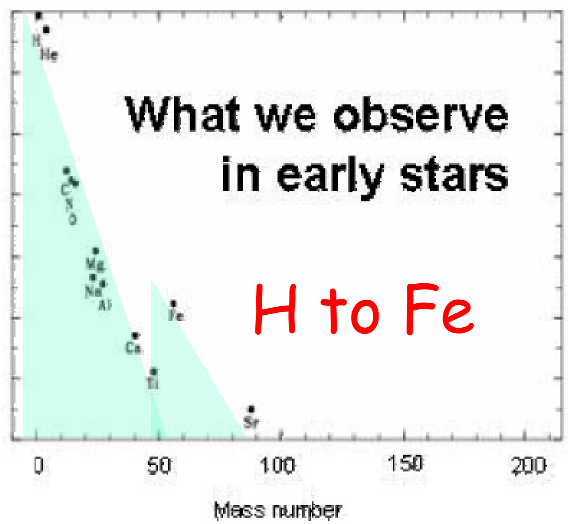

(The abundance pattern in the oldest observed stars He1017 & HH1327)
Anna Frebel (2006)

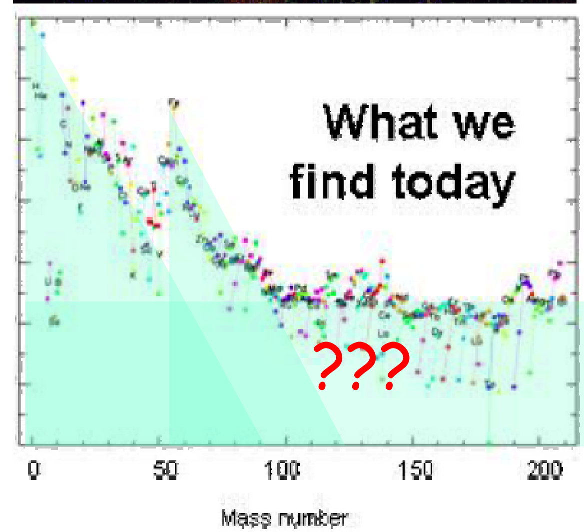

(The solar abundance pattern)
Grevesse & Noels (1995)

Hot r-process: (n,γ)-(γ,n) equilibrium

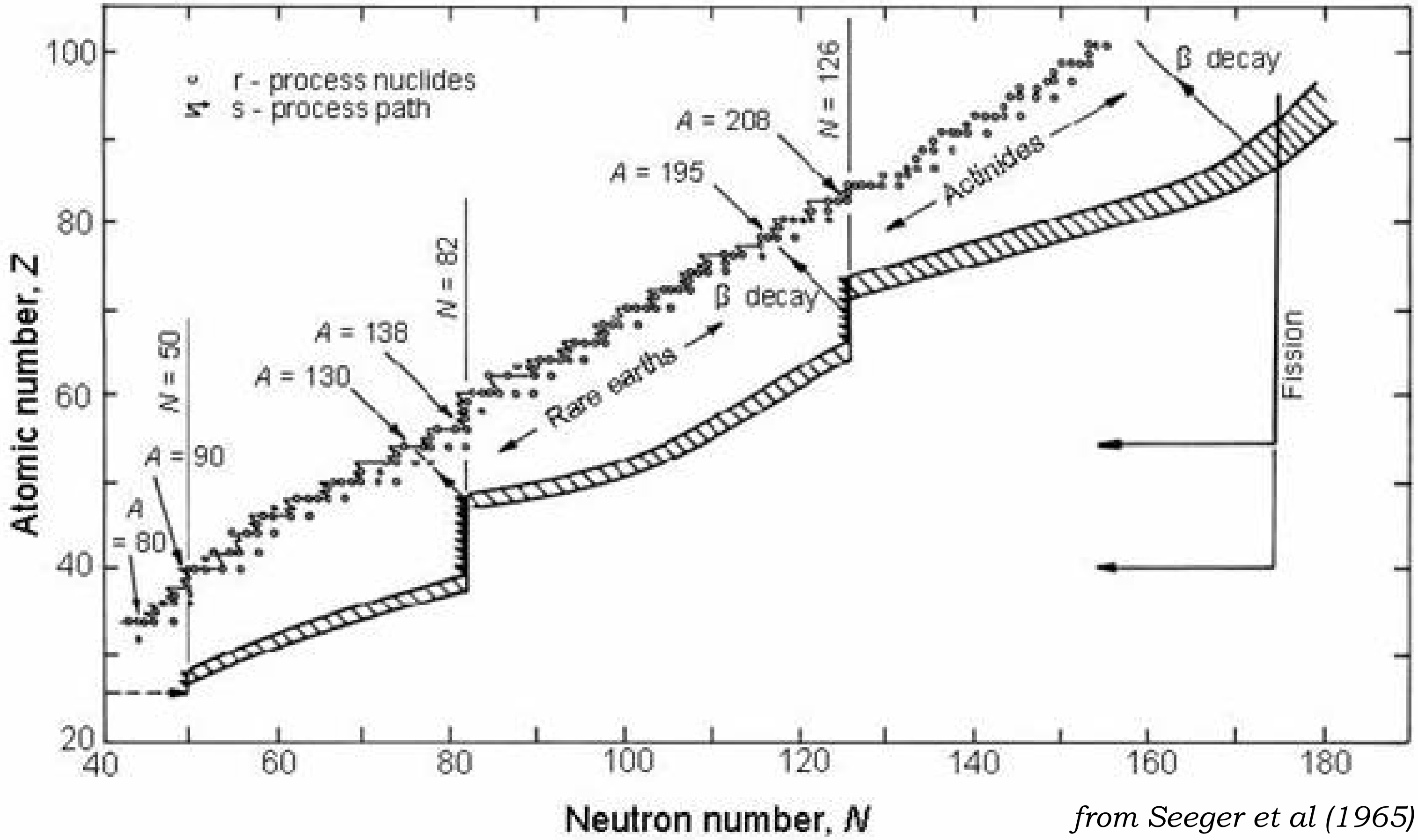

from Seeger et al (1965)

$$S_n(Z,A_{path}) \sim -kT \ln\left\{ \frac{n_n}{2} \left(\frac{2\pi\hbar^2}{m_n kT} \right)^{3/2} \right\}$$

$$S_n(Z,A) = B.E.(Z,A) - B.E.(Z,A-1)$$

n_n neutron number density

T temperature

Hot r-process: (n,γ)-(γ,n) equilibrium

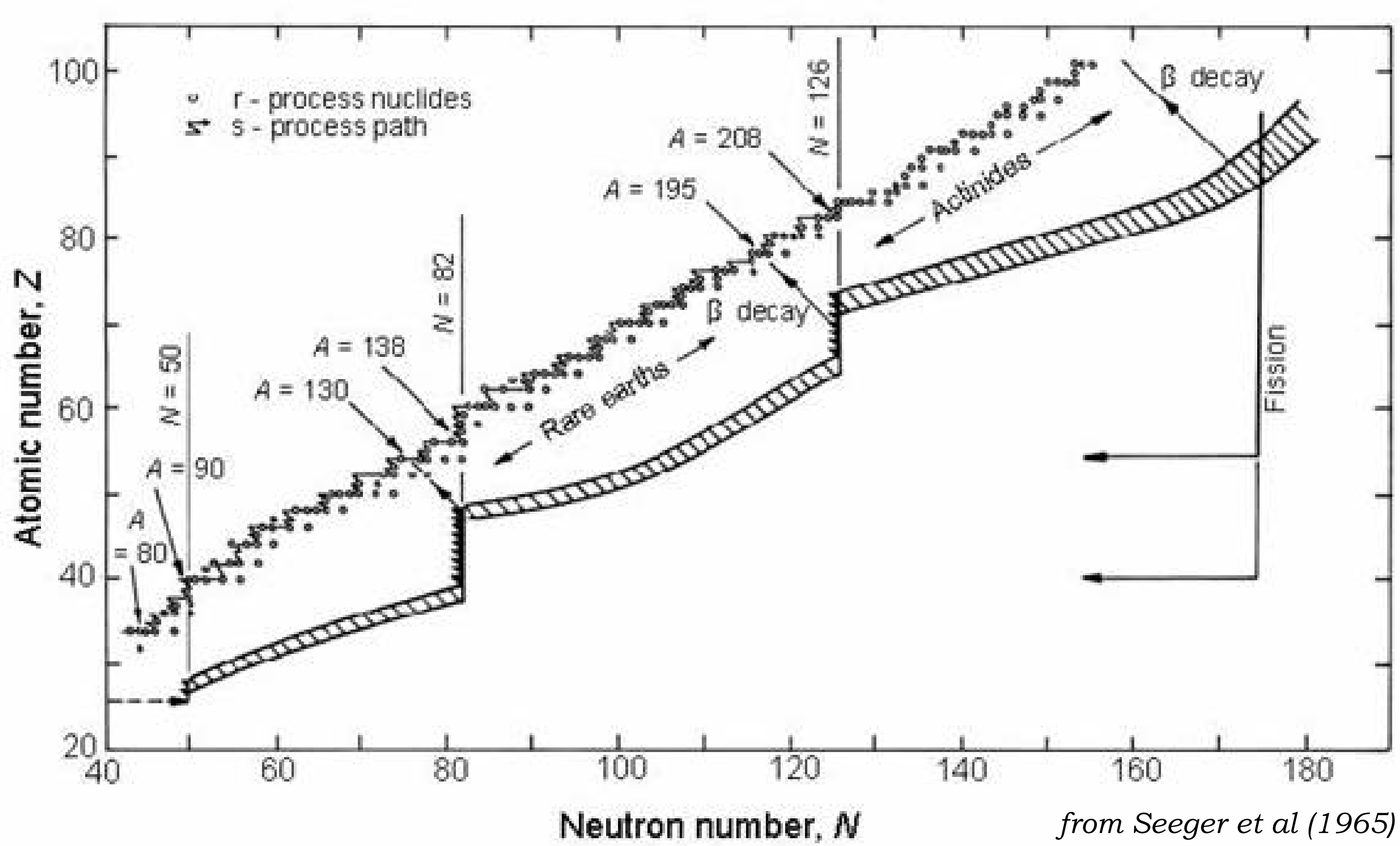

from Seeger et al (1965)

$$S_n(Z,A_{path}) \sim -kT\ln\left\{\frac{n_n}{2}\left(\frac{2\pi\hbar^2}{m_n kT}\right)^{3/2}\right\}$$

$$\lambda_\beta(Z,A_{path})Y(Z,A_{path}) \sim \text{constant}$$

Hot *r*-process: (n,γ)-(γ,n) equilibrium

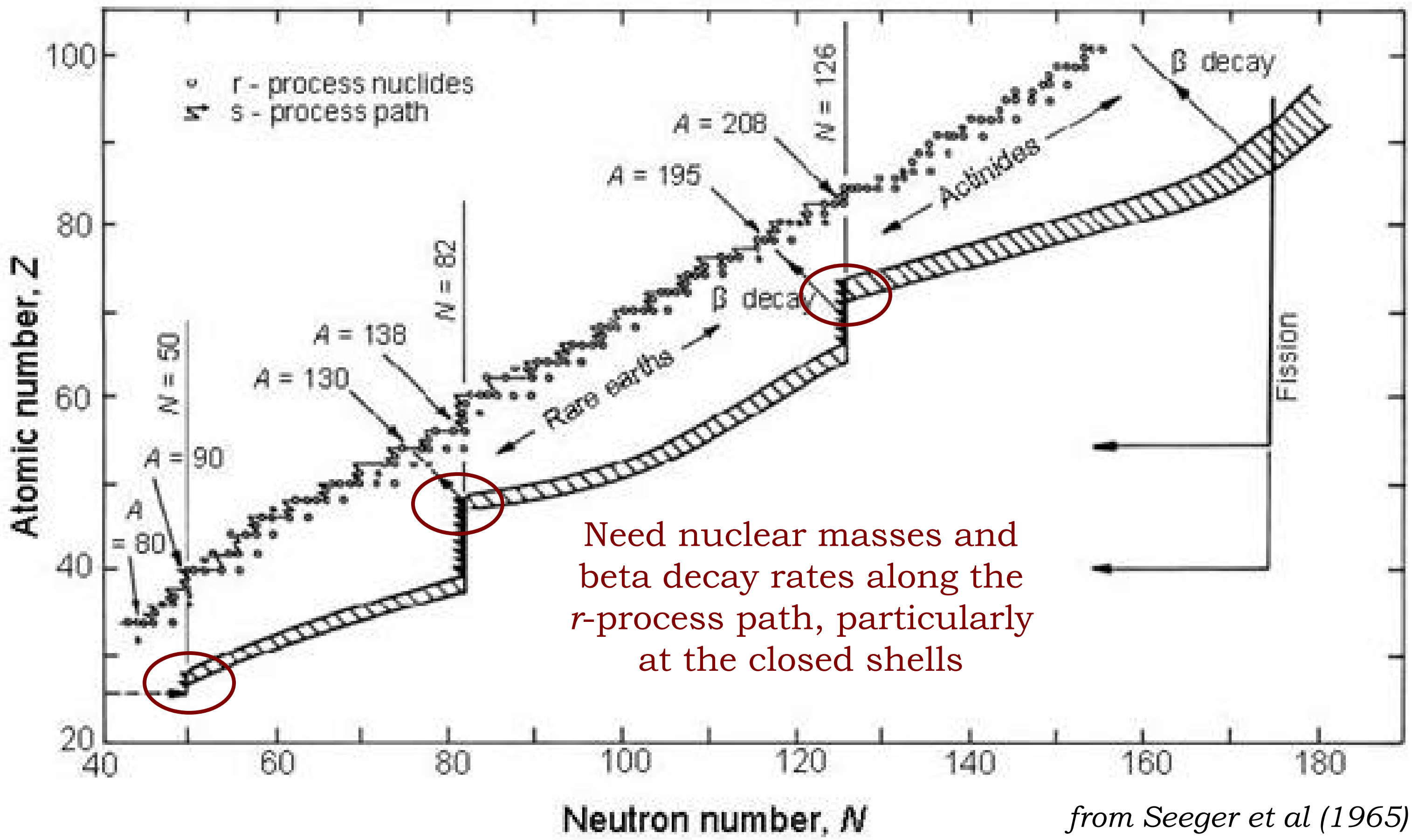

from Seeger et al (1965)

$$\boxed{S_n(Z,A_{path})} \sim -kT\ln\left\{\frac{n_n}{2}\left(\frac{2\pi\hbar^2}{m_n kT}\right)^{3/2}\right\} \qquad \boxed{\lambda_\beta(Z,A_{path})}\,Y(Z,A_{path}) \sim \text{constant}$$

Hot r-process: freezeout from (n,γ)-(γ,n) equilibrium

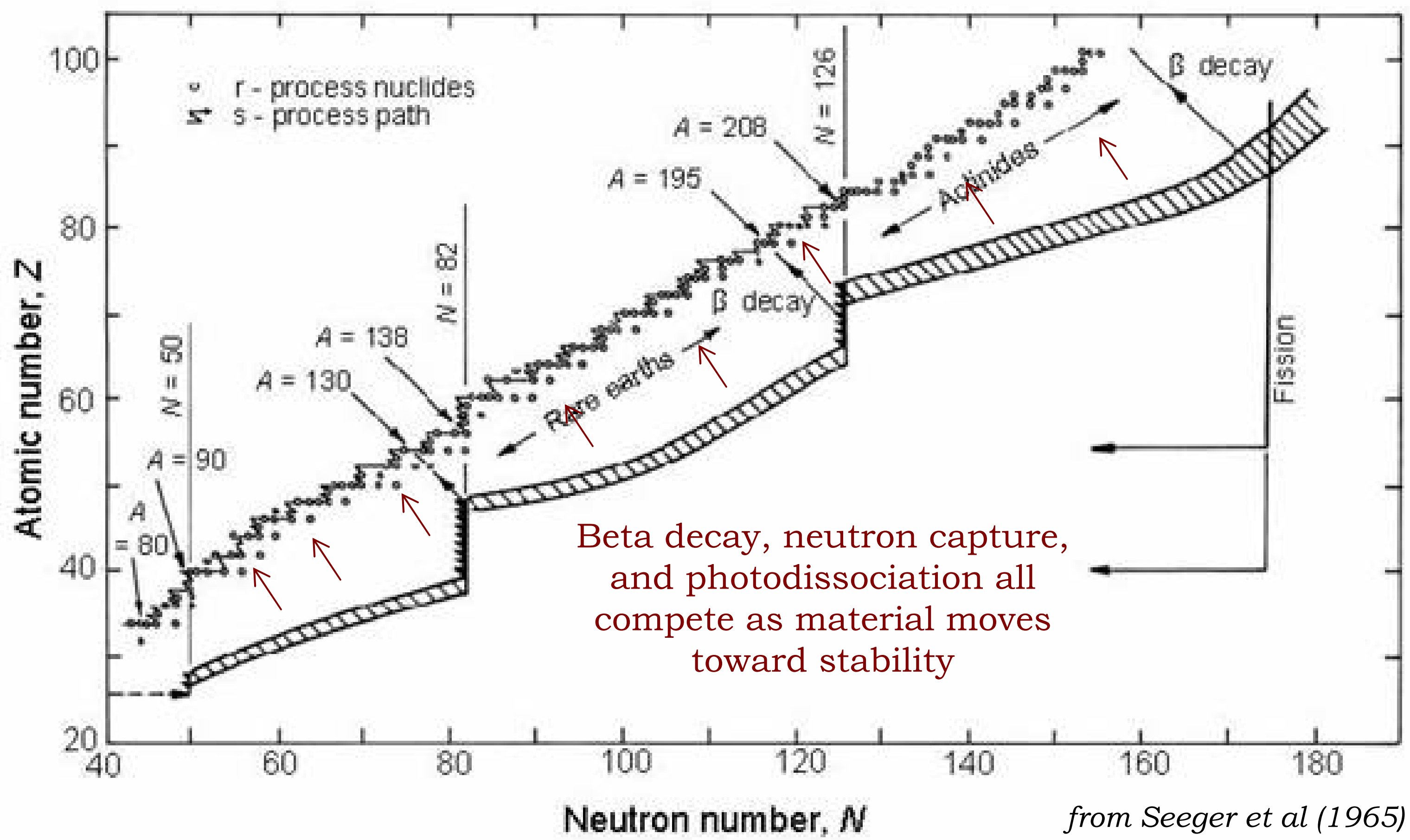

from Seeger et al (1965)

Individual neutron capture and photodissociation rates become important in shaping the final abundance pattern.

Cold *r*-process: equilibrium between (n,γ) and β decay

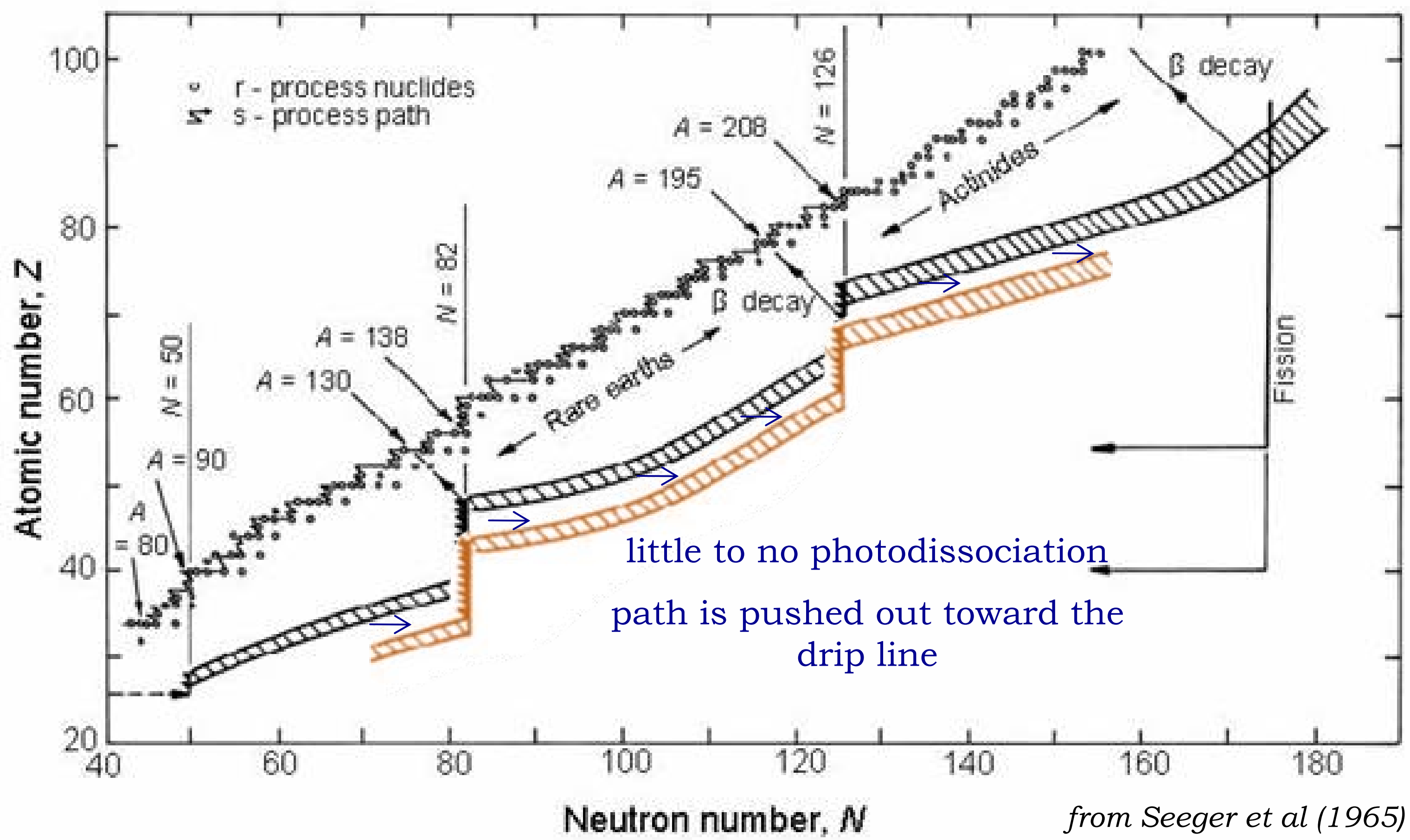

from Seeger et al (1965)

Interplay between beta decay, neutron capture, and beta-delayed neutron emission sets the final abundance pattern.

Neutron separation energy sensitivity study

S. Brett, I. Bentley, N. Paul, A. Aprahamian

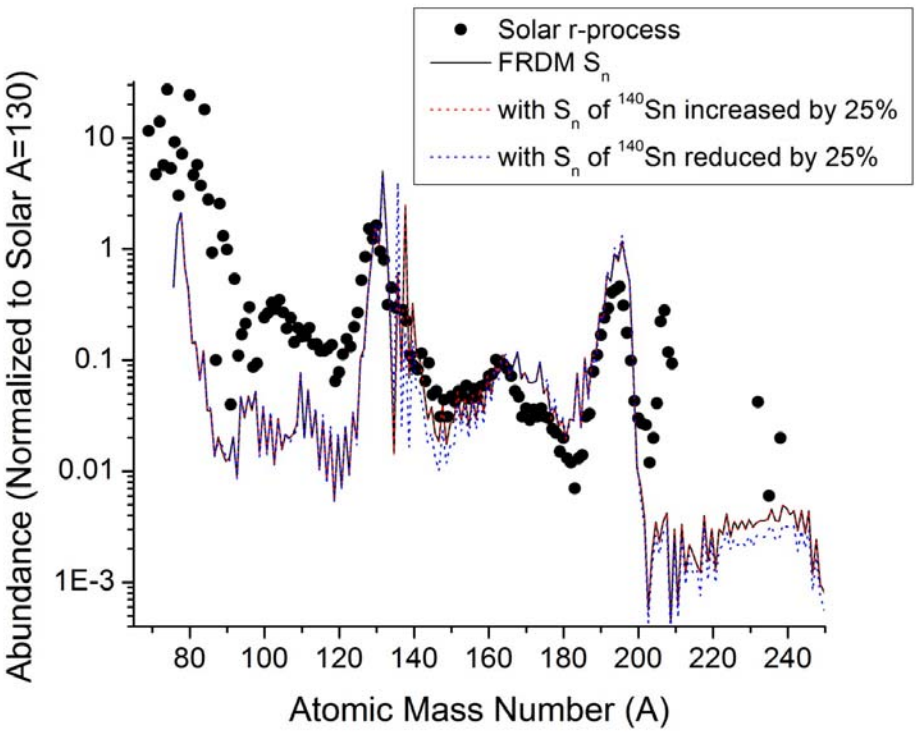

plot by I. Bentley

Start with a baseline simulation

(here, the H-event conditions from Qian et al were used)

Vary one separation energy by 25% and rerun the simulation

Repeat 6957 times

(twice for each heavy nucleus in the network)

$$\Delta Y_{S_n(Z_i, A_i)\pm 25\%} = \sum_A \left[Y_{baseline}(A) - Y_{S_n(Z_i, A_i)\pm 25\%}(A) \right]$$

Neutron separation energy sensitivity study

S. Brett, I. Bentley, N. Paul, A. Aprahamian

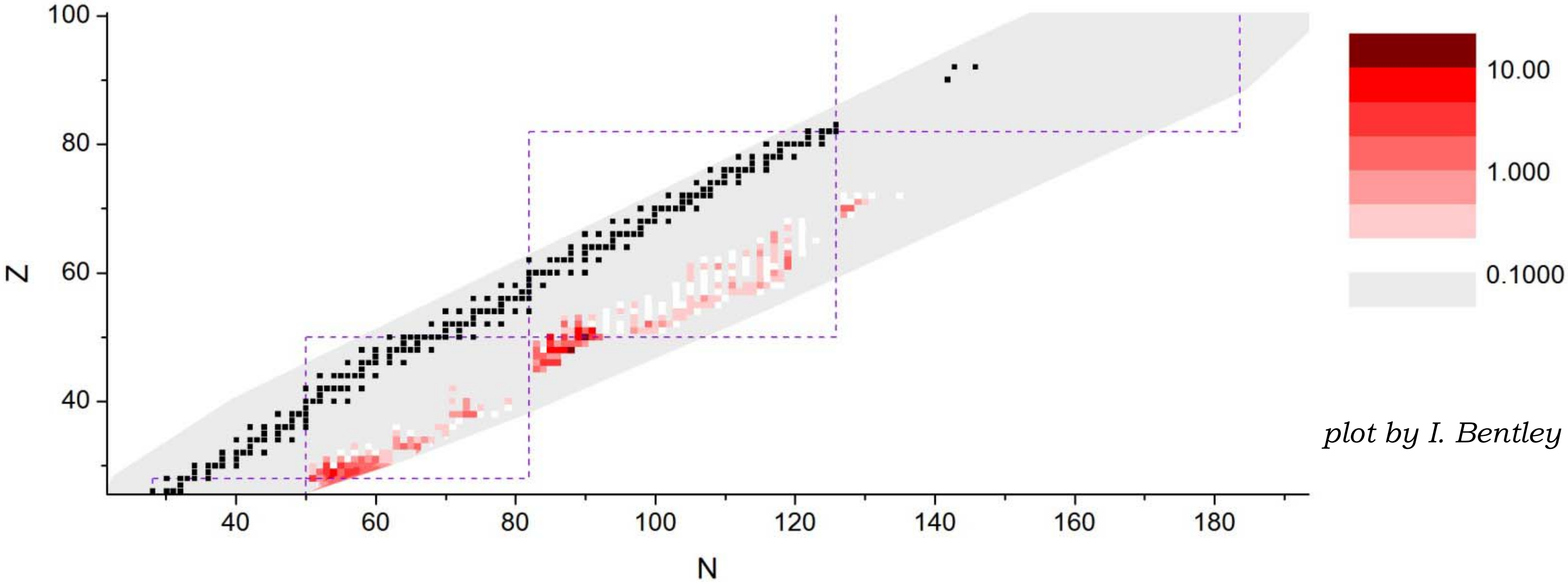

plot by I. Bentley

$$\Delta Y_{S_n(Z_i, A_i)\pm 25\%} = \sum_A \left[Y_{baseline}(A) - Y_{S_n(Z_i, A_i)\pm 25\%}(A) \right]$$

The role of neutron separation energies in a hot *r*-process

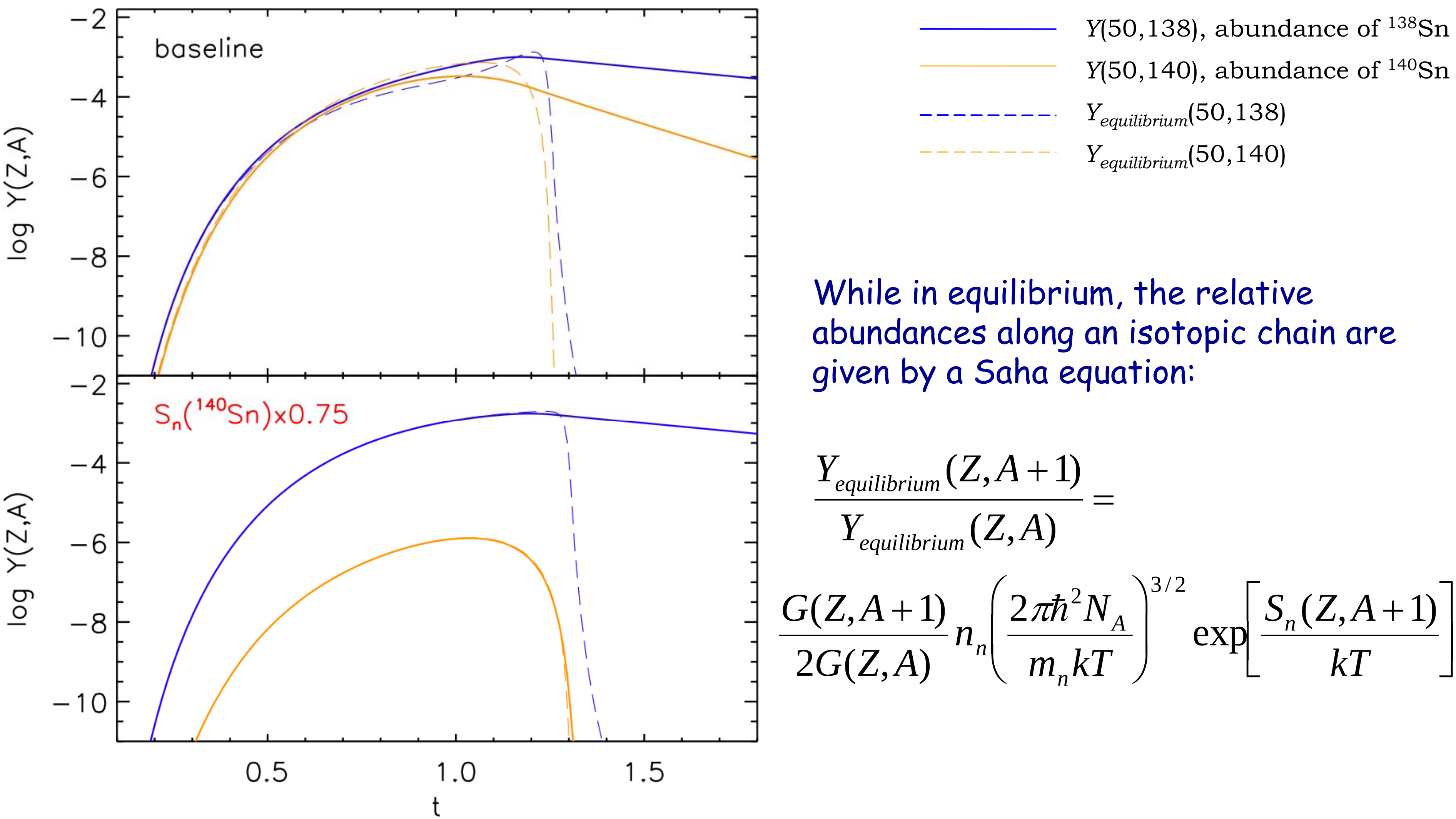

While in equilibrium, the relative abundances along an isotopic chain are given by a Saha equation:

$$\frac{Y_{equilibrium}(Z,A+1)}{Y_{equilibrium}(Z,A)} = \frac{G(Z,A+1)}{2G(Z,A)} n_n \left(\frac{2\pi\hbar^2 N_A}{m_n kT}\right)^{3/2} \exp\left[\frac{S_n(Z,A+1)}{kT}\right]$$

The role of neutron separation energies in a hot *r*-process

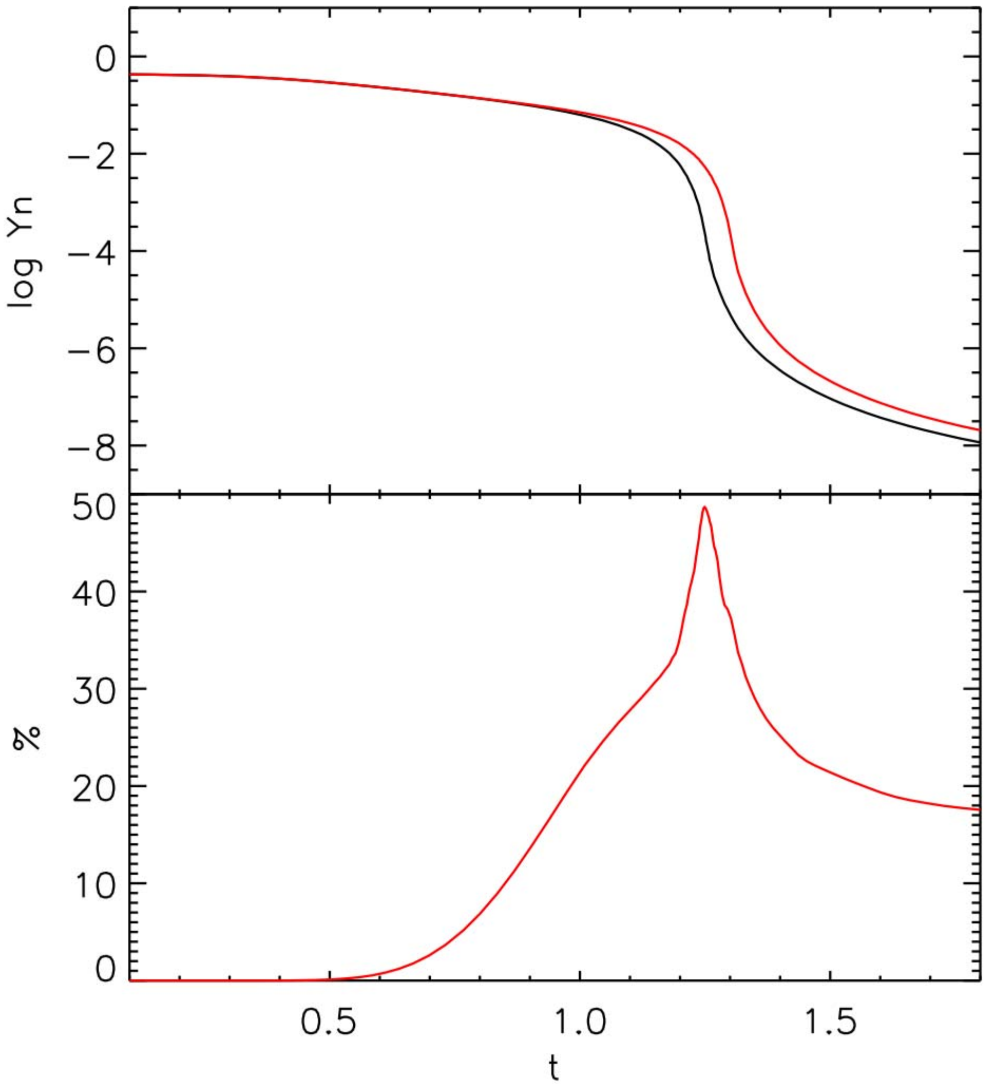

plots by R. Surman

Baseline simulation

Simulation with $S_n(50,140)$ reduced by 25%

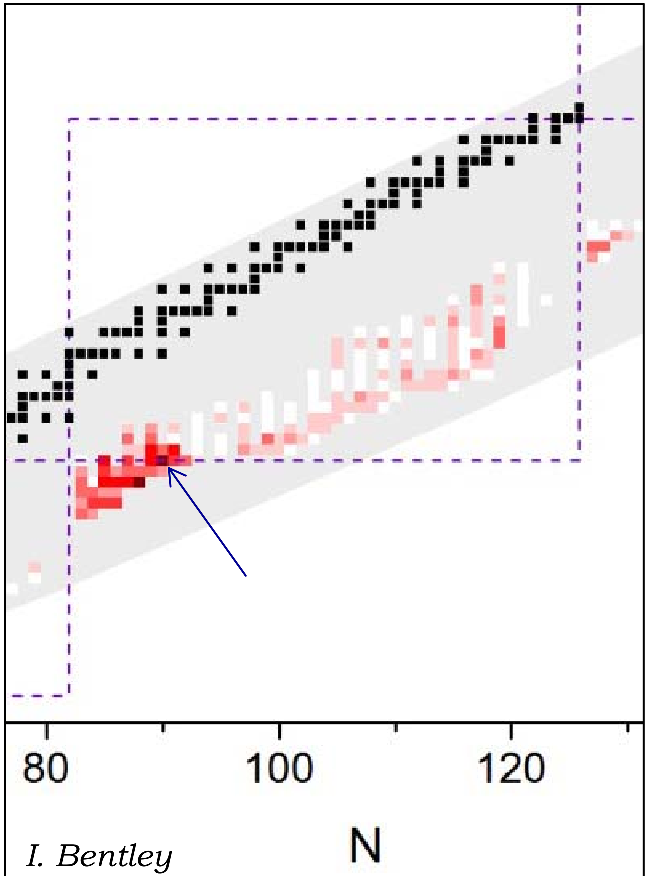

I. Bentley

Beta decay rate sensitivity study

J. Cass, G. Passucci, R. Surman, A. Aprahamian

To start, proceed as in neutron separation energy study:

Vary one beta decay rate by an order of magnitude, rerun the simulation, and compare the final abundance pattern to the baseline

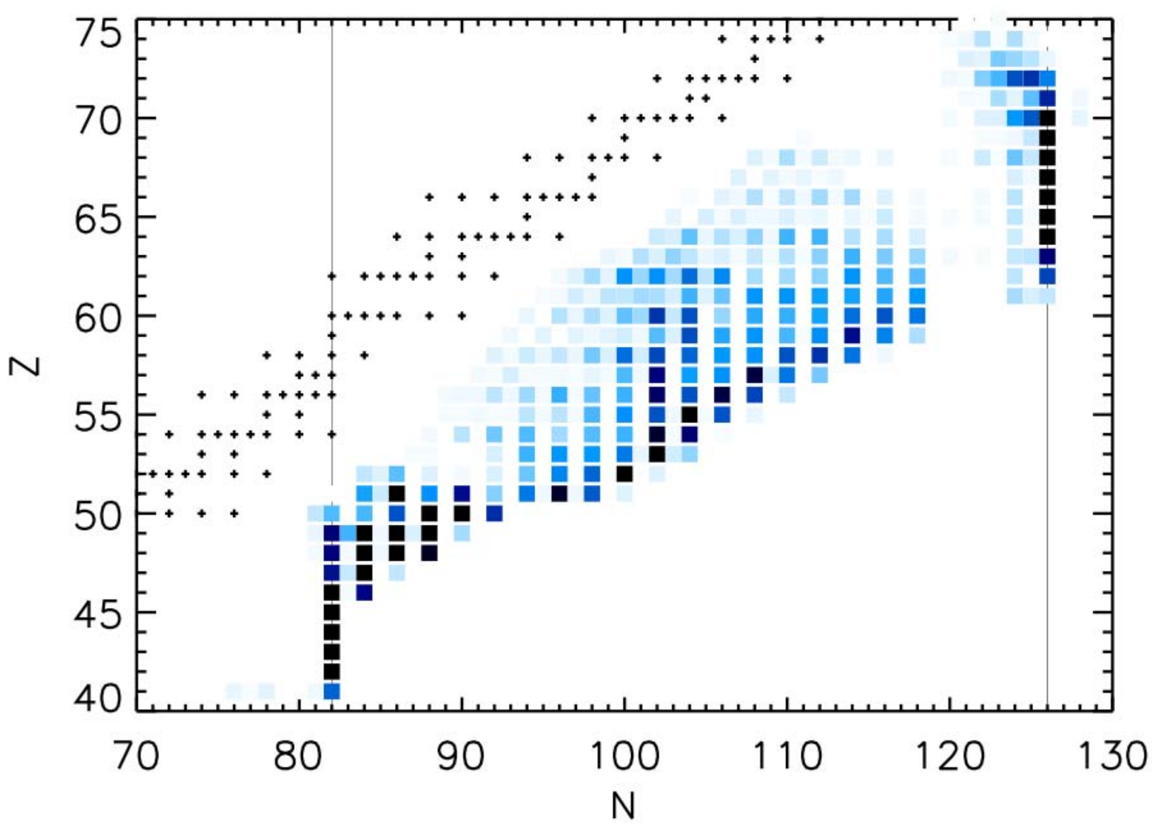

Beta decay rate sensitivity study

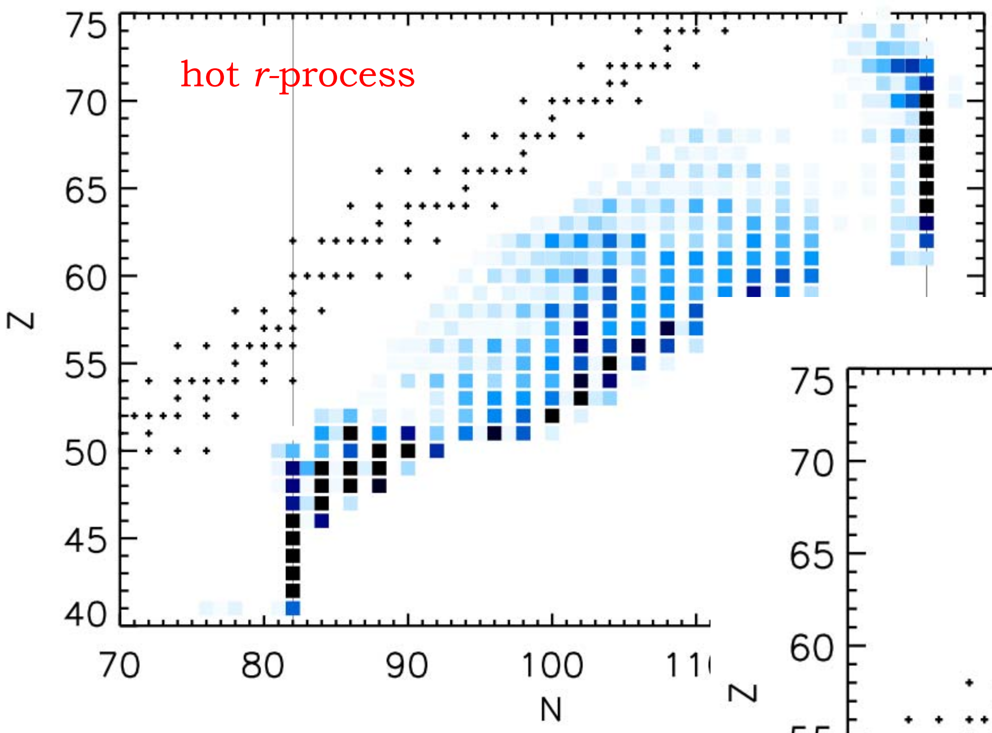

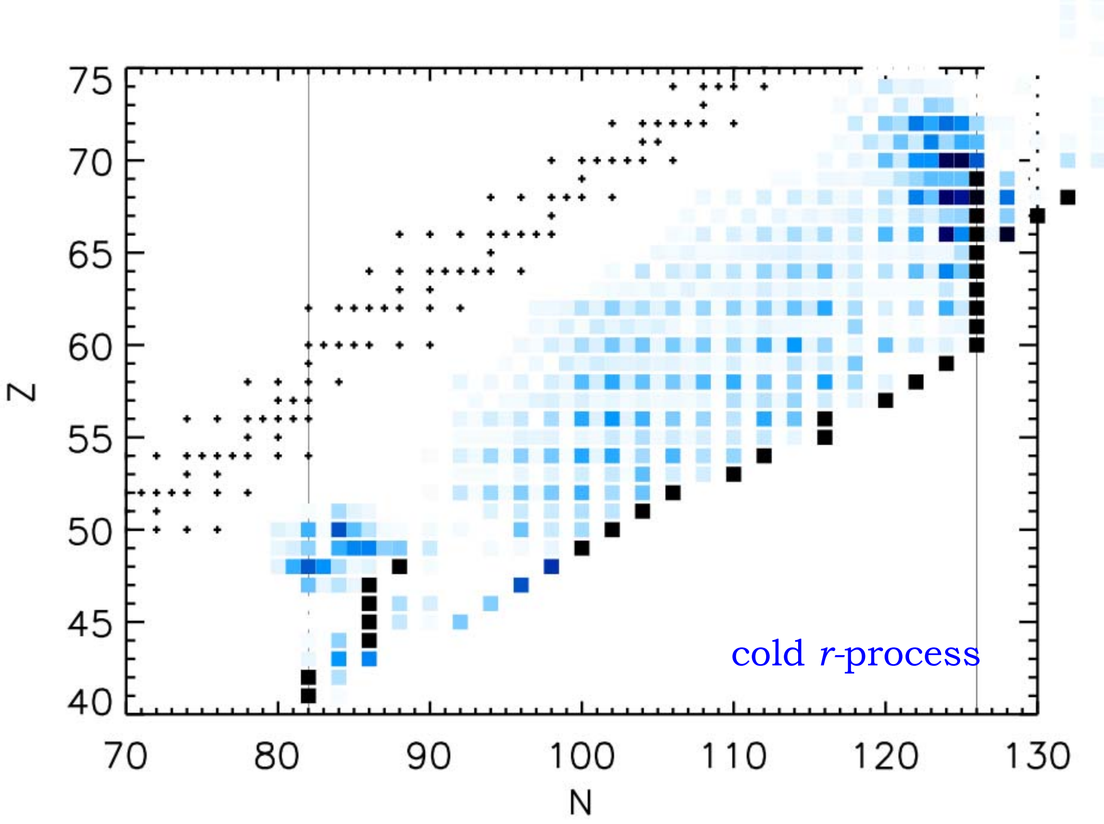

The role of beta decay rates in a hot *r*-process

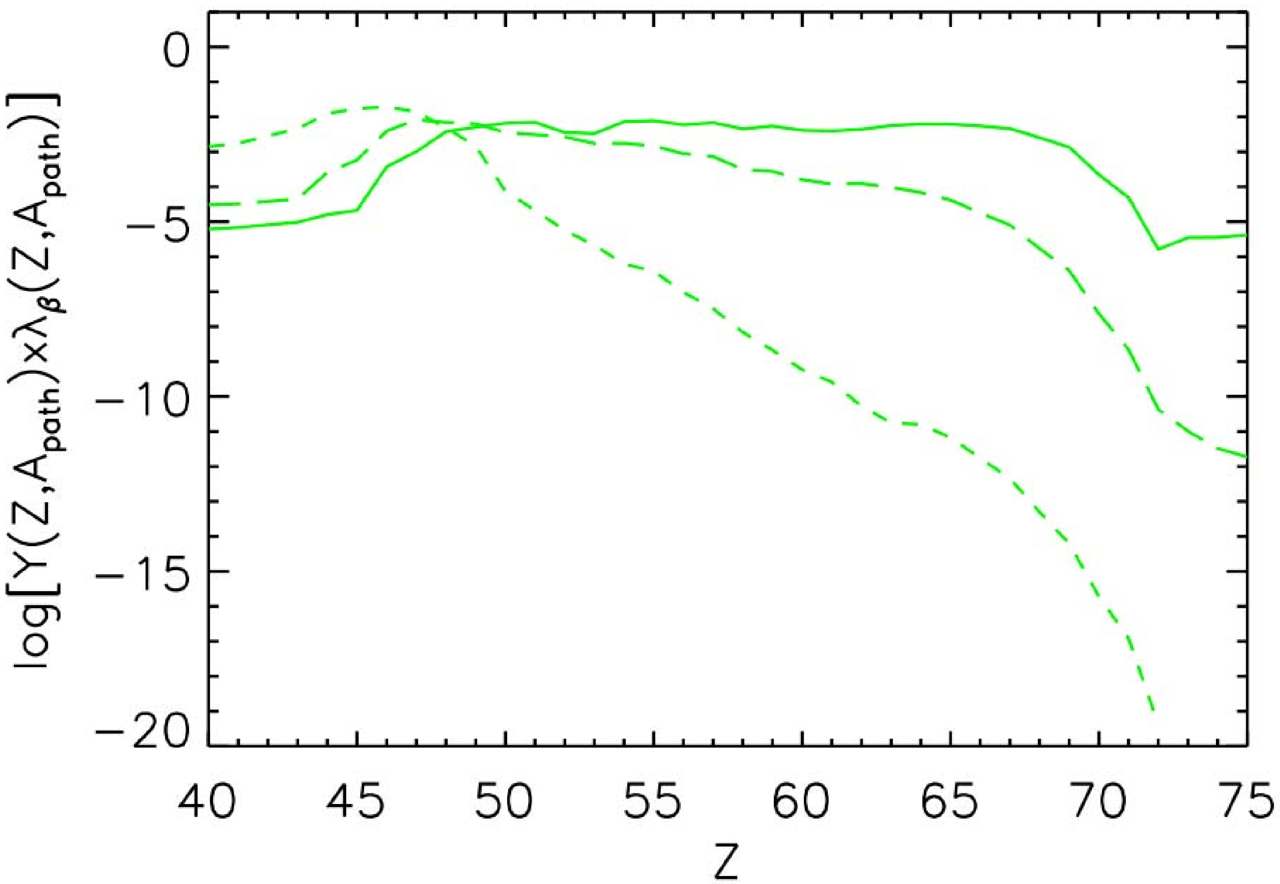

Steady beta flow in the baseline simulation

$$\lambda_\beta(Z,A_{path})Y(Z,A_{path}) \sim \text{constant}$$

The role of beta decay rates in a hot *r*-process

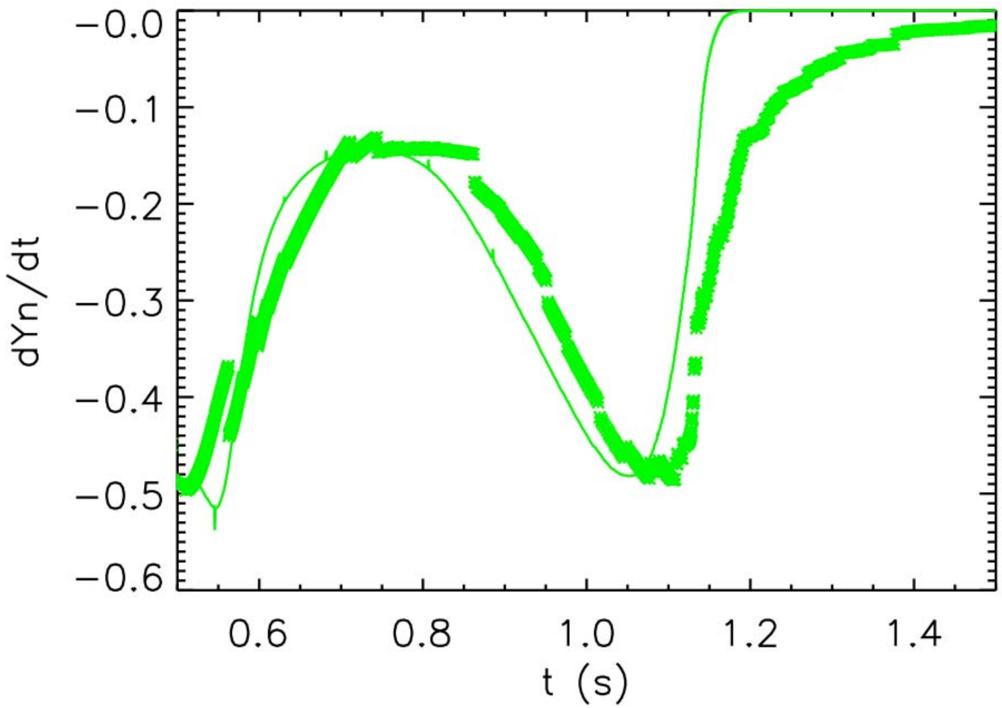

$\frac{dY_n}{dt}$

$\sum_Z \lambda_\beta(Z, A_{path}) Y(Z, A_{path}) N'$

N' neutron captures

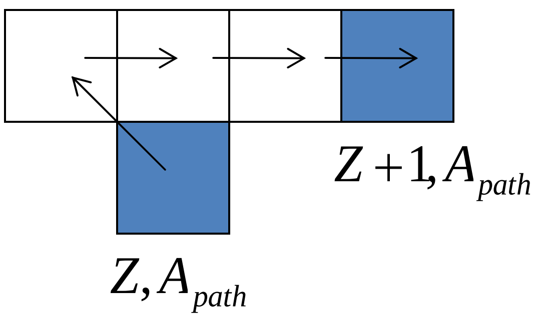

$$\frac{dY_n}{dt} \approx \sum_Z \lambda_\beta(Z, A_{path}) Y(Z, A_{path}) N'$$

where N' is the number of neutrons required to return to the path at $Z+1$ following decay

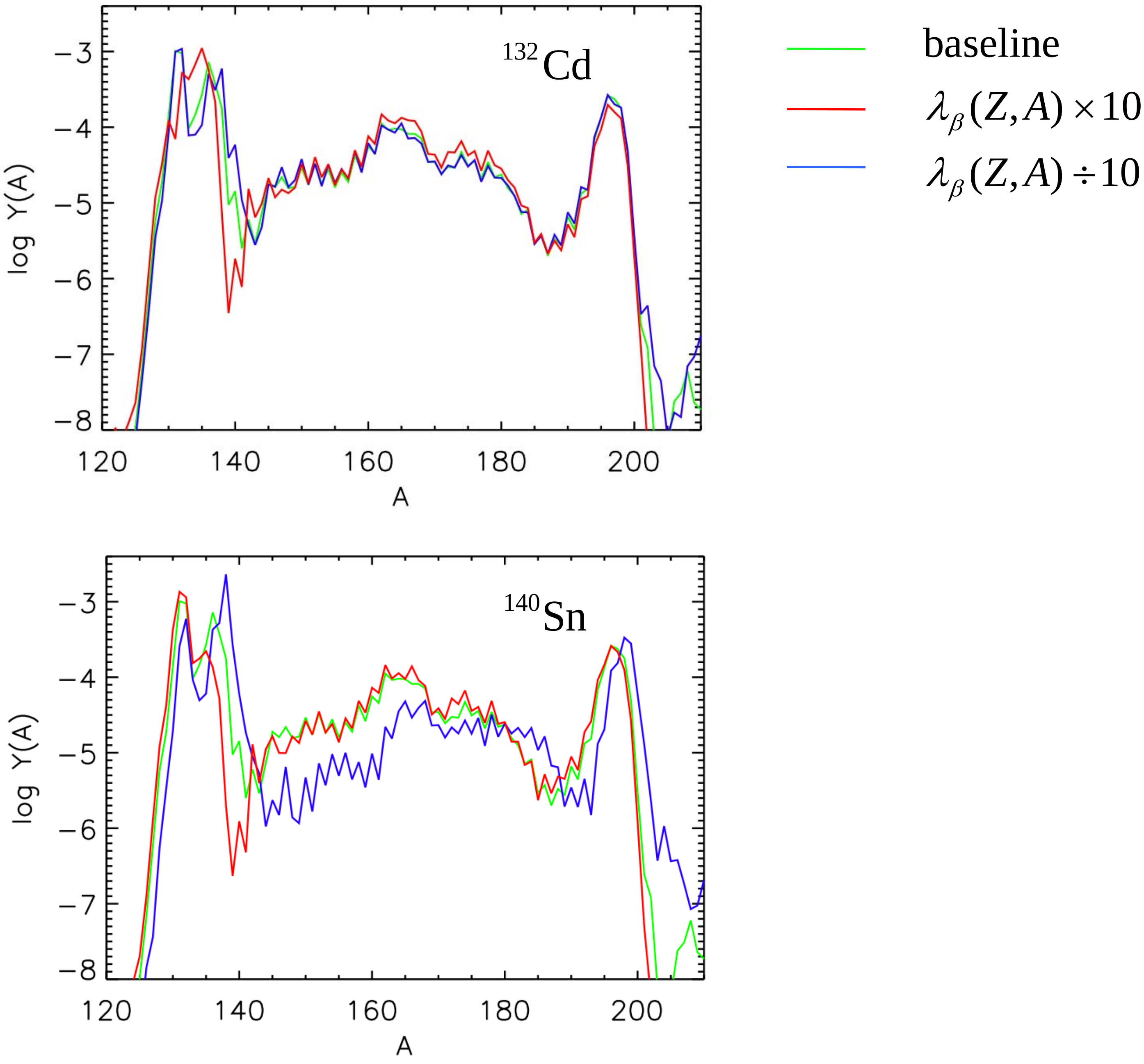

baseline
$\lambda_\beta(Z,A)\times 10$
$\lambda_\beta(Z,A)\div 10$
^{132}Cd
^{140}Sn
log Y(A)
A
−3
−4
−5
−6
−7
−8
120
140
160
180
200

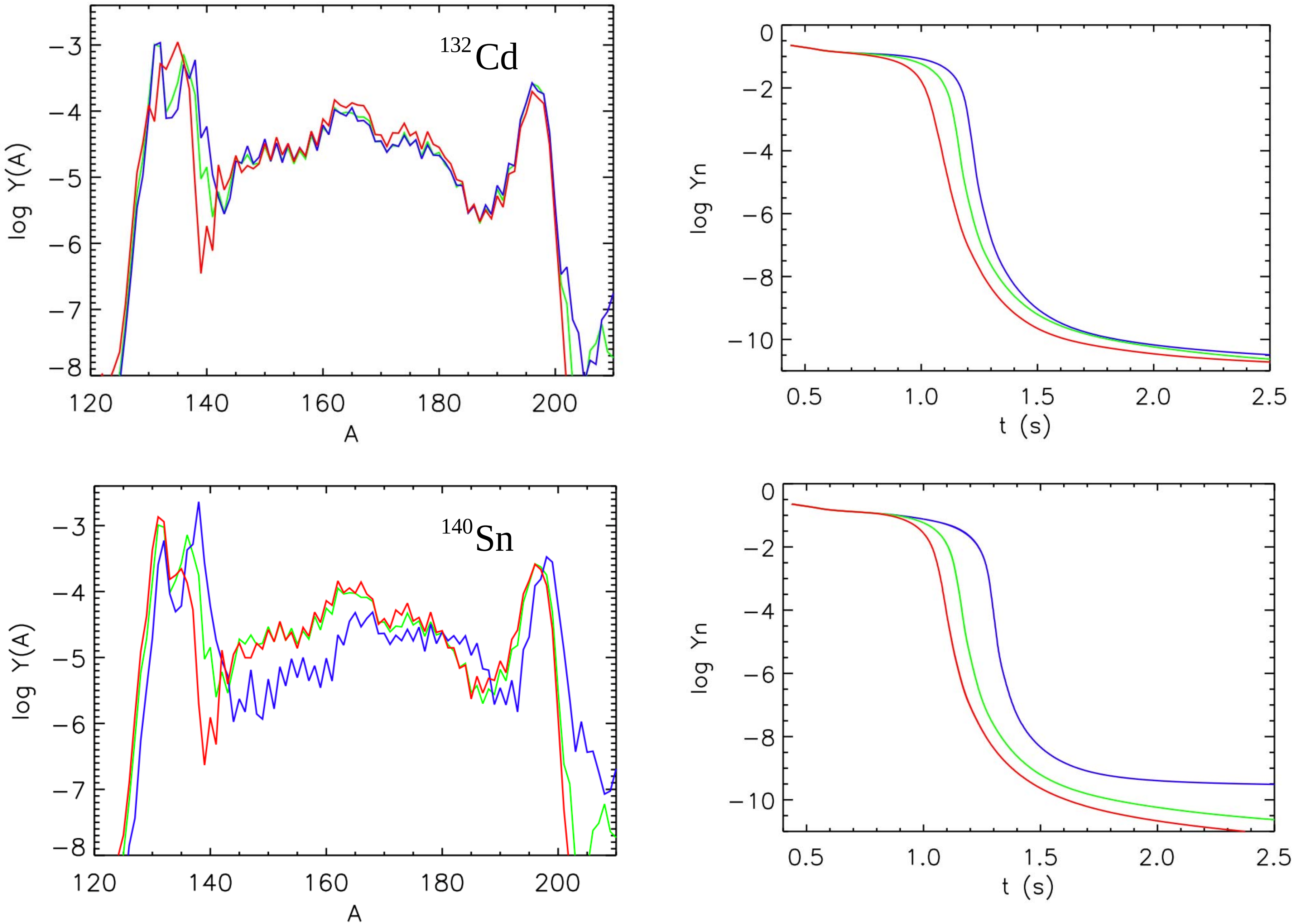

^{132}Cd
log Y(A)
A
log Yn
t (s)
^{140}Sn
log Y(A)
A
log Yn
t (s)

Input Parameters for the Neutrino-less H-event from Qian et. al

Description	Value
Seed Nucleus	^{90}Se
$N_{neutron}/N_{seed}$	86
*Seed Nucleus	^{70}Fe
$*N_{neutron}/N_{seed}$	67
Initial Density ($\rho_5 = 10^5 g/cm^3$)	0.0034
Initial Temperature ($T_9 = 10^9 K$)	1.5
Freeze-out Time	0.86s

$*{}^{90}Se$ was replaced with ^{70}Fe in order to allow for the dependence on the masses of nuclei between $70 \geq A \geq 90$ to be investigated. This was done in such a way that the electron fraction remains constant (Y_e=.19).

ΔY for FRDM

Nucleus	ΔY
^{136}Cd	20.2
^{140}Sn	12.1
^{135}Cd	8.80
^{83}Cu	8.42
^{139}Sn	8.19
^{142}Sb	5.64
^{135}Sn	5.44
^{133}Cd	5.38
^{140}Sb	5.25
^{134}Cd	5.23
^{82}Cu	4.14
^{134}In	4.14
^{131}Pd	3.29
^{137}Sn	2.94
^{141}Sn	2.91
^{83}Zn	2.89
^{85}Zn	2.71
^{85}Cu	2.66
^{130}Pd	2.39
^{132}Pd	2.39

ΔY for ETFSI-Q

Nucleus	ΔY
^{140}Sn	20.1
^{136}Cd	19.0
^{142}Sn	17.3
^{137}Cd	15.3
^{79}Ni	12.5
^{80}Ni	12.0
^{135}Cd	11.5
^{134}Cd	11.5
^{138}Cd	8.57
^{132}Pd	7.66
^{130}Pd	7.34
^{132}In	7.33
^{129}Pd	5.12
^{139}Sn	4.63
^{131}Pd	4.37
^{138}In	3.98
^{139}In	3.95
^{86}Zn	3.21
^{141}Sn	2.92
^{85}Zn	2.86

ΔY for DZ

Nucleus	ΔY
^{80}Ni	13.6
^{79}Ni	9.96
^{138}Cd	7.08
^{137}Cd	5.49
^{83}Cu	4.27
^{131}Pd	3.54
^{82}Cu	3.36
^{132}Pd	3.12
^{136}Cd	3.00
^{130}Pd	2.97
^{86}Zn	2.84
^{129}Pd	1.88
^{85}Zn	1.81
^{134}Ag	1.49
^{142}Sn	1.42
^{135}Ag	1.39
^{135}Cd	1.36
^{133}Cd	1.10
^{141}Sn	1.08
^{144}Sn	1.07

ΔY for HFB21

Nucleus	ΔY
^{136}Cd	22.7
^{137}Cd	10.8
^{138}Cd	10.4
^{135}Cd	6.97
^{140}Sn	5.97
^{130}Pd	5.46
^{83}Cu	5.23
^{142}Sn	4.66
^{134}Cd	4.57
^{141}Sn	4.21
^{86}Zn	3.82
^{133}Cd	3.52
^{132}Cd	3.04
^{137}Sn	2.86
^{82}Cu	2.63
^{138}In	2.47
^{139}In	2.23
^{129}Pd	1.95
^{131}Pd	1.81
^{131}Ag	1.69

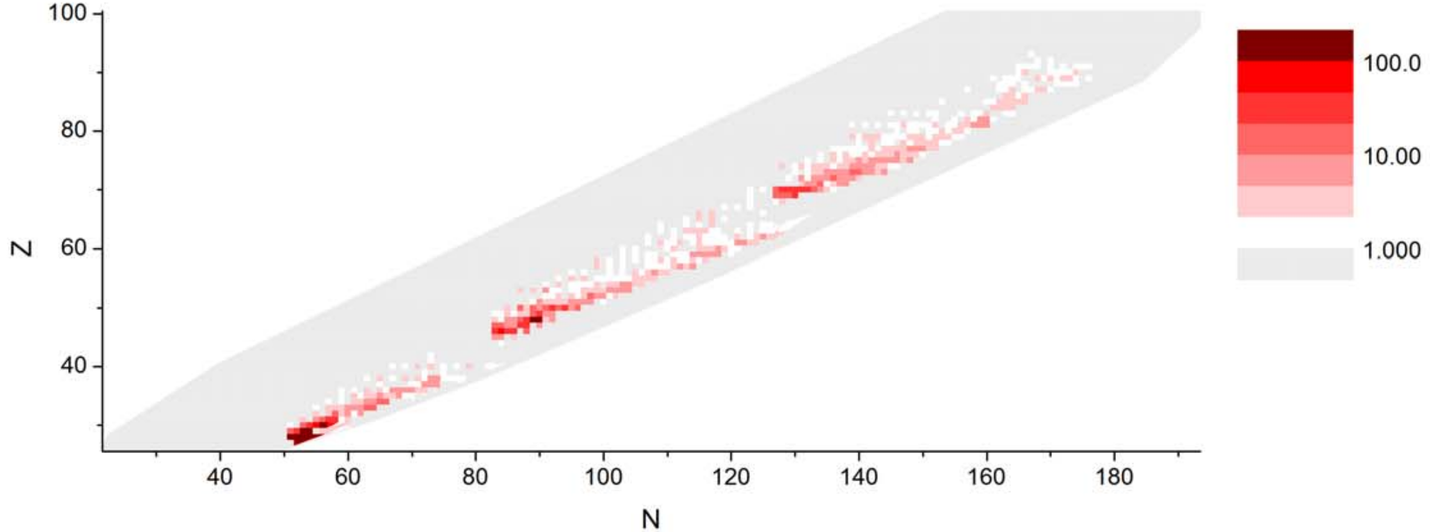

100
80
60
40
Z
40
60
80
100
120
140
160
180
N
100.0
10.00
1.000

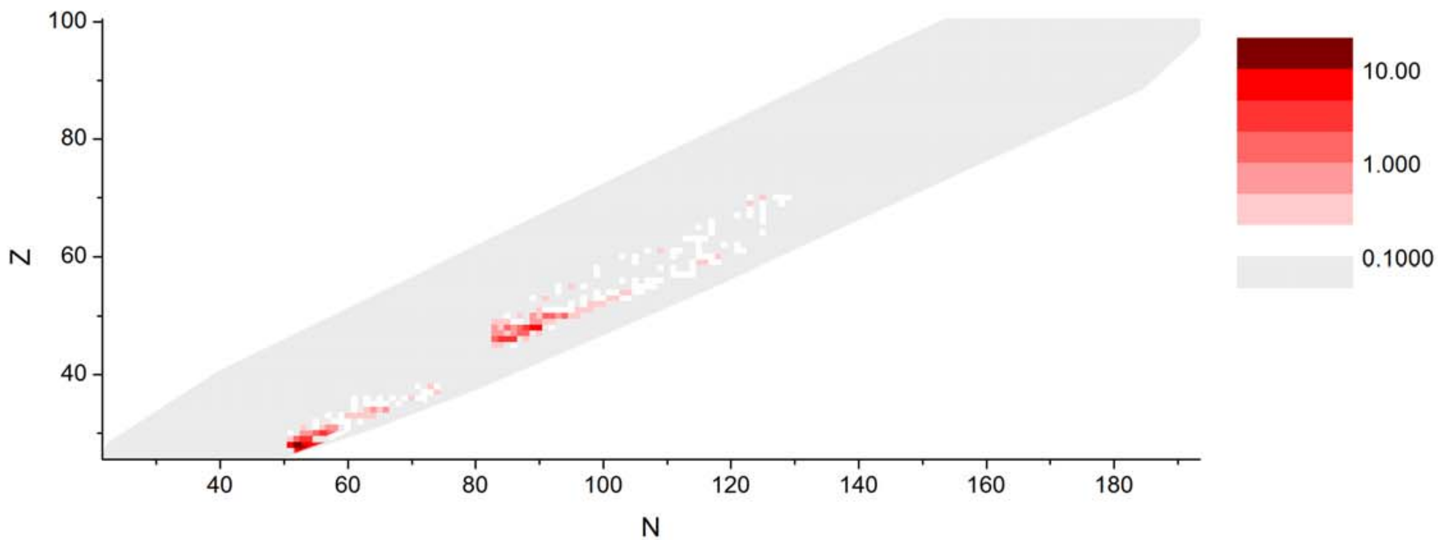

100
80
60
40
Z
40
60
80
100
120
140
160
180
N
10.00
1.000
0.1000

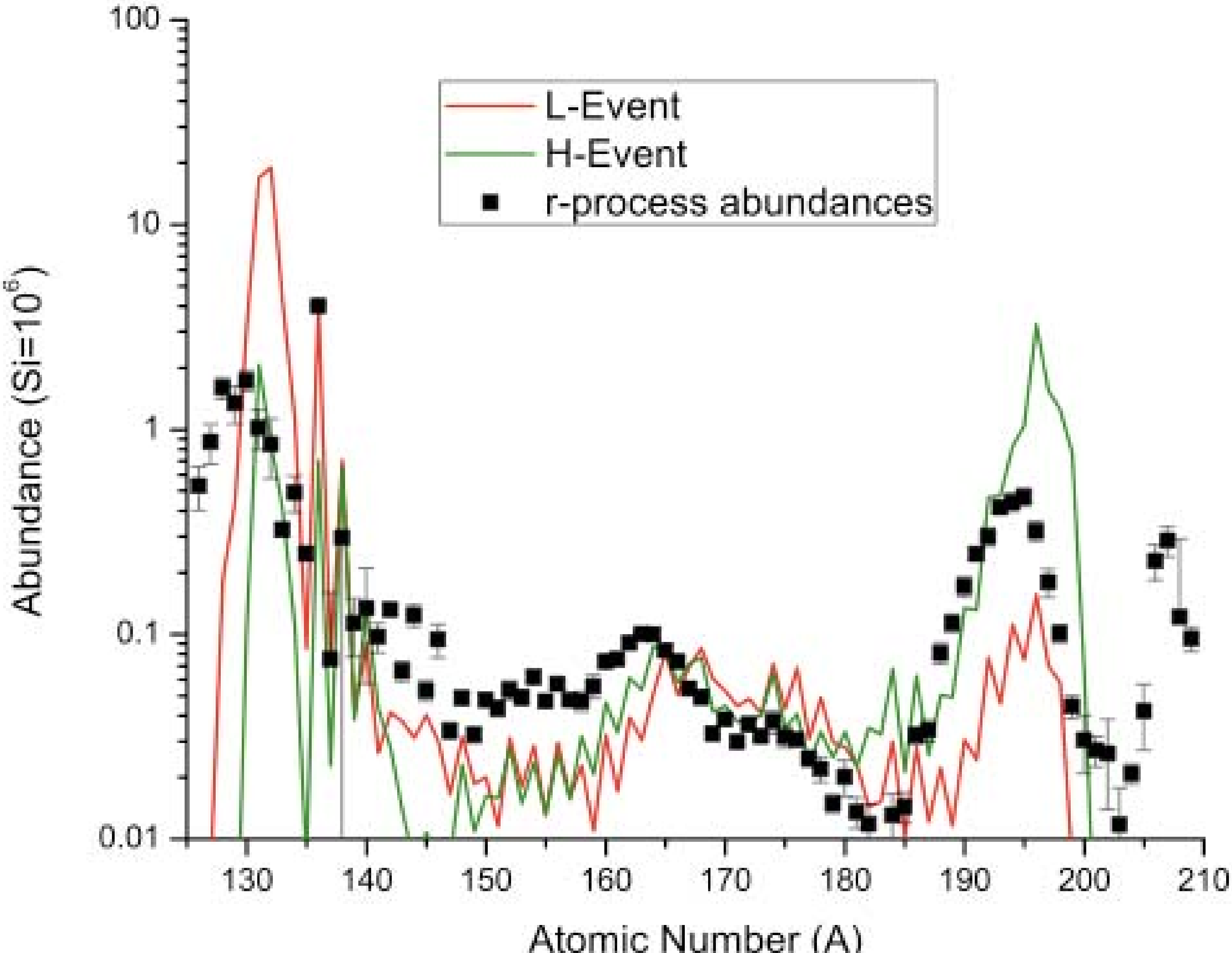

L-Event
H-Event
r-process abundances
Abundance (Si=10^6)
100
10
1
0.1
0.01
130
140
150
160
170
180
190
200
210
Atomic Number (A)

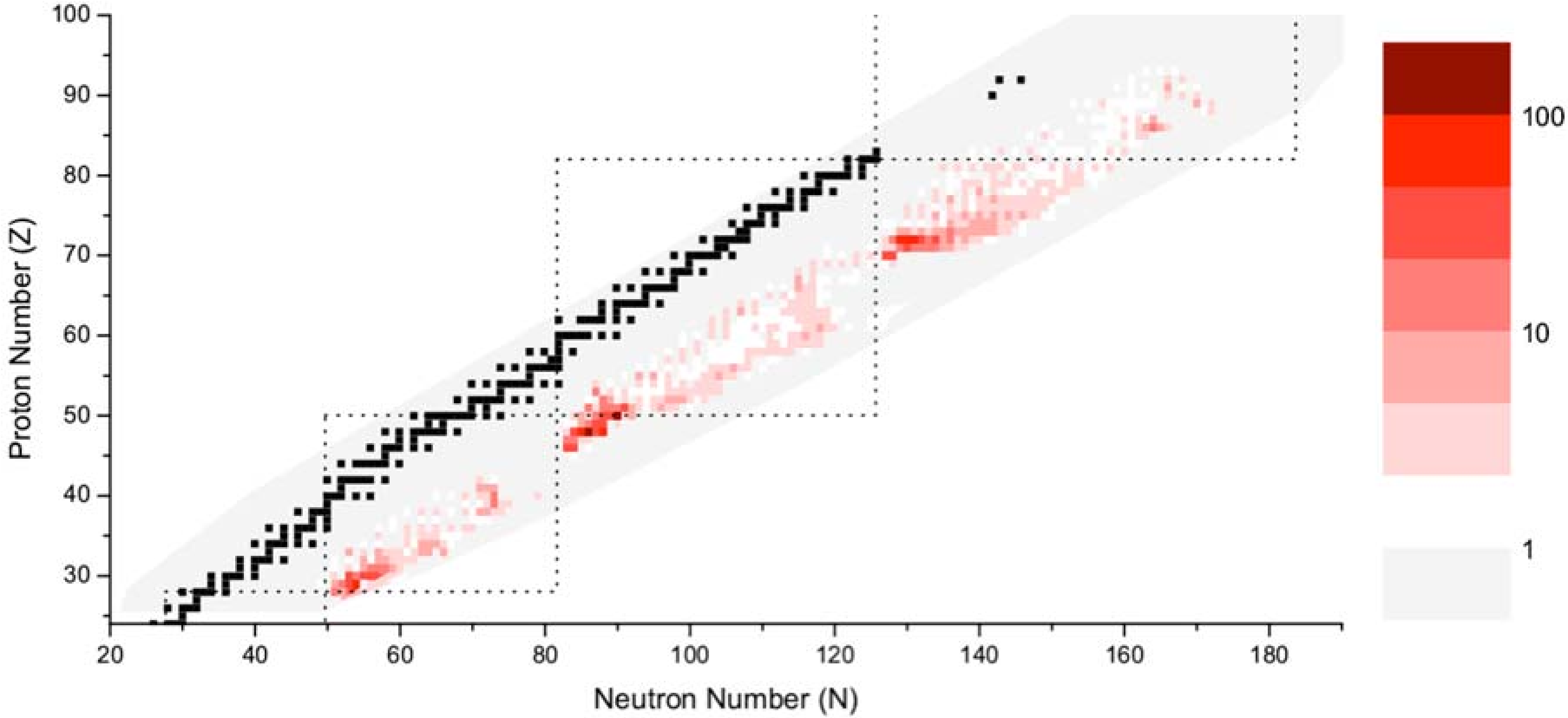

$$\Delta_{\pm 25\%}(N,Z) = \sum_{A} \frac{|Y(A) - Y(A, \pm\Delta S_n(N,Z))|}{Y(A)}.$$

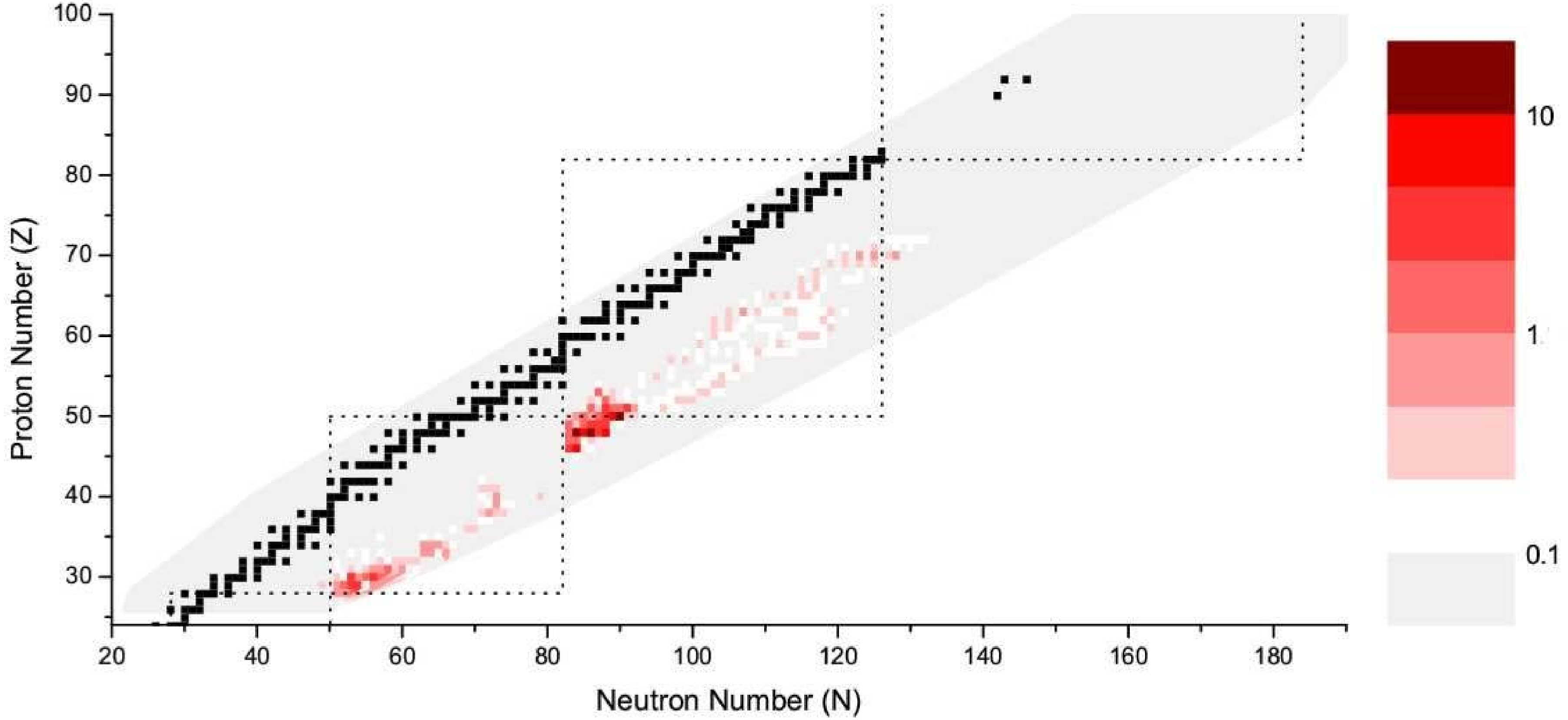

$$\Delta Y_{\pm 25\%}(N,Z) = \sum_{A} |Y(A) - Y(A, \pm\Delta S_n(N,Z))|.$$

Run 23: H-Event with Iron-70 Seed (Z≤50)

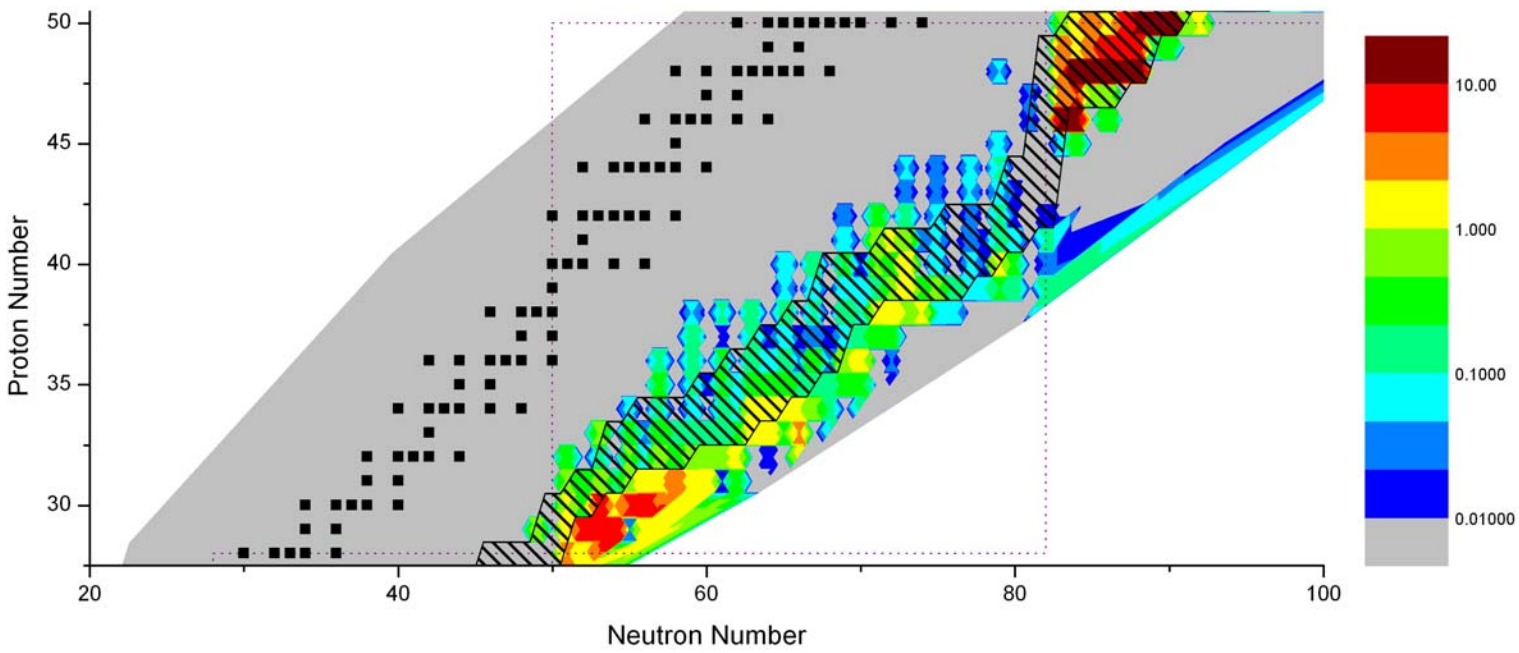

Nucleus	$\Delta_{+25\%}$	$\Delta_{-25\%}$
140Sn	3.59E+00	6.55E+01
134Cd	2.25E+01	1.55E+01
132Cd	2.82E-01	3.09E+01
139Sn	3.71E+00	1.55E+01
136Cd	1.52E+01	1.84E+00
133Cd	5.21E+00	9.65E+00
130Pd	3.18E+00	9.76E+00
129Pd	3.63E+00	7.98E+00
135Cd	8.69E+00	1.68E+00
138Sn	1.71E-01	1.01E+01
83Cu	3.51E+00	4.27E+00
137In	1.22E+00	5.95E+00
135In	7.78E-01	6.39E+00
82Cu	3.01E+00	3.51E+00
83Zn	7.40E-01	5.73E+00
136In	1.55E+00	4.70E+00
86Zn	5.50E-01	5.58E+00
137Sn	8.48E-01	4.79E+00
81Cu	7.61E-02	5.32E+00
131Ag	2.06E+00	2.63E+00

Run #	Description	Seed	Nseed	Nn	T9	density [g/cm^3]	time [sec.]	Source
23	H Qian's neutrinoless model (Iron)	Fe70	0.511	0.489	1.5	3.4x10^2	1.68	Qian et al. ApJ 494 (1998) with Fe70

Run 62: H-Event with Iron-70 Seed

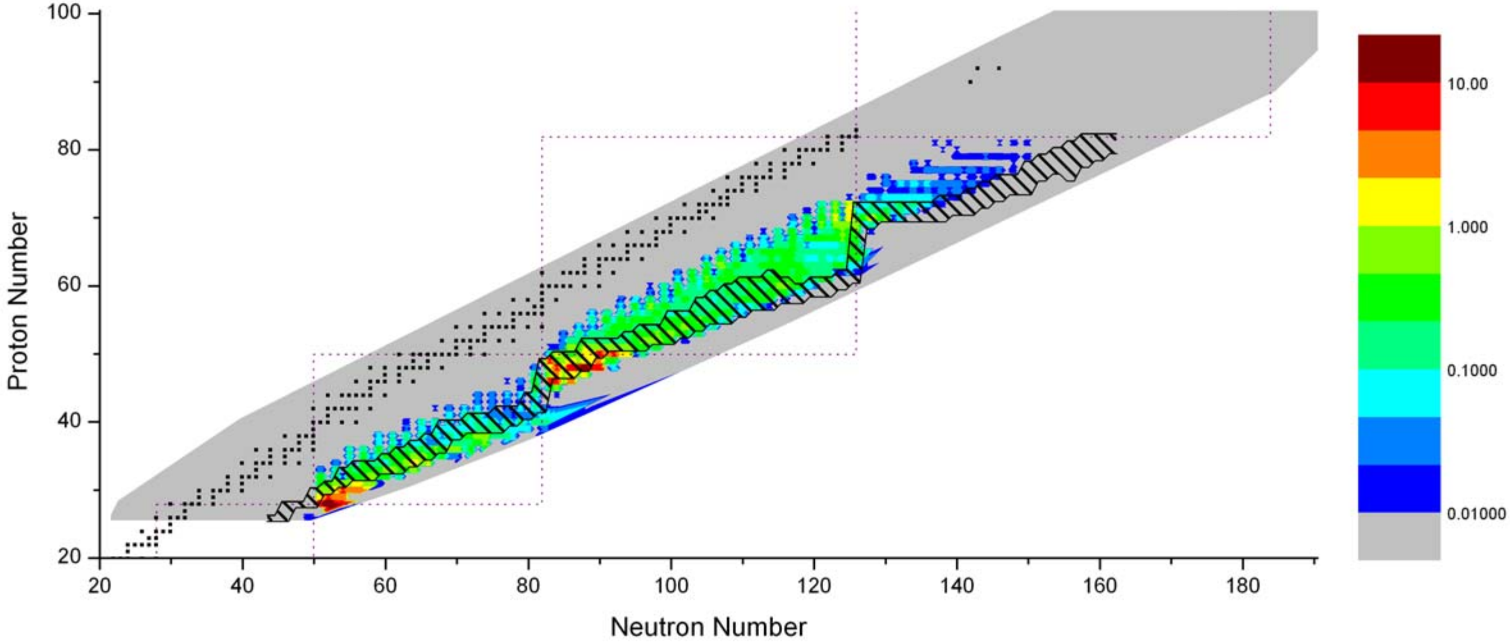

Nucleus	$\Delta_{+25\%}$	$\Delta_{-25\%}$
136Cd	6.79E+00	1.05E+01
80Ni	1.29E+01	2.90E+00
79Ni	7.00E+00	2.64E+00
135Cd	1.90E+00	7.16E+00
134Cd	1.47E+00	5.80E+00
138Cd	5.83E+00	1.26E+00
130Pd	2.92E+00	3.15E+00
140Sn	9.12E-01	4.92E+00
137Cd	4.48E+00	1.19E+00
142Sn	1.12E+00	4.17E+00
81Cu	1.05E+00	3.98E+00
129Pd	2.24E+00	2.78E+00
132In	3.77E+00	1.22E+00
84Zn	2.97E-02	4.93E+00
132Cd	1.76E-01	4.65E+00
132Pd	3.57E+00	4.52E-02
86Zn	2.73E+00	8.48E-01
83Cu	2.64E+00	8.16E-01
141Sn	9.33E-01	2.15E+00
82Cu	2.19E+00	8.38E-01

DUZU mass model

Run #	Description	Seed	Nseed	Nn	T9	density [g/cm^3]	time [sec.]	Source
62	H Qian's neutrinoless model (Iron)	Fe70	0.511	0.489	1.5	3.4x10^2	1.68	Qian et al. ApJ 494 (1998) with Fe70

Run 63: H-Event with Iron-70 Seed

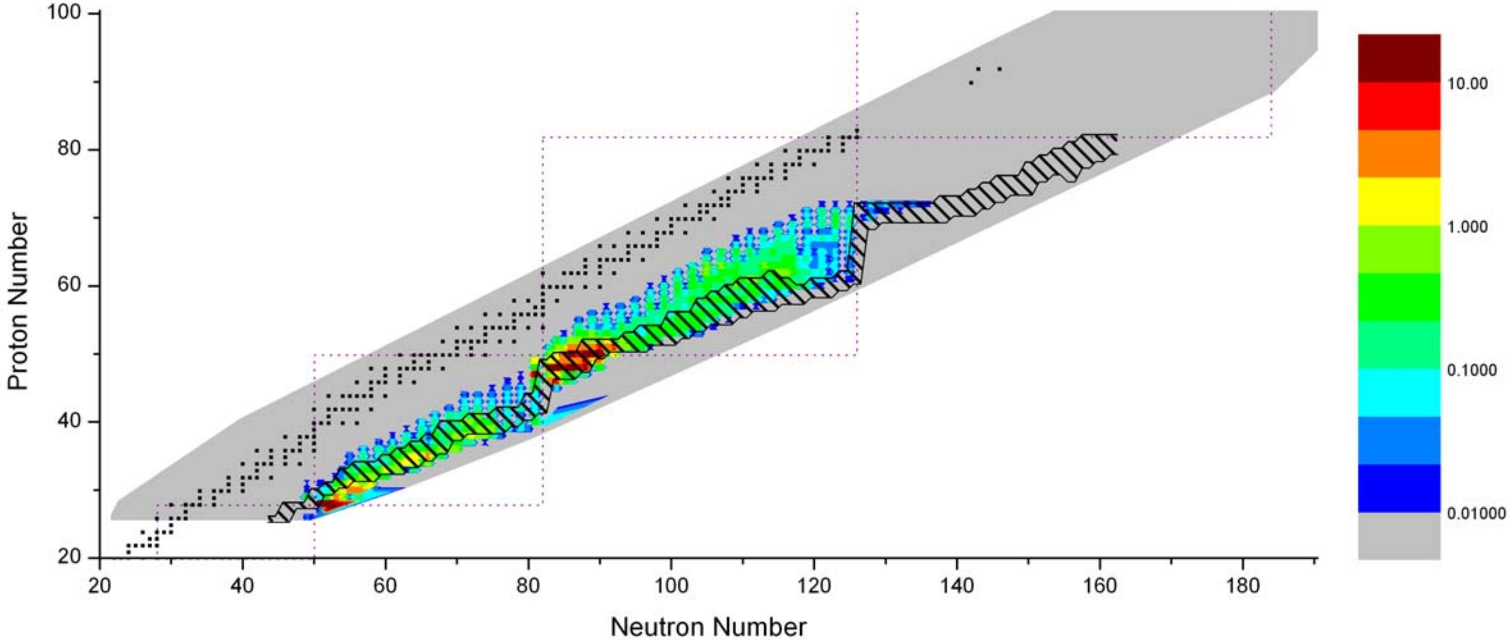

Nucleus	$\Delta_{+25\%}$	$\Delta_{-25\%}$
134Cd	3.45E+01	8.20E+00
140Sn	8.69E+00	2.11E+01
132Cd	2.50E+01	4.61E+00
139Sn	5.41E+00	1.75E+01
80Ni	6.34E+00	1.28E+01
79Ni	6.13E+00	1.28E+01
138Sn	1.00E+01	7.06E+00
136Sn	5.17E-01	1.30E+01
136Cd	1.02E+01	1.35E+00
131Cd	8.38E+00	2.92E+00
128Ag	9.23E-04	1.08E+01
135Cd	6.42E+00	1.32E+00
133Cd	3.73E+00	3.64E+00
137Sn	3.40E+00	2.46E+00
130Pd	5.07E+00	5.09E-01
137In	1.17E+00	4.31E+00
141Sb	1.51E+00	3.82E+00
143Sb	1.26E+00	3.47E+00
135In	1.56E+00	2.87E+00
136In	9.28E-01	3.16E+00

ETFSI-12 mass model

Run #	Description	Seed	Nseed	Nn	T9	density [g/cm^3]	time [sec.]	Source
63	H Qian's neutrinoless model (Iron)	Fe70	0.511	0.489	1.5	3.4x10^2	1.68	Qian et al. ApJ 494 (1998) with Fe70

Run 64: H-Event with Iron-70 Seed

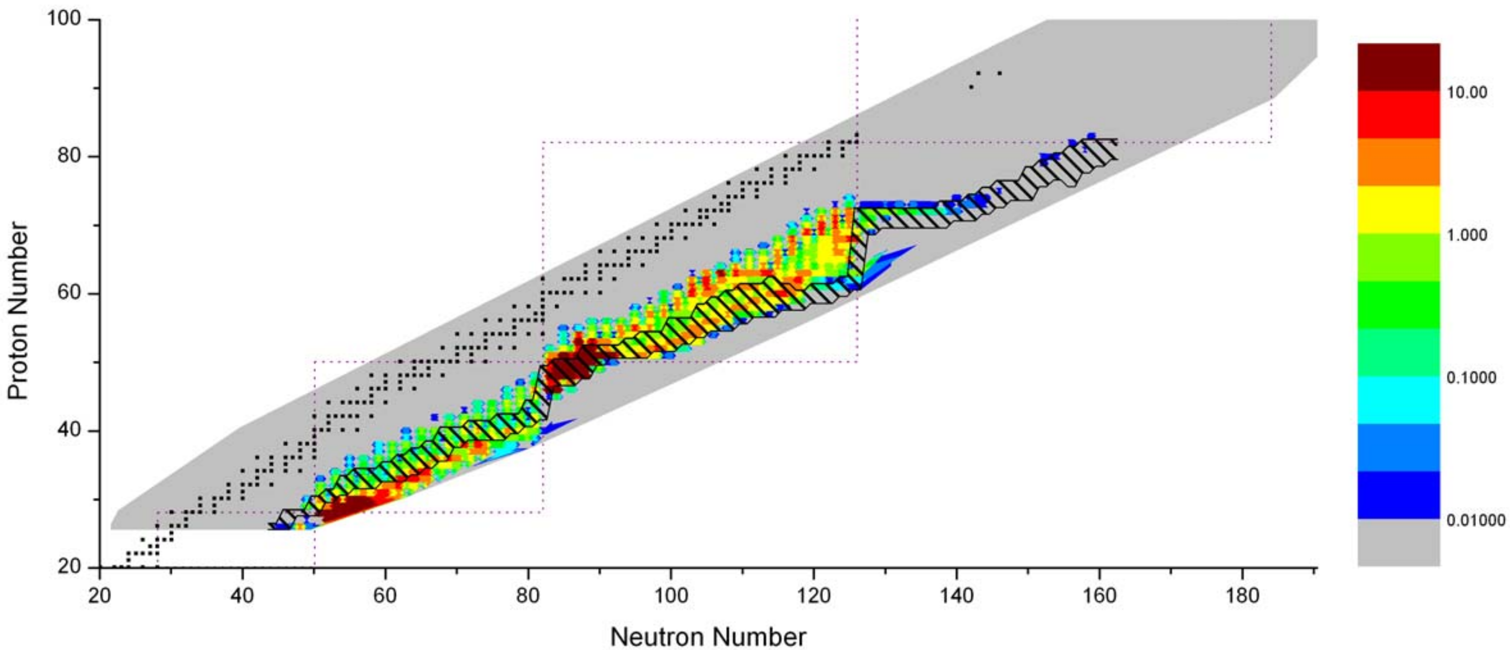

Nucleus	$\Delta_{+25\%}$	$\Delta_{-25\%}$
136Sn	2.87E+00	7.00E+02
80Ni	3.09E+01	1.56E+02
134Cd	1.50E+02	3.33E+01
132Cd	2.96E+00	1.75E+02
138Sn	1.39E+02	3.01E+01
79Ni	3.58E+01	1.13E+02
137Sn	8.82E+01	2.80E+01
130Pd	7.10E+01	2.56E+01
135In	6.17E+00	6.43E+01
133Cd	3.77E+01	3.06E+01
140Sb	1.35E+01	5.30E+01
129Pd	4.18E+01	2.45E+01
136Cd	5.60E+01	6.87E-01
135Sn	9.82E+00	4.63E+01
136In	2.99E+01	2.40E+01
137In	2.84E+01	2.52E+01
83Cu	1.86E+00	4.71E+01
142Sb	2.12E+01	1.84E+01
141Sb	2.18E-03	3.70E+01
136Sb	2.28E+01	1.24E+01

F-spin mass model

Run #	Description	Seed	Nseed	Nn	T9	density [g/cm^3]	time [sec.]	Source
64	H Qian's neutrinoless model (Iron)	Fe70	0.511	0.489	1.5	3.4x10^2	1.68	Qian et al. ApJ 494 (1998) with Fe70

Runs 23, 63, 64

- These runs use the same astrophysical parameters (Qian's H-Event with a ^{70}Fe seed).
- Varied mass models
- The following nuclei are in all three top 20 tables:

^{130}Pd, ^{132}Cd, ^{134}Cd, ^{135}Cd, ^{136}Cd and ^{140}Sn.

Run 24: L-Event with Iron-70 Seed

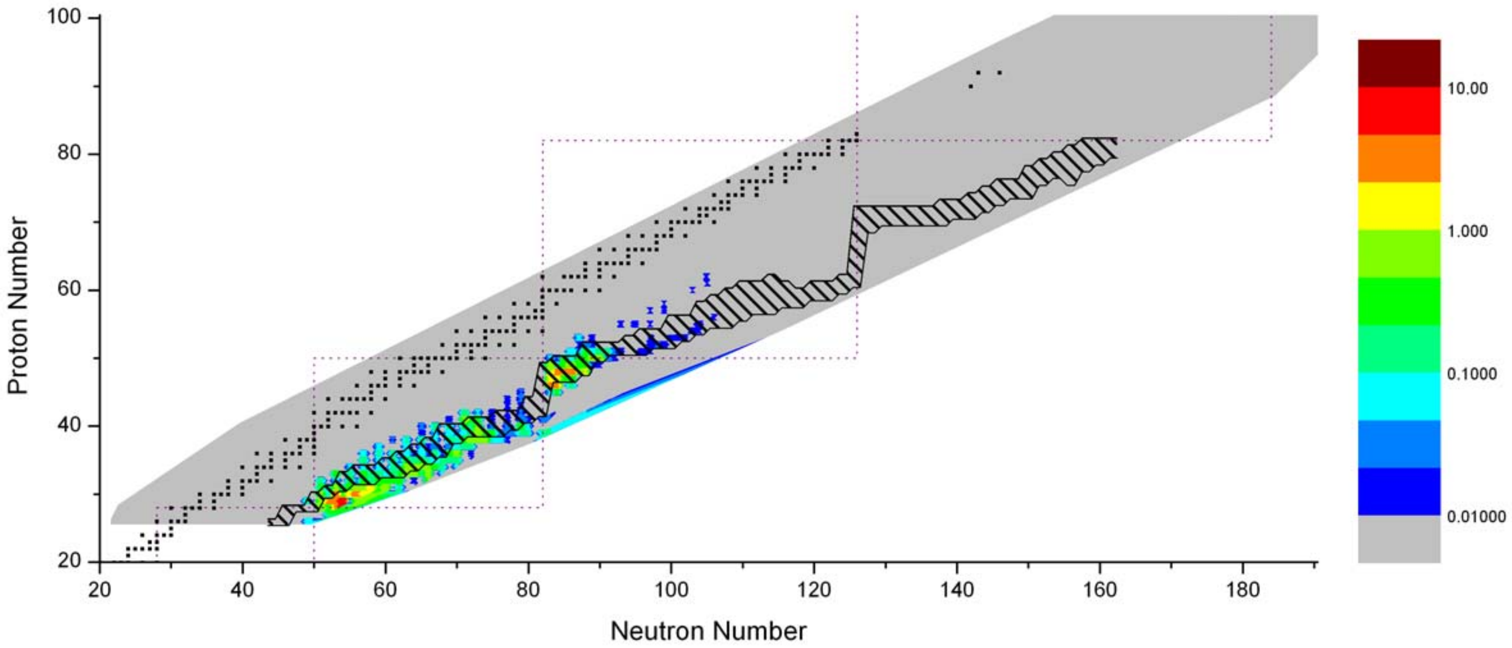

Nucleus	$\Delta_{+25\%}$	$\Delta_{-25\%}$
83Cu	1.92E+00	5.34E+00
82Cu	1.30E+00	3.13E+00
134Cd	1.55E+00	2.27E+00
130Pd	9.98E-01	2.28E+00
83Zn	4.02E-01	2.87E+00
132Cd	6.40E-03	3.06E+00
133Cd	1.26E+00	1.79E+00
129Pd	6.46E-01	1.74E+00
81Cu	1.65E-02	2.33E+00
86Zn	1.67E-01	2.13E+00
85Zn	8.50E-01	1.27E+00
131Ag	3.56E-01	1.67E+00
130Ag	4.13E-01	8.31E-01
89Ga	2.87E-01	9.39E-01
136Cd	9.91E-01	8.64E-02
110Sr	1.46E-02	9.36E-01
140Sn	5.69E-02	8.90E-01
132In	2.71E-02	8.76E-01
79Ni	6.57E-01	2.29E-01
99As	8.53E-01	1.29E-02

Run #	Description	Seed	Nseed	Nn	T9	density [g/cm^3]	time [sec.]	Source
24	L Qian's neutrinoless model (Iron)	Fe70	0.672	0.328	1.5	5.1x10^2	0.78	Qian et al. ApJ 494 (1998) with Fe70

Run 67: L-Event with Iron-70 Seed

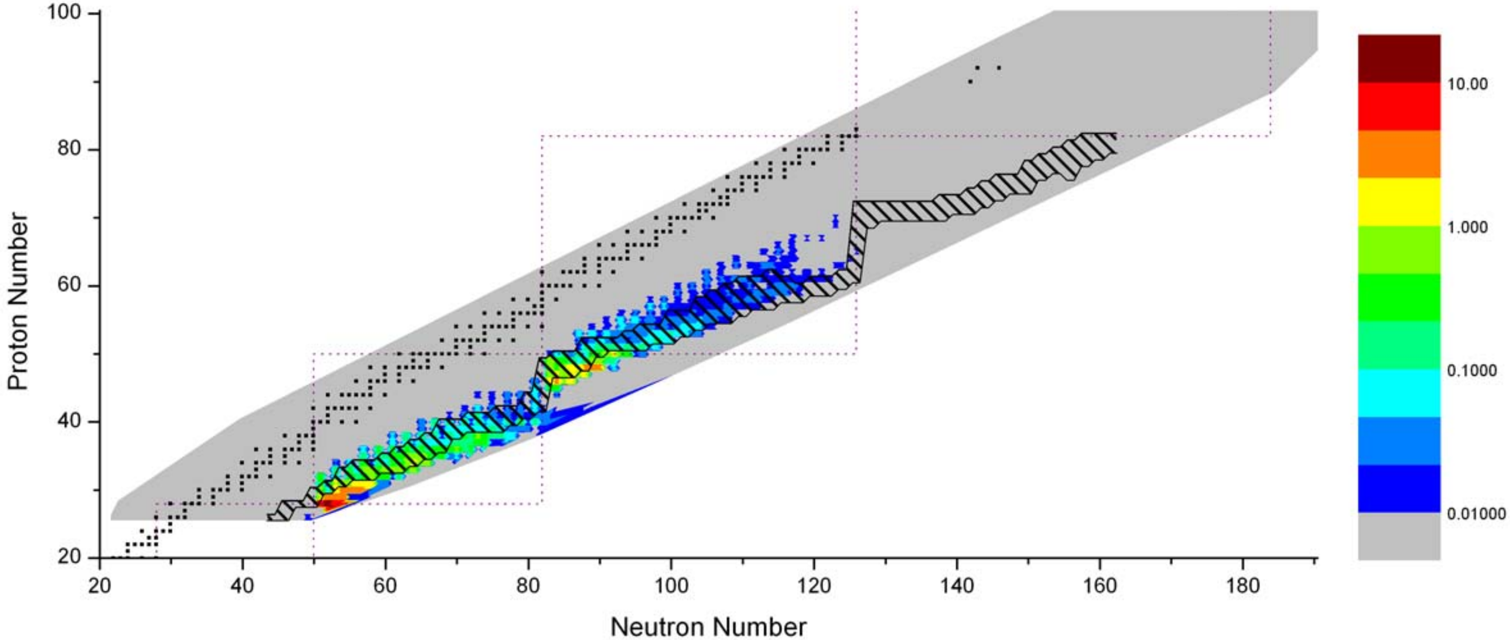

Nucleus	$\Delta_{+25\%}$	$\Delta_{-25\%}$
80Ni	6.56E+00	4.43E+00
79Ni	5.06E+00	3.95E+00
83Cu	2.59E+00	2.00E+00
82Cu	1.87E+00	2.02E+00
86Zn	1.75E+00	1.97E+00
81Cu	3.62E-01	2.93E+00
84Zn	1.13E-02	3.02E+00
85Zn	1.21E+00	1.64E+00
130Pd	1.72E+00	1.06E+00
137Cd	1.91E+00	7.41E-01
138Cd	1.75E+00	7.93E-01
136Cd	5.62E-01	1.84E+00
134Cd	3.66E-02	1.48E+00
83Zn	2.25E-01	1.26E+00
132Pd	1.31E+00	8.11E-02
89Ga	7.33E-01	6.47E-01
129Pd	6.34E-01	7.33E-01
135Cd	2.74E-01	1.04E+00
131Ag	6.44E-01	6.54E-01
87Ga	5.29E-01	7.25E-01

DUZU mass model

Run #	Description	Seed	Nseed	Nn	T9	density [g/cm^3]	time [sec.]	Source
67	L Qian's neutrinoless model (Iron)	Fe70	0.672	0.328	1.5	5.1x10^2	0.78	Qian et al. ApJ 494 (1998) with Fe70

Run 68: L-Event with Iron-70 Seed

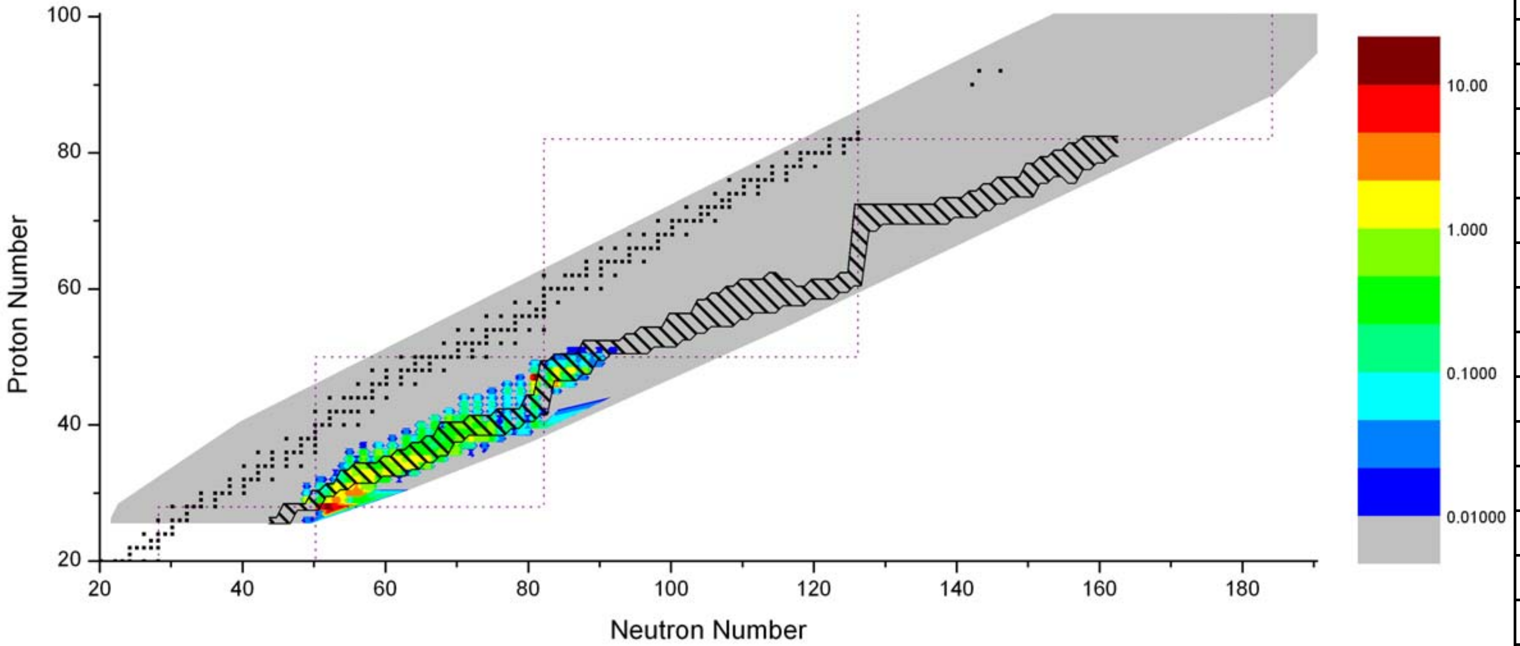

Nucleus	$\Delta_{+25\%}$	$\Delta_{-25\%}$
80Ni	3.47E+00	7.73E+00
128Ag	8.95E-04	1.02E+01
79Ni	1.41E+00	6.29E+00
82Cu	6.57E-01	3.39E+00
86Zn	1.28E+00	2.56E+00
85Zn	1.10E+00	2.46E+00
130Pd	2.23E+00	1.14E-01
87Ga	1.27E+00	1.05E+00
101Br	7.59E-01	1.30E+00
78Cu	2.60E-02	1.87E+00
99Br	6.76E-01	1.22E+00
134Cd	1.73E+00	1.39E-01
132Cd	1.63E+00	2.10E-01
84Zn	6.00E-01	1.23E+00
131Ag	1.53E+00	1.76E-01
98Se	6.51E-01	9.93E-01
91As	2.75E-01	1.33E+00
93As	7.53E-01	8.39E-01
84Ga	1.00E-02	1.53E+00
96Br	8.68E-01	6.06E-01

ETFSI-12 mass model

Run #	Description	Seed	Nseed	Nn	T9	density [g/cm^3]	time [sec.]	Source
68	L Qian's neutrinoless model (Iron)	Fe70	0.672	0.328	1.5	5.1x10^2	0.78	Qian et al. ApJ 494 (1998) with Fe70

Run 69: L-Event with Iron-70 Seed

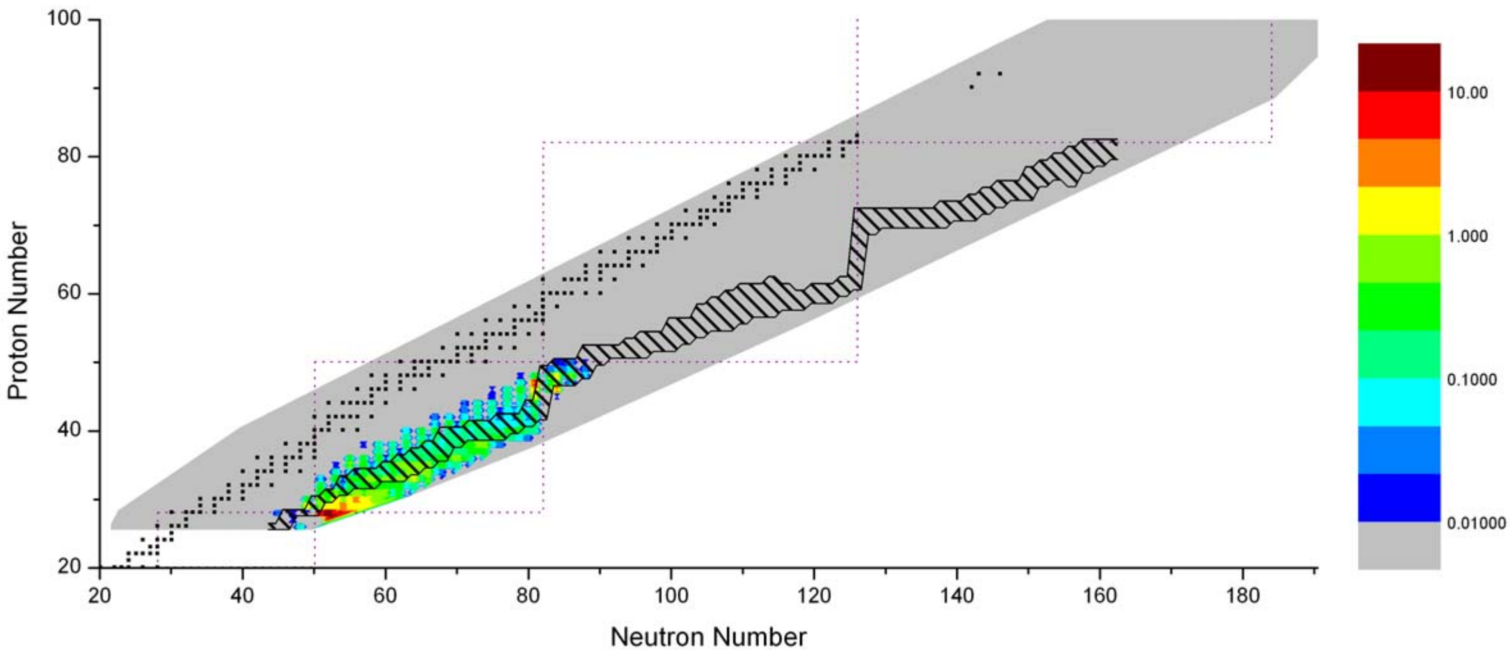

Nucleus	$\Delta_{+25\%}$	$\Delta_{-25\%}$
80Ni	4.00E-01	1.20E+01
79Ni	9.96E-01	7.12E+00
128Ag	2.53E-04	4.68E+00
83Cu	4.78E-01	2.44E+00
86Zn	2.62E-02	2.27E+00
127Pd	4.86E-03	2.18E+00
130Pd	2.06E+00	1.00E-01
83Zn	2.77E-01	1.76E+00
78Cu	1.82E-03	2.00E+00
85Zn	5.55E-01	1.39E+00
85Cu	8.06E-01	6.58E-01
82Cu	3.35E-01	1.12E+00
81Cu	5.13E-02	1.29E+00
132Cd	3.52E-01	9.82E-01
84Cu	6.86E-01	6.04E-01
97As	4.29E-01	6.13E-01
126Rh	3.18E-02	9.72E-01
131Ag	7.92E-01	1.19E-01
95As	4.32E-01	4.66E-01
91As	8.71E-03	8.89E-01

F-spin mass model

Run #	Description	Seed	Nseed	Nn	T9	density [g/cm^3]	time [sec.]	Source
69	L Qian's neutrinoless model (Iron)	Fe70	0.672	0.328	1.5	5.1x10^2	0.78	Qian et al. ApJ 494 (1998) with Fe70

Runs 24, 67, 68

- same astrophysical parameters
- Varied mass models
- The following nuclei are in all three top 20

^{79}Ni, ^{82}Cu, ^{85}Zn, ^{86}Zn, ^{130}Pd, ^{131}Ag, and ^{134}Cd.

TESTING FOR SENSITIVITY

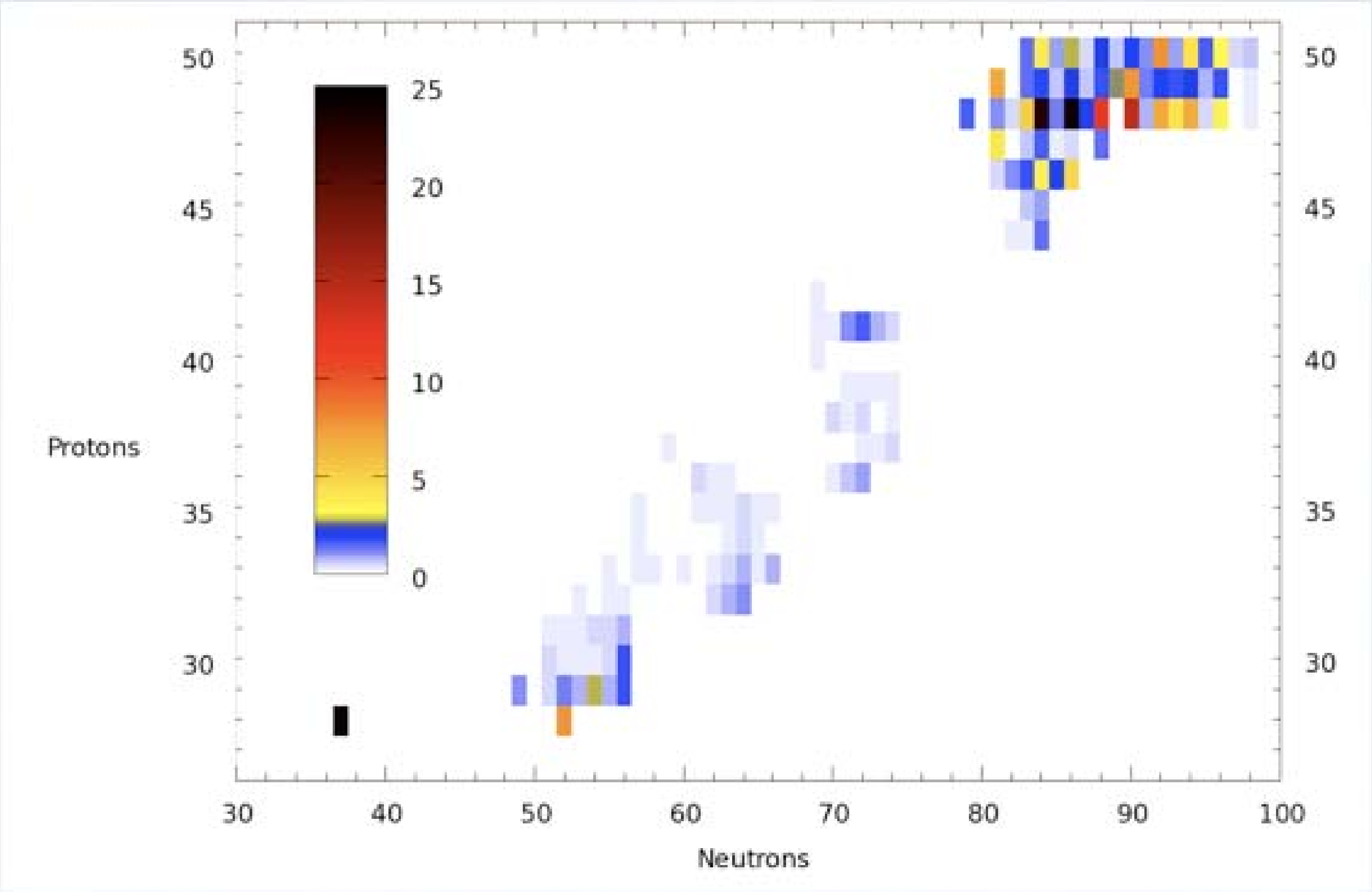

TESTING FOR SENSITIVITY

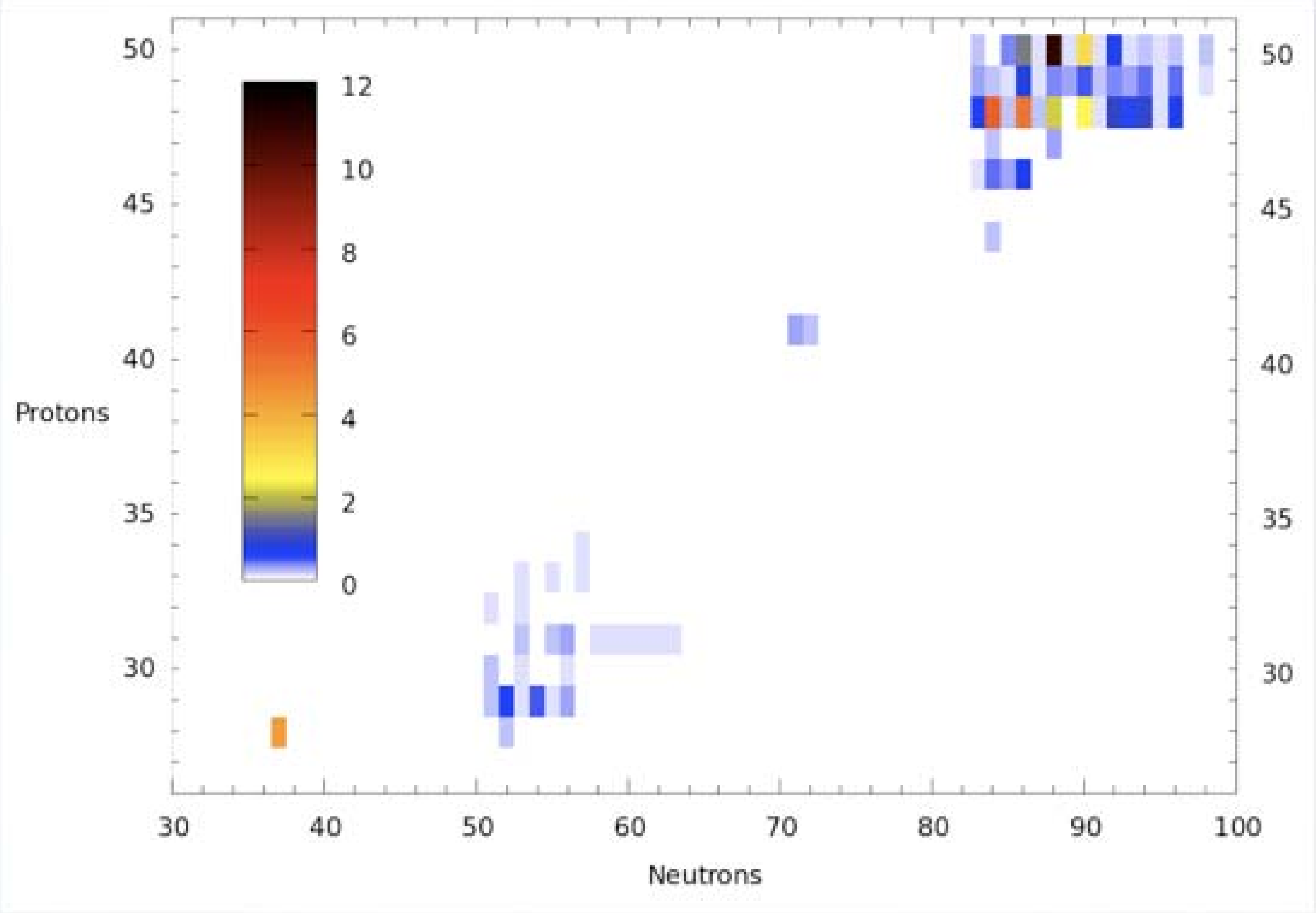

TABLE I: MOST IMPORTANT NUCLEAR MASSES FOR H-SCENARIO WITH ^{70}Fe SEED

^{A}X	Rank $\sum \Delta_{\pm 25}$	Δ_{+25}	Δ_{-25}	Rank $\sum \Delta Y_{\pm 25}$	ΔY_{+25}	ΔY_{-25}
^{140}Sn	1	6.77	262	1	1.34	24.4
^{134}Cd	2	15	119	2	8.39	5.78
^{202}Hf	3	36.4	42.5	165	0.07	0.12
^{201}Hf	4	43.9	34.2	179	0.08	0.09
^{203}Hf	5	39.4	33.9	187	0.07	0.09
^{133}Cd	6	8.62	62.7	6	1.94	3.6
^{136}Cd	7	46.6	8.03	5	5.67	0.69
^{82}Cu	8	17.5	27.8	16	1.12	1.31
^{83}Cu	8	13.6	37.6	12	1.31	1.59
^{204}Hf	10	1.96	41.3	256	0	0.11
^{139}Sn	11	8.21	33	4	1.38	5.78
^{135}Cd	12	32.8	7.31	9	3.24	0.63
^{201}Lu	13	37.2	1.81	273	0.1	0.01
^{132}Cd	14	0.29	38.2	3	0.11	11.5
^{142}Sb	15	11.7	24.9	15	0.92	1.58
^{86}[illegible]	[illegible]	[illegible]	[illegible]	[illegible]	[illegible]	[illegible]

ΔY

- Various mass model neutron separation energies (S_n) were varied by $\pm 25\%$ for each nucleus individually.
- The change in the total abundance curve is then calculated using:

$$\Delta Y_{\pm 25\%}(N,Z)=\sum_{A} Y(A)-Y(A,\pm\Delta S_n(N,Z)).$$

^{78}Ni , ^{77}Ni first measurement of half-lives $110^{+100/-60}$ ms; $128^{+27/-33}$ ms

^{76}Ni, ^{75}Ni more precise measurements $238^{+15/-18}$ ms; $344^{+20/-24}$ ms